



NUREG/CR-7211
PNNL-21589

Application of a Hydrological Uncertainty Methodology to Nuclear Reactor Site Evaluations

AVAILABILITY OF REFERENCE MATERIALS IN NRC PUBLICATIONS

NRC Reference Material

As of November 1999, you may electronically access NUREG-series publications and other NRC records at NRC's Library at www.nrc.gov/reading-rm.html. Publicly released records include, to name a few, NUREG-series publications; *Federal Register* notices; applicant, licensee, and vendor documents and correspondence; NRC correspondence and internal memoranda; bulletins and information notices; inspection and investigative reports; licensee event reports; and Commission papers and their attachments.

NRC publications in the NUREG series, NRC regulations, and Title 10, "Energy," in the *Code of Federal Regulations* may also be purchased from one of these two sources.

1. The Superintendent of Documents

U.S. Government Publishing Office
Mail Stop IDCC
Washington, DC 20402-0001
Internet: bookstore.gpo.gov
Telephone: (202) 512-1800
Fax: (202) 512-2104

2. The National Technical Information Service

5301 Shawnee Rd., Alexandria, VA 22312-0002
www.ntis.gov
1-800-553-6847 or, locally, (703) 605-6000

A single copy of each NRC draft report for comment is available free, to the extent of supply, upon written request as follows:

Address: **U.S. Nuclear Regulatory Commission**
Office of Administration
Publications Branch
Washington, DC 20555-0001
E-mail: distribution.resource@nrc.gov
Facsimile: (301) 415-2289

Some publications in the NUREG series that are posted at NRC's Web site address www.nrc.gov/reading-rm/doc-collections/nuregs are updated periodically and may differ from the last printed version. Although references to material found on a Web site bear the date the material was accessed, the material available on the date cited may subsequently be removed from the site.

Non-NRC Reference Material

Documents available from public and special technical libraries include all open literature items, such as books, journal articles, transactions, *Federal Register* notices, Federal and State legislation, and congressional reports. Such documents as theses, dissertations, foreign reports and translations, and non-NRC conference proceedings may be purchased from their sponsoring organization.

Copies of industry codes and standards used in a substantive manner in the NRC regulatory process are maintained at—

The NRC Technical Library

Two White Flint North
11545 Rockville Pike
Rockville, MD 20852-2738

These standards are available in the library for reference use by the public. Codes and standards are usually copyrighted and may be purchased from the originating organization or, if they are American National Standards, from—

American National Standards Institute

11 West 42nd Street
New York, NY 10036-8002
www.ansi.org
(212) 642-4900

Legally binding regulatory requirements are stated only in laws; NRC regulations; licenses, including technical specifications; or orders, not in NUREG-series publications. The views expressed in contractor-prepared publications in this series are not necessarily those of the NRC.

The NUREG series comprises (1) technical and administrative reports and books prepared by the staff (NUREG-XXXX) or agency contractors (NUREG/CR-XXXX), (2) proceedings of conferences (NUREG/CP-XXXX), (3) reports resulting from international agreements (NUREG/IA-XXXX), (4) brochures (NUREG/BR-XXXX), and (5) compilations of legal decisions and orders of the Commission and Atomic and Safety Licensing Boards and of Directors' decisions under Section 2.206 of NRC's regulations (NUREG-0750).

DISCLAIMER: This report was prepared as an account of work sponsored by an agency of the U.S. Government. Neither the U.S. Government nor any agency thereof, nor any employee, makes any warranty, expressed or implied, or assumes any legal liability or responsibility for any third party's use, or the results of such use, of any information, apparatus, product, or process disclosed in this publication, or represents that its use by such third party would not infringe privately owned rights.

Application of a Hydrological Uncertainty Methodology to Nuclear Reactor Site Evaluations

Manuscript Completed: February 2013
Date Published: August 2016

Prepared by:
P.D. Meyer and C.D. Johnson
Pacific Northwest National Laboratory
Richland, WA 99352

R.E. Cady, NRC Program Manager

NRC Job Code Number V6068

Office of Nuclear Regulatory Research

ABSTRACT

A variety of surface water and groundwater models are often used in the review of applications for new nuclear commercial power reactors. These models are used to evaluate current site hydrology and to provide estimates of future site conditions after facility construction has been completed. Predicted site conditions such as maximum flood and groundwater elevations may be compared to reactor design criteria. The current review guidance emphasizes a conservative approach to hydrologic modeling. The limitations of this approach become apparent when predicted site conditions exceed a design criterion, or when the margin between the two is small. A simple groundwater transport modeling example illustrates how uncertainty concepts can be used to inform regulatory decisions under these conditions. An uncertainty analysis methodology that can be used to estimate the joint impact of parameter, conceptual model, and scenario uncertainties is described, along with available software tools that can be used in a practical implementation of this methodology. The uncertainty methodology is illustrated using an example of reviewing groundwater site characteristics as part of a safety evaluation for a new power reactor. The example uses publicly available information from the Bellefonte Nuclear Station Units 3 and 4 Combined License application. A detailed description of model development is included to illustrate typical modeling decisions that arise in actual reviews. Modeling and uncertainty analyses were carried out using the Groundwater Modeling System (GMS) software, PEST, UCODE, and custom spreadsheets. The example illustrates that following standard procedures for uncertainty analyses can reveal limitations of the hydrologic analyses, e.g., unexamined parameter correlations and outstanding data needs, and results in more consistent reviews. Explicit consideration of alternative models is likely more valuable than quantitative model averaging. However, model averages using linear uncertainty methods can be easily completed and should be considered. Simple approaches to uncertainty evaluation can have great value, contributing to estimates of the degree of conservatism in the analysis, demonstrating an understanding of the system, and providing evidence of due diligence.

CONTENTS

ABSTRACT	iii
LIST OF FIGURES.....	ix
LIST OF TABLES	xv
EXECUTIVE SUMMARY	xvii
ACKNOWLEDGMENTS	xxi
ABBREVIATIONS AND ACRONYMS.....	xxiii
1 INTRODUCTION.....	1-1
2 MODEL USE IN NEW REACTOR REVIEWS.....	2-1
2.1 Use of Hydrologic Models in Nuclear Power Plant Evaluations.....	2-1
2.2 What is the Role of a Model?.....	2-1
2.3 Typical Groundwater Modeling Experience.....	2-2
2.4 Limitations of the Current Approach.....	2-3
2.5 Conservative Models or Conservative Decisions?	2-4
2.6 Groundwater Transport Example	2-5
2.6.1 A Simple Uncertainty Evaluation	2-7
3 UNCERTAINTY METHODOLOGY AND SOFTWARE	3-1
3.1 Uncertainty Methodology Incorporating Parameter, Model, and Scenario Uncertainties.....	3-3
3.2 Implementation of the Uncertainty Methodology	3-6
3.2.1 Software Tools	3-7
3.2.2 Software Capabilities and Limitations.....	3-8
4 EXAMPLE APPLICATION.....	4-1
4.1 Building the Groundwater Model.....	4-1
4.1.1 Gather Relevant Data.....	4-3
4.1.1.1 Site Locale and Topology.....	4-4
4.1.1.2 Site Hydrogeology	4-6
4.1.1.3 Aquifer Properties.....	4-8

4.1.1.4	Precipitation and Land Usage	4-10
4.1.1.5	Hydraulic Information	4-10
4.1.1.6	Conceptual Model Based on the Data	4-13
4.1.2	Define the Geological/Model Structure	4-16
4.1.2.1	Groundwater Model Domain.....	4-16
4.1.2.2	Define Hydrogeological Units as Materials	4-18
4.1.2.3	Build a Solids Model.....	4-18
4.1.2.4	Map the Geological Structure to a MODFLOW Domain.....	4-22
4.1.3	Configure the MODFLOW Model.....	4-29
4.1.3.1	Temporal Nature of the Model.....	4-29
4.1.3.2	Boundary Conditions on Sides of Model Domain.....	4-29
4.1.3.3	Boundary Conditions for Surface Water Features.....	4-29
4.1.3.4	Recharge Boundary Conditions.....	4-31
4.1.3.5	Initial Conditions.....	4-31
4.1.3.6	Configured Model.....	4-32
4.2	Model Calibration.....	4-32
4.2.1	Define Calibration Targets.....	4-33
4.2.2	Define Parameters for Estimation.....	4-33
4.2.3	Calibration Results	4-34
4.2.4	Define Prior Parameter Information	4-38
4.3	Alternative Models Evaluated for the Bellefonte Site.....	4-41
4.3.1	Hydrogeologic Unit Representation.....	4-41
4.3.2	Recharge Representation.....	4-42
4.3.3	Depth of Active Flow	4-42
4.3.4	Alternative Model Designations	4-42
4.4	Calibration Implementation	4-43
4.4.1	Model Evaluation.....	4-43
4.5	Alternative Model Probabilities.....	4-50
4.6	Predictive Modeling	4-51

4.6.1	Modifications for Post-Construction Conditions	4-52
4.6.2	Post-Construction Model Results	4-55
4.6.3	Predictive Uncertainty	4-56
4.6.3.1	Software Used in Estimating Predictive Uncertainty	4-57
4.6.3.2	Predictive Uncertainty Results.....	4-58
5	Conclusions.....	5-1
6	References.....	6-1
	APPENDIX A: Dependence of KIC on Log Transformation of Parameters	A-1
	APPENDIX B: Data Used in Model Development.....	B-1
	APPENDIX C: Spreadsheets for Calculating Model Selection Criteria and Model-Averaged Quantities	C-1

LIST OF FIGURES

Figure 1.	Boxplots of (left) K_s estimates from 11 well tests and (right) Sr-90 K_d estimates from 20 laboratory tests.....	2-6
Figure 2.	Parameter distributions based on data analysis (solid line) and sample distributions (symbols) for (left) K_s and (right) K_d parameters.....	2-7
Figure 3.	Travel time results for the 500 random parameter realizations.....	2-8
Figure 4.	Probability of exceedance for the concentration ratio.....	2-9
Figure 5.	Framework for application of hydrogeologic models. The relatively short history-matching period involves comparison between observations (points) and model simulated equivalents (solid line). The much longer predictive period involves comparison between model simulation results and regulatory or design criteria (e.g., a design maximum groundwater head).	3-2
Figure 6.	Location of the Bellefonte site. Lower image taken from FSAR Figure 2.1-201 (TVA 2009).	4-2
Figure 7.	Steps in building a MODFLOW groundwater model.....	4-3
Figure 8.	Depiction of data inputs used to configure a three-dimensional MODFLOW model for simulating groundwater flow in the subsurface.....	4-5
Figure 9.	DOQQ imagery for the Bellefonte site vicinity. Coordinates are SPCS Alabama East, in feet.	4-5
Figure 10.	Topographic map for the Bellefonte site vicinity.....	4-6
Figure 11.	DEM data in the vicinity of the Bellefonte site (as depicted in Global Mapper).....	4-7
Figure 12.	Conceptual depiction of hydrogeology in a cross-section of the Sequatchie Valley, the location of the Bellefonte site (from Miller 1990).	4-7
Figure 13.	Geological units in the vicinity of the Bellefonte site. Adapted from Irvin and Dinterman (2009).....	4-8
Figure 14.	A geologic cross-section through Units 3 and 4 showing rock units (taken from FSAR Figure 2.5-339, TVA 2009).....	4-9
Figure 15.	Total annual precipitation at COOP station 017304 in Scottsboro, Alabama from 1955 through 2009. The dashed line is the annual average over this time frame.	4-11
Figure 16.	Locations of surface water gaging locations. This figure shows a portion of FSAR Figure 2.4.12-213 (TVA 2009).	4-12
Figure 17.	Locations of streams that discharge into “Town Creek” (marked by the arrows).	4-13

Figure 18.	Hydraulic head data and interpreted contours for the 1961 data (blue contours at west and north sides) and the September 2005 data (black contours in southeast quadrant, all overlain on the Bellefonte area imagery).....	4-14
Figure 19.	Example of recent hydraulic head contours interpreted from November 2006 groundwater headdata.....	4-15
Figure 20.	Conceptual model of karst development at the Bellefonte site (from FSAR Figure 2.5-304, TVA 2009).	4-17
Figure 21.	Groundwater head response to a precipitation event: about 10 cm (4 in) of precipitation were recorded at Scottsboro, Alabama from 9/22/06 to 9/24/06 (Scottsboro 2 NE Experimental Station, downloaded 8/27/10 from http://www.ncdc.noaa.gov). Groundwater head data from FSAR Table 2.4.12-204 for monitoring well MW-1202a screened in the soil unit (TVA 2009).....	4-17
Figure 22.	Extent of the groundwater simulation model grid relative to key features. The grid origin is located in the lower left corner of the model at the bottom of the domain.....	4-19
Figure 23.	Material designations (and corresponding colors) used in GMS to represent the stratigraphic units of the subsurface (Section 4.1.1.6). The “dummy” material was used to facilitate work in GMS, but was not applied in the groundwater model.....	4-19
Figure 24.	DEM data in the vicinity of the Bellefonte site, looking nominally to the NNE. A 10X vertical exaggeration is applied.....	4-20
Figure 25.	Set of TINs defining the Soil (between green ground surface and orange) and the Weathered Rock (between orange and yellow). The zone of low data density represents where ground surface elevations from wells at the Bellefonte site were used in place of the DEM data. The orange and yellow TINs are offset from ground surface by the nominal thickness of each material. View is nominally to the NNE with a 10X vertical exaggeration.	4-21
Figure 26.	Solids models for the Soil and weathered rock (WeRo) materials based on a uniform thickness of each material from ground surface. View is nominally to the NNE with a 10X vertical exaggeration.....	4-21
Figure 27.	Examination of TINs representing the contacts between bedrock units. The left image depicts the TINs based on borehole data for contacts between the units, while the right image shows the parallel planes used to represent the unit contacts. The view is along a strike of 42.5° with a 10X vertical exaggeration.....	4-23
Figure 28.	Solids representing the USR, the MSR units A to F, and the contacts with the NV and LSR units. View is nominally to the NNE with a 10X vertical exaggeration.....	4-24

Figure 29. View of solids used to fill in space such that the groundwater model domain is encompassed (left) and the solid used for clipping the top of the solids representing the bedrock units (right). The rightmost block representing the NV unit has been hidden in the right image so that the variation of the clipping solid surface is visible. Note that although the clipping solid is green, it does not represent Soil. The view is nominally to the NNE with a 10X vertical exaggeration but with 25° (left) and -25° (right) dip viewing angles.....	4-24
Figure 30. Solids representing bedrock stratigraphic units after being clipped so the top elevation matches with the bottom elevation of the WeRo solid. View is nominally to the NNE with a 10X vertical exaggeration.....	4-25
Figure 31. Final set of solids representing all materials and trimmed to the lateral and bottom extent of the groundwater flow model domain. View is nominally to the NNE with a 10X vertical exaggeration.....	4-25
Figure 32. Deformation of an originally orthogonal model grid after mapping the solids model (Figure 31) to the MODFLOW LPF package using the Grid Overlay option. The grid layers follow the topography (using equal grid cell thickness for all layers in a given vertical column of grid cells). The water table would cut through multiple layers. View is nominally to the NNE with a 10X vertical exaggeration.	4-27
Figure 33. MODFLOW model grid for the LPF package, showing the materials (hydrogeological units) applied to the grid cells. This model was created by splitting the solids model into two portions, mapping (using the Grid Overlay option) to two model grids, and then merging both grids into a single model grid. Grid cells beyond the shoreline of the Tennessee River have been inactivated. View is nominally to the NNE with a 10X vertical exaggeration.....	4-28
Figure 34. Fence diagram of MODFLOW model grid for the HUF package, showing the hydrogeological units applied to the grid cells along selected cross sections. View is nominally to the NNE with a 10X vertical exaggeration.....	4-28
Figure 35. Hydraulic head data from 1961 relative to the model domain boundary. Data from numbered wells were used to define the boundary conditions along the northwest side. Filled circles indicate wells impacted by pumping and thus not used in this analysis.	4-30
Figure 36. Boundary conditions for the groundwater model. Internal boundary conditions (green drain and purple constant head) apply to layer 1, others (yellow) to all layers.	4-30
Figure 37. Zones for the recharge boundary conditions.....	4-31
Figure 38. MODFLOW groundwater model for the Bellefonte site as configured with the hydrogeological units (HUF package), constant head boundary conditions (purple points), and drains (white points).	4-32

Figure 39.	Locations of hydraulic head calibration targets for the four groups of data. Points outside the model domain boundary were not included as calibration targets.	4-34
Figure 40.	Hydraulic head contours (every 2 feet) resulting from the initial PEST calibration.	4-35
Figure 41.	Unweighted residuals (observed minus simulated, in feet) for the 1961 data. Positive (blue) and negative (pink) residual magnitudes are proportional to symbol size.	4-36
Figure 42.	Unweighted residuals (observed minus simulated, in feet) for the September 2005 data. Positive (blue) and negative (pink) residual magnitudes are proportional to symbol size.	4-36
Figure 43.	Unweighted residuals (observed minus simulated, in feet) for the average 2006/2007 “Bedrock” data. Positive (blue) and negative (pink) residual magnitudes are proportional to symbol size.	4-37
Figure 44.	Unweighted residuals (observed minus simulated, in feet) for the average 2006/2007 “Soil” data. Positive (blue) and negative (pink) residual magnitudes are proportional to symbol size.	4-37
Figure 45.	Correlation between hydraulic conductivity and recharge prevents unique parameter estimates unless one value is fixed (e.g., recharge here) or prior values of parameters are applied. Here the prior mean recharge was 8 in/yr; the prior mean hydraulic conductivity was 0.438 ft/d.	4-39
Figure 46.	Prior parameter distributions derived from data and assumptions discussed in the text: horizontal hydraulic conductivity (top) and recharge (bottom).	4-40
Figure 47.	Pathlines from points around the Units 3 and 4 reactor buildings computed in GMS using MODPATH: plan view (top) and cross-section through the reactor building areas (bottom, 10x vertical exaggeration).	4-46
Figure 48.	Graphical evaluation of residuals for model H4R1D1: observed vs. simulated heads (feet) (top left), unweighted residuals vs. observed heads (top right), weighted residuals vs. simulated heads (middle left), quantile-quantile plot of weighted residuals (middle right), and boxplot of weighted residuals (bottom, with explanatory legend).	4-47
Figure 49.	Parameter estimates and 95% confidence intervals for hydraulic conductivity (top, ft/d) and recharge (bottom, ft/d). See text for explanation of parameters.	4-49
Figure 50.	Composite sensitivities for model H4R1D1 at the final parameter values as computed following Hill and Tiedeman (2007).	4-50
Figure 51.	Model probabilities computed with AICc and KIC, and the weighted sum of squared residuals for the alternative models.	4-51

Figure 52. Figures depicting the depth of the reactor building excavation (left), changes in topography, the locations of reactor buildings, and the groundwater model grid zones representing fill material and reactor building excavations (right). Figures adapted from FSAR Figure 2.5-348a and Figure 2.5-362.	4-53
Figure 53. Refined recharge zones for the post-construction scenario. A portion of the Lowlands zone was incorporated into the northern corner of the Developed Area zone.	4-53
Figure 54. Details of the post-construction recharge zones around Units 3 and 4. Reactor and other significant buildings and the main parking areas are set to zero recharge. Note that the colors are simply used to distinguish zones and are unrelated to materials.	4-54
Figure 55. Pre-construction topography and materials (left) and modifications to represent the post-construction scenario (right) in the vicinity of Units 3 and 4. The topography was flattened at the site and the Category 1 building foundations were represented by inactive grid cells surrounded by fill material. View is nominally to the ENE with a 10X vertical exaggeration.	4-55
Figure 56. Hydraulic head contours for model H4R1D1 with the post-construction model configuration modifications. The purple rectangles indicate the location of Units 3 and 4, where inactive cells represent building foundations and fill material surrounds the foundations.	4-56
Figure 57. Comparison of pre-construction (left) and post-construction scenario hydraulic head contours for model H4R1D1. Contour intervals are 1 ft.	4-56
Figure 58. Detail from the post-construction groundwater model showing the locations of the predicted heads at the corners of the reactor units.	4-59
Figure 59. Prior parameter distribution for the hydraulic conductivity of the fill material.	4-60
Figure 60. Predicted heads (top of colored bars) and 95% confidence interval upper limits for the individual models and the model average.	4-61
Figure 61. Effect on model-averaged predicted head of including the fill material hydraulic conductivity uncertainty.	4-61

LIST OF TABLES

Table 1.	Hydraulic conductivity (K_s) for subsurface materials near the Bellefonte site. Minimum and maximum values reported in TVA (2009); midpoints and averages were calculated.	4-9
Table 2.	Porosity for subsurface materials in the vicinity of the Bellefonte site.....	4-10
Table 3.	Average stage observed at surface water measurement locations.	4-12
Table 4.	Initial model grid description.	4-18
Table 5.	Head observation error intervals, standard deviations, and calibration weights.....	4-33
Table 6.	Materials represented by hydraulic conductivity parameters in alternative models.....	4-48
Table 7.	Model selection criteria values and model probabilities for alternative models.....	4-51
Table 8.	Averaged observed head (calibration target), maximum observed head, and simulated equivalent head from the calibrated H4R1D1 model for three wells near the desired location of predicted head. All heads in feet.	4-59

EXECUTIVE SUMMARY

A variety of surface water and groundwater models are often used in the review of applications for new nuclear commercial power reactors. Models are used to improve understanding of site behavior, e.g., by synthesizing a conceptual understanding of site hydrology with observations of the site-specific and regional hydrologic characteristics. Ultimately, however, Nuclear Regulatory Commission (NRC) staff need to reach conclusions about site hydrologic characteristics and the magnitude of hydrologic hazards and environmental impacts that directly support regulatory decisions about facility safety and environmental acceptability. These conclusions often require the estimation of some quantitative measure of future site behavior, for example, maximum flood and groundwater elevations after plant construction, that can be compared to reactor design criteria. To improve the defensibility of decisions informed by the results of predictive modeling, it is important to be transparent in describing the development of the model and explicit in communicating the uncertainties in model results. This viewpoint is consistent with NRC policy in the sense that risk-informed decisions require some understanding of uncertainty, which includes the uncertainty of model results used as the partial basis for those decisions.

As a practical matter, hydrologic models are not an end in themselves, but are usually part of a larger project. Because of this, the way in which hydrological models are developed and used is constrained by budget and schedule factors that may be beyond the control of those responsible for the hydrologic analysis. For example, groundwater model developers supporting a Combined License (COL) applicant and NRC staff reviewing the application share a common experience: typically all the data are collected prior to model development. As a result there is little (or no) opportunity for the modeling to influence data collection and there are significant constraints on the ability to evaluate the model and improve it when model limitations/errors become apparent. This situation can lead to relaxation of calibration criteria (i.e., accepting a larger error in the calibration) and a greater need for sensitivity analyses and consideration of alternative conceptualizations to adequately address uncertainties. Because opportunities for feedback from model evaluation are limited, it is important that the NRC staff's review plans and regulatory guidance are explicit about modeling expectations, including the role of uncertainty assessment. These expectations should be consistent with established standards and accepted procedures.

With regard to hydrology-related review of new reactor applications, the current review criteria and technical procedures contained in NRC staff guidance describe a predominantly deterministic approach that emphasizes conservatism in the analysis. This approach can be problematic when either the acceptance criteria are not satisfied (or the margin of acceptance is small), or when the models and technical evaluation methods are not demonstrably conservative. Examples are given where these issues have arisen in actual reviews. Instead of focusing on the conservatism of models (e.g., bounding assumptions and extreme parameter values), it is recommended that the focus be on conservative decisions. The latter implies that uncertainties in model outcomes can be properly accounted for; the conservatism in this case enters when comparing model outcomes to regulatory or design requirements. For example, a decision based on the 95th percentile outcome is more conservative than one based on the mean outcome. Focusing on a conservative decision is consistent with a risk-informed approach, and it allows for the natural consideration of consequences (e.g., the safety consequences of exceeding a design flood elevation). A simple groundwater transport modeling example is used to demonstrate the advantage of a risk-informed approach focused on conservative decisions with a quantitative consideration of uncertainties.

An uncertainty analysis methodology that can be used to estimate the joint impact of parameter, conceptual model, and scenario uncertainties is described. This methodology is comprehensive in that it considers multiple sources of uncertainty while providing a means to focus on those of most relevance. It is quantitative, allowing model results to be compared with regulatory criteria or design requirements. It is systematic, applicable to a wide range of sites and objectives. And the methodology is practical, able to be implemented with standard methods and existing software tools.

Implementation of the uncertainty methodology requires two basic activities: development of two or more models to represent unresolved conceptual and structural uncertainties associated with the representation of the site, and calculations to estimate parameter values, parameter uncertainties, model probabilities, and predicted values (including predictive uncertainty). Model development is a site-specific and labor-intensive process, making it difficult to apply standards or generalizable procedures. The Groundwater Modeling System (GMS) package and its associated process codes were the primary software used in model development for the example discussed in this report. Parameter estimation and uncertainty calculations are more amenable than model development to the application of standards and generalizable procedures. PEST and UCODE were the principal software packages used to carry out these calculations for the example in this report. Due to limitations in software capabilities, calculation of model probabilities and model-averaged predictions were carried out using custom spreadsheets.

A practical application of the uncertainty methodology is demonstrated in this report through the review of groundwater site characteristics as part of a safety evaluation for a new power reactor. Although the example uses publically available information from the Bellefonte Nuclear Station Units 3 and 4 COL application, the groundwater models developed for the example are solely the product of the coauthors of this report. Information used in model development included digital imagery and topographic data, a regional hydrogeologic description, geologic unit contacts from site characterization borehole logs, aquifer properties from site characterization hydraulic and physical tests, regional precipitation data, surface water elevation data, and observation well groundwater head measurements.

A detailed description of conceptual model development in GMS is included to illustrate typical modeling decisions that arise in actual reviews. The conceptual model was mapped in GMS to a MODFLOW groundwater flow model. Alternative models were developed to represent uncertainties in the representation of the hydrogeologic units, the variation in recharge, and the depth of active flow. Sixteen alternative models were considered. Each model was calibrated to a set of groundwater head observations and prior information on parameters for saturated hydraulic conductivities and recharge values. Model evaluation was carried out within GMS and using custom spreadsheets. With the exception of outliers located in two areas of the model domain, the residuals appeared to be normally distributed. Weighted residuals for the calibrated models were, however, larger than indicated by the assumed head observation errors. These results suggest that, although model error is significant, predictive uncertainties from the models can be accurate.

Model probabilities were calculated using a custom spreadsheet to eliminate the potential effect of parameter transformations on the probabilities, something that is not considered in existing software. Results showed that only four of the sixteen alternative models were assigned substantial model probabilities. High probability models were neither the most complex, nor the simplest.

Predictive models were developed for the high probability models to estimate post-construction groundwater head in the reactor power block area. Building foundation locations, the addition of fill material, changes in topography due to cut and fill, and changes in recharge were implemented in the predictive models to represent post-construction conditions. Parameter uncertainty was based on the calibration results with the addition of uncertainty in the hydraulic conductivity of the fill material. Predictive uncertainties were estimated using linear methods to calculate the mean and variance of the predicted groundwater head values. Results indicated that the depth of flow had little impact on the head near the reactor units. The depth of flow likely would have a much greater impact on predicted travel time. Model-averaged predicted values and predictive uncertainty were found to depend on the model selection criterion used to calculate the model probabilities. Since no single criterion has been shown to be superior in all cases, multiple criteria should be used.

The upper limit of the 95% confidence interval for the predicted groundwater head was increased by the inclusion of uncertainty in the fill material hydraulic conductivity, as much as one foot depending on the model selection criterion used. This result demonstrates the potential importance of even localized changes to the model under post-construction conditions. The fill material occupies a small portion of the model domain, but it is a potentially critical feature given that the design criterion for maximum groundwater head is within the excavation. In this case, including a reasonable uncertainty estimate for this material of limited extent had a noticeable impact on the predicted regulatory value to be compared to the design criterion. Whether or not this is significant would depend on the margin between the upper limit and the design criterion.

The example illustrates that following standard procedures for uncertainty analyses can reveal limitations of the hydrologic analyses, e.g., unexamined parameter correlations and outstanding data needs, and results in more consistent reviews. Explicit consideration of alternative models is likely more valuable than quantitative model averaging. However, model averages using linear uncertainty methods can be easily completed and should be considered. Simple approaches to uncertainty evaluation can have great value, contributing to estimates of the degree of conservatism in the analysis, demonstrating an understanding of the system, and providing evidence of due diligence.

ACKNOWLEDGMENTS

The authors gratefully acknowledge the financial assistance of the Office of Nuclear Regulatory Research of the U.S. Nuclear Regulatory Commission (NRC), the guidance of the NRC Project Manager, Ralph E. Cady, and the publication assistance of Mark Fuhrmann. We also appreciate the comments of NRC staff members Thomas J. Nicholson and Joseph F. Kanney during presentation of the contents of this report, and the comments of NRC staff members Mark S. McBride and Nebiyu Tiruneh on the final written version of the report.

ABBREVIATIONS AND ACRONYMS

ACRS	Advisory Committee on Reactor Safety
AICc	Akaike Information Criterion, corrected
ANSI	American National Standards Institute
ANS	American Nuclear Society
ASTM	American Society of Testing and Materials
ASWP	Alabama State Water Program
BCF	Block-Centered Flow
CFR	Code of Federal Regulations
COL	Combined Operating License
COOP	U.S. Cooperative Network
DEM	Digital Elevation Model
DOQQ	Digital Orthographic Quarter Quad
DRG	Digital Raster Graphic
ECL	Effluent Concentration Limit
ER	Environmental Report
FSAR	Final Safety Analysis Report
GHCN	Global Historical Climatology Network
GIS	Geographical Information System
GMS	Groundwater Modeling System
HCN	U.S. Historical Climatology Network
HDF	Hierarchical Data Format
HUF	Hydrogeologic-Unit Flow
KIC	Kashyap Information Criterion
LPF	Layer Property Flow
LSR	Lower Stones River
MMA	Multi-Model Analysis Software
MODFLOW	Groundwater Flow Modeling Software
MODPATH	Groundwater Flow Path Modeling Software
MSR	Middle Stones River
MT3DMS	Groundwater Transport Modeling Software
NAD27	North American Datum of 1927
NAD83	North American Datum of 1983
NE	Northeast

NNE	North Northeast
NRC	Nuclear Regulatory Commission
NV	Nashville
NW	Northwest
PCRDP	Historical precipitation data
PDF	Portable Document Format
PEST	Parameter Estimation Software
PRA	Probabilistic Risk Assessment
RAI	Request for Additional Information
RQD	Rock Quality Designation
SE	Southeast
SPCS	State Plane Coordinate System
SPT	Standard Penetration Test
SRP	Standard Review Plan
SSWR	Sum of Squared Weighted Residuals
SW	Southwest
TIN	Triangulated Irregular Network
TVA	Tennessee Valley Authority
UCODE	Parameter Estimation Software
USACE	U.S. Army Corps of Engineers
USGS	U.S. Geological Survey
USR	Upper Stones River
UTM	Universal Transverse Mercator
WeRo	Weathered Rock
WGS84	World Geodetic System of 1984

1 INTRODUCTION

In its review of applications for new nuclear power plants, U.S. Nuclear Regulatory Commission (NRC) staff are responsible for evaluating the hydrologic characteristics of proposed sites and assessing the impacts of the facilities on the hydrology and water resources of the surrounding area. Current guidance for these staff evaluations (NRC 2007; NRC 1999) describe technical procedures without explicit reference to the use of models. In practice, however, NRC staff often use hydrologic models as part of their evaluations. Models are used to synthesize a conceptual understanding of site hydrology and observations of the site-specific and regional hydrologic characteristics. This type of model use, to improve understanding of site behavior, is generally uncontroversial.

Understanding of the hydrology of a site is not an end in itself, however. Ultimately NRC staff need to reach conclusions about site hydrologic characteristics and the magnitude of water-related hazards and environmental impacts that directly support regulatory decisions about facility safety and environmental acceptability. These conclusions often require the estimation of some quantitative measure of future site behavior, for example, a flood elevation after plant construction. These estimates may be based in part on the results of modeling. This type of model use - to make predictions about the future state of a hydrologic system - is not without controversy (e.g., Pilkey and Pilkey-Jarvis 2007). It is nonetheless generally viewed as a central component of estimating the future effects of regulatory decisions (National Research Council 2007). To improve the defensibility of decisions informed by the results of predictive modeling, it is important to be transparent in describing the development of the model and explicit in communicating the uncertainties in model results (National Research Council 2007, 2012). This viewpoint is consistent with NRC policy in the sense that risk-informed decisions require some understanding of uncertainty, which includes the uncertainty of model results used as the partial basis for those decisions.

This report discusses the analysis of uncertainty in hydrologic modeling used in the review of applications for new nuclear commercial power reactors. Although the examples provided in the report are for groundwater modeling, the methods and principles discussed are applicable to other hydrologic models as well.

Chapter 2 of the report describes the types of hydrologic models used in new reactor reviews and the role of modeling in the regulatory process. The current review guidance emphasizes a conservative approach to modeling. The limitations of this approach are discussed and a simple groundwater transport modeling example is provided to illustrate how uncertainty concepts can be used to inform regulatory decisions. Chapter 3 describes an uncertainty analysis methodology that can be used to estimate the joint impact of parameter, conceptual model, and scenario uncertainties. The practical implementation of this methodology is also described, including a discussion of the capabilities and limitations of applicable software tools. Chapter 4 contains an example application of the uncertainty methodology as it might be used in reviewing groundwater site characteristics conducted as part of a safety evaluation for a new power reactor. The example uses publically available information from the Bellefonte Nuclear Station Units 3 and 4 Combined License application. A detailed description of model development is included to illustrate typical modeling decisions that arise in actual reviews. The utility and limitations of the software for modeling and uncertainty analysis are discussed throughout the example. Concluding remarks and observations are provided in the final chapter of the report.

2 MODEL USE IN NEW REACTOR REVIEWS

2.1 Use of Hydrologic Models in Nuclear Power Plant Evaluations

Hydrologic models are used to support NRC staff reviews of nuclear power plant applications in the evaluation of both safety and environmental impacts. For the evaluation of hydrologic site characteristics related to safety under Section 2.4 of the Standard Review Plan (SRP) (NRC 2007), models are often used as part of the determination of flood elevations. Applications of models may include determining watershed response to extreme precipitation events, site drainage in response to locally intense precipitation, and surge or wave runup due to events such as hurricanes and tsunamis. Groundwater flow and transport models are also likely to be used under SRP Section 2.4 reviews to evaluate the maximum post-construction groundwater elevations on site, to identify and characterize potential transport pathways, and estimate the effects of an accidental release of radioactive liquid effluents.

Hydrologic models may also be used in the review of a nuclear power plant application for the evaluation of environmental effects as part of the production of an environmental impact statement. For example, models are used to evaluate the impact of plant water use on downstream water users and to assess the impact of plant discharge on water quality. Similarly, groundwater flow models have been used to evaluate the impacts of plant groundwater use on nearby wetlands, on flow in streams on or near the site, and on off-site users of groundwater.

There are also other NRC regulatory actions that may use hydrologic models for similar purposes. Models of groundwater flow and transport may be used to evaluate the safety and environmental impacts of a proposed *in situ* uranium recovery operation, for example by determining the role of low permeability units and structural faults in controlling flow. Hydrologic models may also be used in evaluating potential doses resulting from the disposal of radioactive waste and in the decommissioning of licensed facilities.

2.2 What is the Role of a Model?

Models of hydrologic systems are generally used for two purposes. The first of these is to develop and demonstrate an understanding of the hydrologic behavior of the site. To serve this purpose, the model integrates the conceptual understanding of the site (e.g., the geologic structure and the active flow and transport processes), observations of site properties and behavior (e.g., hydraulic conductivity and head), and the forces acting on the system (e.g., precipitation). The model is typically used in this context by comparing model results to observations. Inability of the model to reproduce observed conditions indicates a flaw in the model, which can be explored by reevaluating assumptions and exploring the sensitivity of model outputs to the model structure, parameterization, and boundary conditions. This analysis may also suggest where additional data would be useful in improving the understanding of the site. Sensitivity analyses can also be used to evaluate the potential impact of design and operational changes on site hydrology.

The second purpose for which models are generally used is as a means to make predictions about future hydrologic conditions. In this context, the output of a model is compared to a quantitative design requirement or regulatory criterion. For example, a flood prediction is compared to the design basis flood elevation, maximum groundwater levels are compared to the design basis groundwater elevation, and predicted concentration from the accidental release of radioactive liquid effluents are compared to the concentration limits identified in 10 CFR 20, Appendix B. While the models generating these predictions can be based on prior knowledge of

the hydrologic system and site-specific observations, the predictions are made under post-construction conditions that can be substantially different than those used to develop the models. To compensate for the resulting uncertainties and to ensure some margin of safety, the models are typically based on conservative assumptions.

2.3 Typical Groundwater Modeling Experience

As a practical matter, hydrologic models are not an end in themselves, but are usually part of a larger project. This is certainly the case for a nuclear power plant application. Because of this, the way in which hydrologic models are developed and used by an applicant is constrained by budget and schedule factors that may be beyond the control of those responsible for the hydrologic analysis. This has implications for the review of modeling carried out by NRC staff as part of the safety and environmental evaluations.

Bredehoeft (2010) recently described a typical “recipe” for groundwater model development and use, consisting of the following steps.

- Collect all available data.
- Create cross-sections and isopach maps.
- Decide the information is insufficient.
- Drill more wells.
- Build a groundwater model.
- Run the model. Discover that it is sensitive to data that was not collected, or that the concept of the system is in error.
- Out of money/time. “Further work is indicated.”

The primary flaw in this approach as identified by Bredehoeft (2010) is that the conceptualization is not tested (by running the groundwater model) until the end of the process, leaving little or no opportunity for (1) the modeling to influence data collection, and (2) the conceptualization and groundwater model to be modified.

It is instructive to compare the “recipe” described by Bredehoeft (2010) to the typical experience of groundwater modeling associated with new reactor applications. From the perspective of reviewers following procedures in SRP 2.4.12 as part of a safety evaluation, the typical experience can be described as follows.

- The Final Safety Analysis Report (FSAR) and supporting documents contain all the data that will be available for the review.
- The FSAR describes a single groundwater conceptualization.
- Analysis of post-construction conditions is initially not supported by modeling or is supported with a simple model with minimal discussion of limitations and uncertainty.
- One or more rounds of additional requests are required to obtain sufficient information on alternative groundwater conceptualizations, assumptions, and uncertainties.
- Schedules are often impacted by repeated requests for additional information.

From the perspective of the model developer (supporting applicants), Findikakis and Waterman (2010) described a typical situation as follows.

- Development of a groundwater model occurs after data collection.
- Different project teams are responsible for data collection and modeling.
- Data are collected to satisfy geotechnical needs and minimum site characterization requirements, not groundwater modeling needs.

- Drilling and well development techniques may be inappropriate for aquifer characterization methods.

Model developers supporting an applicant and application reviewers thus share a common experience that reflects the flaws identified by Bredehoeft (2010). Typically, all the data are collected prior to model development. As a result there is little (or no) opportunity for the modeling to influence data collection and there are significant constraints on the ability to evaluate the model and improve it when model limitations/errors become apparent. Findikakis and Waterman (2010) stated that this situation leads to relaxation of calibration criteria (i.e., accepting a larger error in the calibration) and a greater need for sensitivity analyses and consideration of alternative conceptualizations to adequately address uncertainties.

The experience described above suggests that the groundwater modeling process associated with new reactor applications could be improved. Because the process of model development as part of the FSAR preparation and the review of that modeling as part of the safety evaluation are performed sequentially with limited opportunities for feedback, it is important that the NRC staff's review plans and regulatory guidance are explicit about modeling expectations, including the role of uncertainty assessment. These expectations should be consistent with established standards such as ANSI/ANS-2.17-2010 (ANS 2010) and accepted procedures such as the guidelines for effective modeling discussed in Hill and Tiedeman (2007). Each of these referenced documents contains a detailed discussion of uncertainty in the context of groundwater modeling.

2.4 Limitations of the Current Approach

The NRC has a policy to include risk information in the review process. But what does “risk-informed” mean in the context of hydrologic analyses for new reactor safety evaluations? The current review criteria and technical procedures contained in the hydrology section of the SRP (NRC 2007) describe a predominantly deterministic approach that emphasizes conservatism in the analysis. There are, in fact, no explicit probability or risk concepts identified. For example, the flooding evaluation refers to probable maximum precipitation, flood, hurricane, storm surge, and tsunami. The “probable maximum” concept is a conservative and deterministic construct with a nonzero, but unquantified probability of exceedance.

Groundwater analyses are similarly described in deterministic, conservative terms. For example, the maximum groundwater elevation expected at the site must be determined. Accidental releases of radioactive liquid effluents are determined using the “bounding set of plausible surface and subsurface pathways” and assuming “worst-case contamination.”

Two conditions are required for a conservative approach to be adequate: (1) the acceptance criteria must be satisfied, and (2) the models and technical evaluation methods must be demonstrably conservative. When one of these conditions is not met, a conservative approach is inconclusive, thereby raising additional questions. For example, what is the path forward when the acceptance criteria are not met or when the margin is unacceptably small? This question is of practical importance as the issue has arisen in multiple reviews of new reactor applications, including with respect to storm surge exceeding the design basis flood elevation and locally intense precipitation exceeding the capacity of the site drainage system.

One approach is to relax the conservatism in the evaluation, moving gradually from a demonstrably conservative analysis to a less conservative, but presumably more realistic, analysis. This is sometimes referred to as a hierarchical approach. As an example of this approach, the analysis of the accidental release of radioactive liquid effluents might begin by

assuming purely advective groundwater transport, but introduce dispersion to the transport evaluation if radionuclide concentrations exceed the limits. This will tend to cause the acceptance criteria to be satisfied, but by reducing the conservatism of the analysis, the second condition above may not be satisfied, or at the least the degree of conservatism in the modified approach may need to be addressed.

Another approach when the acceptance criteria are violated or the margin is small is to introduce mitigating features in the facility design. For example, additional flood protection measures could be included, or the plant elevation could be raised. The potential danger in this approach is that it may result in over-design and unnecessary costs.

The second condition required for a conservative approach to be adequate, that the models and technical evaluation methods must be demonstrably conservative, may fail to be satisfied when the model and methods are based on limited data.

This issue is of practical concern as it has been raised during Advisory Committee on Reactor Safety (ACRS) review of a safety evaluation in the context of the analysis of accidental release of radioactive liquid effluents in groundwater. Specifically, the ACRS staff questioned whether selecting minimum measured values of the adsorption coefficients (K_d) could be justified given the observed variability in K_d and the limited number of samples. The specific question from the transcript was,

“These K_d values vary quite a bit. When you ask for the minimum value, then you have to think about whether the sample is big enough for the minimum to be reasonable. If you have two values, taking the lower one is not very sensible. If you have 100 values, taking the minimum is probably excessive. So do they have enough samples in order for taking the minimum to be a meaningful thing to do?” (NRC 2009, p. 138).

The question indicates not only a concern that the method for selecting a model parameter (using the extreme observation as the parameter value) could be nonconservative when data are limited, but also a concern that the method could be overly conservative when data are abundant.

Another situation in which the conservatism of a model may be questioned is when a model is used for predictions under unobserved conditions. For example, a groundwater model that is developed using data for current site conditions, may be used to predict groundwater elevations and transport pathways under post-construction conditions. This issue has also been raised by the ACRS in reviewing draft interim staff guidance on implementing SRP Section 2.4.12,

“You characterize the site before, let’s say, presubstantial construction. Now you have a predictive model which takes into account the effective construction...How do you know at the end that your predictive model is right?” (NRC 2010, p. 47).

While the concern in the question may have been whether a model remains accurate in predicting post-construction conditions, a “right” model could also be one that remains conservative.

2.5 Conservative Models or Conservative Decisions?

A focus on conservative models, i.e., bounding assumptions and extreme parameter values, can lead to an exaggeration of uncertainties (in the sense of relying on overly conservative results) and often implies a failure to realistically quantify uncertainties. This approach is not

risk-informed. In contrast, a focus on conservative decisions implies that uncertainties in model outcomes can be properly accounted for; the conservatism in this case enters when comparing model outcomes to regulatory or design requirements. For example, a decision based on the 95th percentile outcome is more conservative than one based on the mean outcome. Similarly, tolerating a failure probability of one per thousand is more conservative than accepting a one percent failure rate. Focusing on a conservative decision thus is consistent with a risk-informed approach. In addition, it allows for the natural consideration of consequences (e.g., the safety consequences of exceeding a design flood elevation).

The following section describes the application of a groundwater transport model to illustrate the limitations of the current deterministic approach focused on conservative models and to demonstrate the advantage of a risk-informed approach focused on conservative decisions with a quantitative consideration of uncertainties.

2.6 Groundwater Transport Example

Consider a simple transport model that might be relevant to the review under SRP Section 2.4.13 (NRC 2007) of an accidental release of radionuclide liquid effluents to groundwater. Under a conservative release scenario, liquid effluent containing a radionuclide mixture is assumed to be released from a tank directly to groundwater, with the initial concentration (activity) of any specific radionuclide given by C_0 . Transport is assumed to occur via advection, with radionuclides subject to decay and adsorption. Under these conditions, the concentration at any downgradient location is given by

$$C = C_0 e^{-\lambda t} \quad (1)$$

where λ is the radionuclide-specific decay coefficient and t is the travel time. This concentration can be compared to a radionuclide-specific effluent concentration limit (ECL) from 10 CFR 20 Appendix B, Table 2.

Travel time is given by

$$t = \frac{D\theta}{(K_s \nabla h)} R_f \quad (2)$$

where D is the travel distance, θ is the effective porosity, K_s is the saturated hydraulic conductivity, ∇h is the magnitude of the hydraulic head gradient, and R_f is the retardation factor, defined as

$$R_f = 1 + \frac{\rho_b K_d}{\theta} \quad (3)$$

with ρ_b the bulk density and K_d the adsorption coefficient. This model is conservative in that the only processes affecting transport are advection and adsorption.

Site data available to support the accidental release analysis included measurements of groundwater head (to estimate the gradient), measurements of the physical properties of soil and rock (to estimate the bulk density and porosity), well tests for estimating hydraulic conductivity, and laboratory measurements of adsorption on core samples for estimating adsorption coefficients. Measures of the latter two parameters exhibited significant variability, with a range of [0.08, 2.64] m/d for the 11 K_s estimates and a range of [3.6, 166.4] ml/g for the

K_d estimates (Sr-90 is considered here). Figure 1 contains boxplots of the K_s and K_d estimates, showing the median, interquartile range, limits (excluding outliers), and estimated outliers.

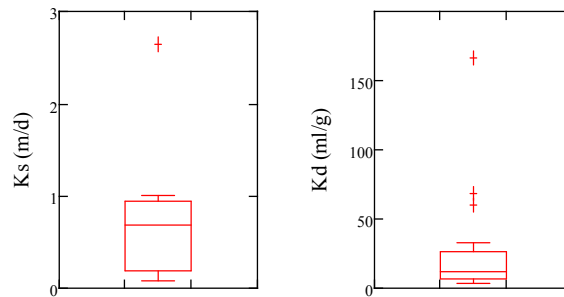


Figure 1. Boxplots of (left) K_s estimates from 11 well tests and (right) Sr-90 K_d estimates from 20 laboratory tests

From the transport perspective, a conservative approach would result in concentration values that are maximized to some extent. For the model of Eq. (1), this corresponds to a minimum travel time, which occurs when using large values of K_s and small values of K_d . The conservative data in this case are the maximum K_s of 2.64 m/d and the minimum K_d of 3.6 ml/g for Sr-90. By assigning these conservative data values to the parameters of Eq. (2), and choosing representative (average) values for the remaining parameters (that exhibit less variability than K_s and K_d), a deterministic, conservative evaluation of the concentration from an accidental release to groundwater was completed. The resulting concentration ratio was

$$C/ECL_{Sr-90} = 3.25$$

As in any conservative analysis in which the result exceeds or is close to the design or regulatory criterion, the question immediately arises: what is the degree of conservatism in this result? In particular, is this value conservative enough? For example, are there sufficient data to substantiate that the most conservative data represent a bounding case? Conversely, is it possible that the analysis is overly conservative? For example, is it unreasonable to characterize a long transport pathway with a minimum K_d value when a broad range of values was observed at the site? These questions can be only partially addressed by carefully examining the assumptions made in deriving the model and determining the parameter values.

In this example the concentration exceeded the regulatory limit defined by the ECL. Given that the result represents some unknown degree of conservatism, how should the analysis proceed? Would it be best to relax some of the conservative model assumptions? For example, dispersion could be included in the transport model. In that case, however, a dispersion coefficient would have to be chosen. As a result, there is a risk that the analysis moves from something that can be defended (e.g., an analysis based on data) to something that is more difficult to defend (e.g., an analysis based on a dispersivity value without data support). Would it be better to relax the assumptions on the parameter values, for example, by assuming that the transport pathway is better represented by a less extreme K_d value? This would require justifying the apparently nonconservative parameter value. Whichever approach is taken, the question still remains - what is the degree of conservatism in the analysis? The fundamental issue is that this question cannot be adequately addressed without some examination of uncertainty in the transport analysis.

2.6.1 A Simple Uncertainty Evaluation

To illustrate how consideration of uncertainties can, with relatively little effort, provide useful information on the degree of conservatism in the transport evaluation, the conservative model of Eq. (1) was combined with an assessment of the uncertainties in the model parameters. Estimates of the probability distributions of the parameters were based on an analysis of the data. K_s and K_d were best fit with lognormal distributions; the parameters of the distributions were estimated from the sample mean and variance of the data sets. The hydraulic gradient and porosity were assumed to follow normal distributions with standard deviations equal to ten percent of the mean values. In the absence of any information to the contrary, the parameters were assumed to be uncorrelated with one another.

Five-hundred random realizations of the parameters were generated based on the data analysis. The resulting parameter probability distributions for K_s and K_d are shown in Figure 2 along with the sample distributions for the measured data. Additional analyses could be completed, such as nonparametric tests for the assumption of lognormality in the parameters and application of a Bayesian method to include uncertainties in the estimated moments of the parameter probability distributions. For this example, parameter distributions were considered reasonable given the qualitative comparison of Figure 2 and the conservative assumptions of the transport model.

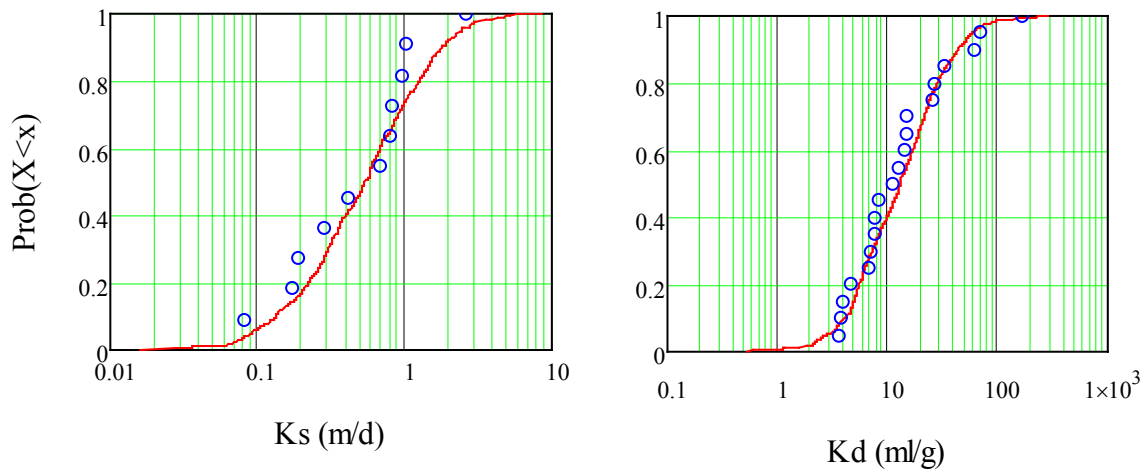


Figure 2. Parameter distributions based on data analysis (solid line) and sample distributions (symbols) for (left) K_s and (right) K_d parameters

Travel time was computed using Eq. (2) for each of the 500 random realizations of parameter values. The resulting distribution of travel time (in years) is shown in Figure 3 for each of the random parameters used in the calculation. As illustrated in the apparent relationships (or lack thereof) between travel time and the parameter values, the relatively small coefficient of variation of the hydraulic head gradient and effective porosity result in the domination of travel time variability by the hydraulic conductivity and the retardation coefficient. This has some implications for site characterization. Although travel time is sensitive to the gradient and the porosity, additional data characterizing these parameters would be expected to have little impact on the distribution of travel time.

The distribution of travel time is highly skewed (note the use of a log scale in Figure 3), with a minimum travel time of 13.2 years, a median of 882 years, and a geometric mean travel time of 857 years. In this simulation, the minimum travel time did not occur at either the maximum hydraulic conductivity or the minimum adsorption coefficient. The extreme parameter values were unlikely to occur in the same realization because the parameters were assumed to be uncorrelated.

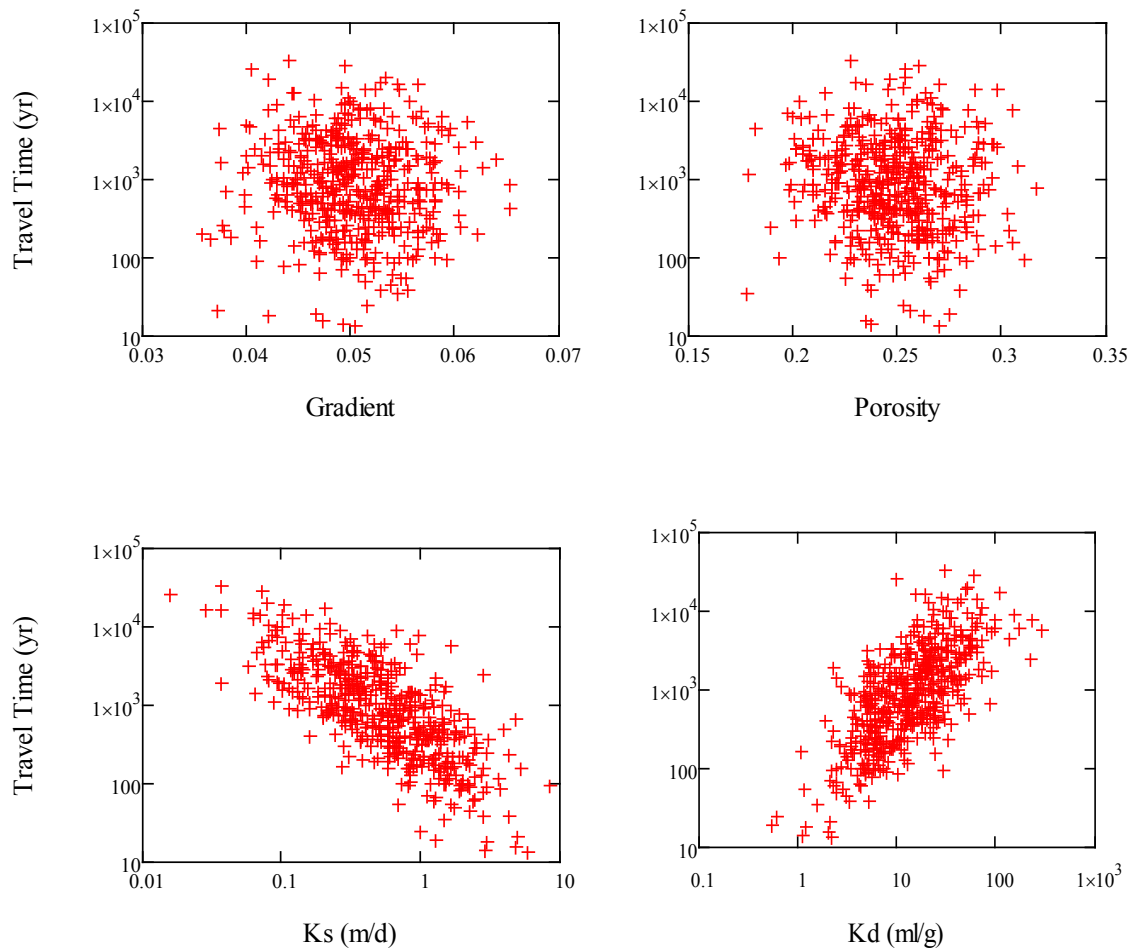


Figure 3. Travel time results for the 500 random parameter realizations

The distribution of travel times results in a distribution of concentration values (or C/ECL concentration ratios) when applied to Eq. (1). The concentration ratio distribution is shown in Figure 4 as a complementary cumulative distribution function for those C/ECL ratios greater than about 0.03. This figure shows the probability of exceeding a given concentration ratio; only the probabilities for the largest ratios are shown as these would be of most concern in a safety evaluation.

As discussed above, the maximum observed K_s value and the minimum observed K_d value resulted in a concentration ratio of 3.25, which falls at the 98th percentile of the distribution of Figure 4. That is, there is an estimated two percent probability that the concentration ratio will be larger than 3.25.

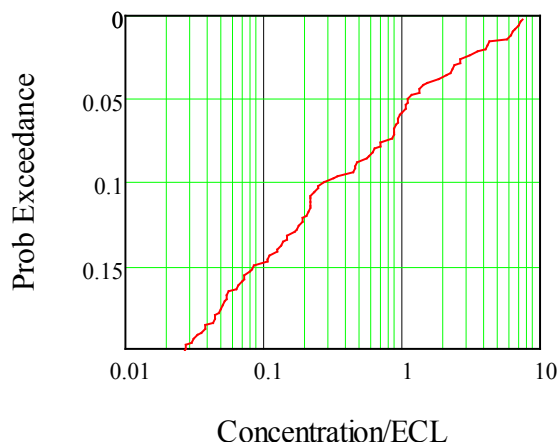


Figure 4. Probability of exceedance for the concentration ratio

From the measurements and fitted parameter distributions shown in Figure 2, the most conservative measured K_s and K_d values (2.64 m/d and 3.6 ml/g, respectively) correspond to the 96th and 8th percentiles. That is, there is a 4% (for K_s) and 8% (for K_d) probability of values leading to worse outcomes – higher concentrations. These probabilities are less conservative than the outcome from using the most conservative measured parameters in the transport model, which resulted in a 2% chance of a worse outcome as described above.

There are a number of factors that could affect these results. Parameter correlations would modify the way in which conservative parameter values combine to produce outcomes with a comparable, or greater, degree of conservatism. In this example, a negative correlation between K_s and K_d would result in more comparable values. In addition, the example results were based on a fit to the sampling distributions, which represent the population of parameter values. This reflects a judgment that the bulk of transport is most likely to occur along high-velocity, low-reactivity pathways. In some cases, it may be more justifiable to use distributions representing the probability density of the mean values, reflecting a judgment that the outcome is more responsive to average conditions.

Irrespective of the particular assumptions or methods used in conducting the analysis, however, the explicit modeling of parameter uncertainty provides a quantitative estimate of how these uncertainties affect the outcome of interest. This information can be used to estimate the degree of conservatism in the decision, given the assumptions inherent in the model (a conservative transport model in the example) and what is known about the site (measurements of the site groundwater flow and transport characteristics in the example). This focus on the outcome is appropriate. As seen in the example, a focus on the degree of conservatism in the model parameters can lead to an overly conservative outcome.

The consideration of the degree of conservatism contributes to a risk-informed analysis. Consistent values of the degree of conservatism can be used as a matter of policy. As shown in Figure 4, for example, the concentration ratio corresponding to a 5% probability of exceedance (the 95th percentile) is 1.09. The ratio corresponding to a 10% probability of exceedance (the 90th percentile) is 0.25. One of these values may be appropriate for use in a safety evaluation. Given a mixture of radionuclides, each with its own travel time distribution, the probability of exceedance for the entire mixture could be easily computed, from which the probability of exceeding a concentration ratio of 1.0 is easily determined. This result could be evaluated for acceptability with due consideration of an acceptable degree of conservatism.

The example discussed here was for an accidental release of radioactive liquid effluents in groundwater, but the concepts apply to other hydrologic analyses and outcomes. For example, the probability of exceeding the design basis flood level or groundwater elevation could be similarly addressed in the safety evaluation. Ultimately, probabilistic outcomes and consequences could be combined to include hydrology in a probabilistic risk assessment (PRA). For flood analyses, including uncertainty in the probability distribution used to represent flood frequencies is likely to be important. This is analogous to including uncertainty in the distributions of Figure 2 from the groundwater transport example.

3 UNCERTAINTY METHODOLOGY AND SOFTWARE

The previous section illustrated the potential benefits of a relatively simple consideration of uncertainty in the application of a groundwater transport model. A more general methodology for uncertainty evaluation has the following desirable characteristics.

- Comprehensive: it should consider many sources of uncertainty while providing a means to focus on those of most relevance.
- Quantitative: it should be possible to compare results with regulatory criteria or design requirements.
- Systematic: it should be applicable to a wide range of sites and objectives and enable the common application of computer codes and methods.
- Practical: it should allow for the use of a simple approach first and it should use existing software tools when possible.

Meyer et al. (2007) described an uncertainty evaluation methodology that exhibited the first three characteristics. In this report we demonstrate that the methodology is also practical for application to groundwater modeling for environmental and safety evaluations associated with nuclear power plant licensing. This is accomplished by illustrating some simplifications in the methodology and describing the capabilities of available software that can be helpful in implementing certain aspects of the methodology.

The framework in which hydrogeologic models are applied to nuclear power plant evaluations is illustrated in Figure 5. Site characterization and data gathering provide information in the history-matching period that can be used to develop and evaluate models. While some historical data may be applicable, it is not uncommon for site-specific measurements of hydrologic behavior (such as groundwater heads) to cover a period of time as short as one year, as indicated in the figure. Uncertainty is assessed in the history-matching period based on a combination of expert judgment and a quantitative measure of the ability of the model to reproduce observations. Many of these uncertainties can be reduced to some extent by collecting additional data, but as noted previously this is not always a practical option.

Models are applied in the predictive period to evaluate site behavior under post-construction conditions with regard to regulatory requirements and design criteria. Models used in the predictive period are derived from the models developed in the history-matching period, but may have significant differences. For example, history matching is conducted under pre-construction conditions, but estimates of maximum groundwater head are required under post-construction conditions. Construction of a nuclear power plant will substantially modify local conditions, likely including site topography, recharge, and subsurface materials.

The modifications may affect site groundwater heads and transport pathways. The predictive period generally extends over the regulatory period of the facility, potentially up to 80 years for a nuclear power plant. The predictive period may be longer if this is required to capture important temporal effects: for example, the impact of plant operations on downstream water use under variable climatic conditions.

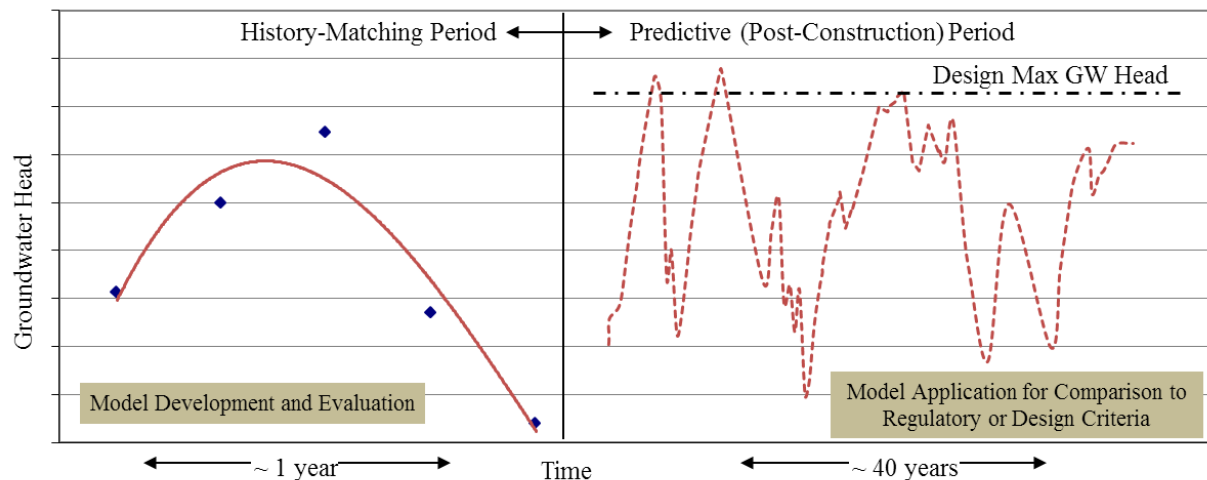


Figure 5. Framework for application of hydrogeologic models. The relatively short history-matching period involves comparison between observations (points) and model simulated equivalents (solid line). The much longer predictive period involves comparison between model simulation results and regulatory or design criteria (e.g., a design maximum groundwater head).

The uncertainties determined in the history-matching period are propagated into the predictive period with the addition of uncertainties that apply only in the predictive period (for example, uncertainties in the properties of the fill materials used in construction). Because the predictive period characterizes unobservable future conditions, some of these uncertainties are irreducible characteristics of the system being modeled (for example, recharge with modified surface conditions and subsurface materials).

The uncertainties addressed by Meyer et al. (2007) fell into three categories.

Conceptual model uncertainty. As described by Neuman and Wierenga (2003), the conceptual model is a hypothesis about the behavior of the system being modeled and the relationships between the components of the system. It is typically represented mathematically to render quantitative predictions (conceptual-mathematical model). Uncertainties in the conceptual model are generally assessed in the history-matching period and applied in the predictive period. However, there may be unique features of the predictive model that introduce additional uncertainties to the predictive period conceptualization.

Parameter uncertainty. Parameters are quantities required to obtain a solution from the mathematical model and are thus model-specific. They generally represent a characteristic of the site (such as the saturated hydraulic conductivity), but may be only indirectly related to measurements of those characteristics due to differences between the scale of measurements and the scale represented by parameters, and due to the potential dependence of parameter values on model assumptions. Parameter uncertainties are generally assessed in the history-matching period and applied in the predictive period. However, there may be additional uncertainties that only apply to parameters of the predictive model.

Scenario uncertainty. A scenario is a future state or condition assumed for a system that affects the hydrology (e.g., post-construction changes in surface topography, recharge, and ground-water extraction). These types of uncertainties apply only to the predictive period.

3.1 Uncertainty Methodology Incorporating Parameter, Model, and Scenario Uncertainties

This section summarizes a method, described fully in Meyer et al. (2007), to provide an optimal way of assessing predictive uncertainty with consideration of parameter, conceptual model, and scenario uncertainties. This method relies on the specification of a set of alternative models and scenarios and weights the alternative model results by a measure of the model probabilities and the alternative scenarios by a measure of the scenario probabilities. The method closely follows the description of Draper (1995).

The contribution of parameter uncertainty to a model-predicted output, Δ , can be written as

$$p(\Delta|M_k, \mathbf{D}, S_i) = \int p(\Delta|M_k, \mathbf{D}, S_i, \boldsymbol{\theta}_k) p(\boldsymbol{\theta}_k|M_k, \mathbf{D}, S_i) d\boldsymbol{\theta}_k \quad (4)$$

where $p(\Delta|M_k, \mathbf{D}, S_i)$ is the probability density function of Δ conditioned on a specific model, M_k , a set of measurements of system behavior (e.g., hydraulic head), \mathbf{D} , and a specific scenario, S_i . The model is characterized by a set of uncertain parameters, $\boldsymbol{\theta}_k$, with a distribution of $p(\boldsymbol{\theta}_k|M_k, \mathbf{D}, S_i)$.

Referring to the modeling framework of Figure 5, Δ , M_k , $\boldsymbol{\theta}_k$, and S_i apply in the predictive period. The data, \mathbf{D} , are obtained from the history-matching period. M_k is possibly modified from a corresponding model in the history-matching period, M'_k , whose parameters, $\boldsymbol{\theta}'_k$, are contained in $\boldsymbol{\theta}_k$. Δ is conditioned on \mathbf{D} because M'_k and $\boldsymbol{\theta}'_k$ are conditioned on \mathbf{D} in the history-matching period.

Model uncertainty is included by postulating a set of K alternative models that represent conceptual and structural uncertainties, and then calculating the weighted average of the models' predictions of Δ from Eq. (4). In doing so, each model must be capable of predicting the same output, Δ , and each model's parameter set, $\boldsymbol{\theta}_k$, in Eq. (4) must be conditioned (through history matching) on the same data set, \mathbf{D} . The weighted average prediction is written as

$$p(\Delta|\mathbf{D}, S_i) = \sum_{k=1}^K p(\Delta|M_k, \mathbf{D}, S_i) p(M_k|\mathbf{D}, S_i) \quad (5)$$

where the weights, $p(M_k|\mathbf{D}, S_i)$, are the posterior probabilities of each model k conditioned on the data and the scenario.

Scenario uncertainty is included in a similar manner by postulating a set of I alternative scenarios and calculating a weighted average of the predicted output.

$$p(\Delta|\mathbf{D}) = \sum_{i=1}^I p(\Delta|\mathbf{D}, S_i) p(S_i) \quad (6)$$

Here the weights are prior scenario probabilities; they are not conditioned on the data because they represent a primarily subjective judgment regarding the likelihood of the specific scenario's conditions occurring in the future (Meyer et al. 2007).

The posterior model probabilities of the history-matching models are calculated using Bayes' theorem.

$$p(M'_k | \mathbf{D}, S_i) = \frac{p(\mathbf{D} | M'_k) p(M'_k | S_i)}{\sum_{l=1}^K p(\mathbf{D} | M'_l) p(M'_l | S_i)} \quad (7)$$

where $p(M'_k | S_i)$ is the subjective, prior model probability for model M'_k (for a given scenario S_i) and $p(\mathbf{D} | M'_k)$ is the model likelihood for M'_k (which is independent of the scenario as explained in Meyer et al. [2007]). The posterior model probabilities of the predictive models, $p(M_k | \mathbf{D}, S_i)$ in (5), are then assumed to be equivalent to the corresponding values in (7),

$$p(M_k | \mathbf{D}, S_i) = p(M'_k | \mathbf{D}, S_i). \quad (8)$$

When Eqs. (7) and (8) are applied to Eq. (4), the resulting method is called Bayesian Model Averaging (Draper 1995; Hoeting et al. 1999).

The calculations involved in Eqs. (4) to (7) were simplified for this report. First, Eq. (4) is approximated as

$$p(\Delta | M_k, \mathbf{D}, S_i) \approx p(\Delta | M_k, \mathbf{D}, S_i, \hat{\boldsymbol{\theta}}_k) \quad (9)$$

where $\hat{\boldsymbol{\theta}}_k$ is an estimate of $\boldsymbol{\theta}_k$ and can be written as

$$\hat{\boldsymbol{\theta}}_k = \begin{pmatrix} \hat{\boldsymbol{\theta}}'_k \\ \hat{\boldsymbol{\theta}}^+_k \end{pmatrix}. \quad (10)$$

Here $\hat{\boldsymbol{\theta}}'_k$ is the least squares estimate of $\boldsymbol{\theta}'_k$ (the parameters of the history-matching model M'_k) and $\hat{\boldsymbol{\theta}}^+_k$ is the prior estimate of any additional parameters applying only to the predictive period model M_k . Second, instead of calculating complete probability distributions, results were obtained only for the mean and variance of the predicted value. Given Eq. (9), for an individual model, the estimated moments are

$$E(\Delta | M_k, \mathbf{D}, S_i) = \Delta|_{\hat{\boldsymbol{\theta}}_k} \quad (11)$$

$$Var[\Delta | M_k, \mathbf{D}, S_i] = \left(\frac{\partial \Delta}{\partial \boldsymbol{\theta}_k} \right)^T \Sigma_k^{LS} \left(\frac{\partial \Delta}{\partial \boldsymbol{\theta}_k} \right) \quad (12)$$

(see Hill and Tiedeman 2007). The mean predicted value is the prediction evaluated at $\hat{\boldsymbol{\theta}}_k$. The variance is estimated from prediction sensitivities $\left(\frac{\partial \Delta}{\partial \boldsymbol{\theta}_k} \right)$ evaluated at $\hat{\boldsymbol{\theta}}_k$ and the parameter covariance matrix

$$\boldsymbol{\Sigma}_k^{LS} = \begin{bmatrix} \boldsymbol{\Sigma}_k'^{LS} & 0 \\ 0 & \boldsymbol{\Sigma}_k^{+LS} \end{bmatrix}. \quad (13)$$

Here

$$\boldsymbol{\Sigma}_k'^{LS} = \hat{\sigma}_{LS}^2 (\mathbf{J}_k^T \boldsymbol{\omega} \mathbf{J}_k)^{-1} \quad (14)$$

is the parameter covariance matrix from the regression used to estimate the parameters of the

history-matching model, $\hat{\sigma}_{LS}^2 = \frac{\mathbf{e}^T \boldsymbol{\omega} \mathbf{e}}{N_z - P_k} \Big|_{\boldsymbol{\theta}_k = \hat{\boldsymbol{\theta}}_k}$ is the least squares estimate of the calculated error

variance, $\mathbf{e}^T \boldsymbol{\omega} \mathbf{e}$ is the sum of squared weighted residuals (SSWR) from the regression (\mathbf{e} being the vector of residuals and $\boldsymbol{\omega}$ being the weight matrix), N_z is the number of data in \mathbf{D} , P_k is the

number of estimated hydrologic parameters in $\boldsymbol{\theta}'_k$, and \mathbf{J}_k is the Jacobian, or sensitivity, matrix

from the regression as evaluated at $\hat{\boldsymbol{\theta}}_k$. $\boldsymbol{\Sigma}_k^{+LS}$ in Eq. (13) is the prior covariance for the additional parameters of the predictive model, $\boldsymbol{\theta}_k^+$.

The first two moments of Eq. (5) are given by

$$E[\Delta | \mathbf{D}, S_i] = \sum_{k=1}^K E[\Delta | \mathbf{D}, M_k, S_i] p(M_k | \mathbf{D}, S_i) \quad (15)$$

$$\begin{aligned} Var[\Delta | \mathbf{D}, S_i] &= \sum_{k=1}^K Var[\Delta | \mathbf{D}, M_k, S_i] p(M_k | \mathbf{D}, S_i) \\ &+ \sum_{k=1}^K (E[\Delta | \mathbf{D}, M_k, S_i] - E[\Delta | \mathbf{D}, S_i])^2 p(M_k | \mathbf{D}, S_i) \end{aligned} \quad (16)$$

while the moments of Eq. (6) are given by

$$E(\Delta | \mathbf{D}) = \sum_{i=1}^I E(\Delta | \mathbf{D}, S_i) p(S_i) \quad (17)$$

$$\begin{aligned} Var(\Delta | \mathbf{D}) &= \sum_{i=1}^I Var(\Delta | \mathbf{D}, S_i) p(S_i) \\ &+ \sum_{i=1}^I [E(\Delta | \mathbf{D}, S_i) - E(\Delta | \mathbf{D})]^2 p(S_i). \end{aligned} \quad (18)$$

Calculations are also simplified by estimating the model likelihoods in Eq. (7) using

$$p(\mathbf{D} | M'_k) = \exp\left(-\frac{1}{2} IC_k\right) \quad (19)$$

where IC_k is one of a number of model selection criteria that have been proposed and evaluated for use in hydrologic analyses (Neuman 2003; Ye et al. 2004; Poeter and Anderson 2005; Tsai and Li 2008; Ye et al. 2008, Singh et al. 2010). For this report, two model selection criteria were used,

$$AICc_k = N_z \ln \hat{\sigma}_{ML}^2 + 2P_k + \frac{2N_k(N_k + 1)}{N_z - N_k - 1} \quad (20)$$

$$KIC_k = N_z \ln \hat{\sigma}_{ML}^2 - 2 \ln p(\hat{\theta}'_k) - P_k \ln 2\pi - \ln |\Sigma_k'^{ML}| \quad (21)$$

as presented in Ye et al. (2008). Here, $N_k = P_k + 1$, $\hat{\sigma}_{ML}^2 = \frac{N_z - P_k}{N_z} \hat{\sigma}_{LS}^2$ is the maximum likelihood estimate of the calculated error variance, $p(\hat{\theta}'_k)$ is the prior parameter probability density evaluated at $\hat{\theta}'_k$, and $\Sigma_k'^{ML} = \frac{N_z - P_k}{N_z} \Sigma_k'^{LS}$ is the maximum likelihood parameter covariance matrix.

In computing the model likelihoods and model probabilities using Eqs. (19) and (7), only one of the model selection criteria in Eqs. (20) and (21) should be used. The absolute values of the criteria are not meaningful; it is only the differences between values that are important. Because of the exponential form of Eq. (19), two alternative models with a difference in AICc (or KIC) values of more than six or seven implies dominance of one model over the other (i.e., the probability of the less likely model will be a small fraction of the high likelihood model).

3.2 Implementation of the Uncertainty Methodology

To implement the uncertainty methodology described above requires two basic activities: model development and parameter estimation/uncertainty calculation.

Model development. Two or more alternative models must be developed, that together represent the unresolved conceptual and structural uncertainties associated with the representation of the site. Model development in the context of the uncertainty methodology described above involves the following.

- Each model must describe hydrologic conditions in the history matching period and must be capable of simulating the observations used in the parameter estimation.
- Each model, possibly with modification, must be capable of representing the predictive period and must be capable of simulating the desired predictive outputs.
- Each model, possibly with modification, must be capable of representing each alternative scenario.
- A common dataset of observations from the history-matching period must be used for parameter estimation. Errors in these observations must be characterized by a (possibly diagonal) covariance matrix, which is used to determine weights for the parameter estimation.
- Prior model and scenario probabilities (possibly uniform) must be specified, usually based on expert judgment.
- If prior parameter estimates are used, the prior distributions for these estimates must be specified.

Parameter estimation & uncertainty calculation. Following model development and specification of scenarios, the following calculations are required to implement the uncertainty methodology.

- Parameter estimates for the history-matching models are calculated for Eq. (9) using weighted, least squares regression and parameter uncertainties are calculated using Eq. (14).
- Regression results for each model are used in Eq. (19) and (20) or (21) to calculate model likelihoods. Model probabilities are calculated from Eq. (7) using the model likelihoods (and

prior model probabilities) from the set of alternative models characterizing the history-matching period.

- Predictive period models are used to calculate predictive values and uncertainties from Eqs. (11) and (12). The latter involves calculation of prediction sensitivities.
- Model- and scenario-averaged predictions and prediction uncertainties are calculated using Eqs. (15) to (18).

3.2.1 Software Tools

This section primarily discusses software tools that were used in the application described in the following chapter; this section is not intended to be a review of available software. Failure to describe any particular software tool here does not imply a judgment about its applicability or usefulness.

Model development is site-specific and labor-intensive, requiring the interjection of experience and subjective decisions at many points in the process. This makes it difficult to apply standards or generalizable procedures, although some guidance does exist (e.g., ANS 2010; ASTM 2008; ASTM 2010). As discussed previously, for best results model development should be integrated with site characterization. However, specific tools or methods to complete this integration (e.g., to determine what additional data would be most valuable) are not discussed here.

Model development typically is based on a set of diverse data obtained during site characterization and monitoring. In addition, modeling and other analyses can generate substantial amounts of data. Management of this data involves documentation of sampling and analysis methods, data quality, and data uncertainties. With respect to a nuclear power plant application, data management is primarily the responsibility of the applicant. To clearly document the technical basis for their conclusions, however, reviewers should carefully manage any data used or generated in the application review. Spreadsheet software¹ was the primary data management tool used in the application described in the following chapter.

Conceptual model development typically involves preparation of figures to aid in interpretation of data (e.g., stratigraphic fence diagrams based on borehole data, time series of groundwater head measurements, etc.) and data analysis to derive parameter estimates (e.g., saturated hydraulic conductivity estimates from pump or slug test data) and to characterize uncertainties. Again, documentation of the conceptual model is primarily the responsibility of the applicant. For the application described here, some multipurpose software was used in developing the conceptual model (spreadsheet and Mathcad²), as was the specialized modeling software, Groundwater Modeling System (GMS³). Global Mapper (GM 2005) was used to prepare spatial GIS data for use in GMS. The Corpscon utility (USACE 2004) was used to convert point data from one coordinate system to another, also for use in GMS.

The conceptual model serves as the basis for a mathematical/numerical model. Implementation of a numerical model requires specification of boundaries, spatial and temporal discretization, parameter values, and initial conditions, among other activities. GMS was used as the principal tool to translate the conceptual model into a numerical model. GMS was also used as the

¹ Excel 2007/2010, ©2006/2010 Microsoft Corporation, Redmond, Washington.

² Mathcad v. 15.0, ©2010 Parametric Technology Corporation, Needham, Massachusetts.

³ GMS v. 7.1.10, ©2012 Aquaveo LLC, Provo, Utah.

primary user interface to the model codes, several of which were used in the application: MODFLOW-2000 (Harbaugh et al. 2000; McDonald and Harbaugh 1988) for groundwater flow, MODPATH (Pollock 1994) to evaluate pathways, and MT3DMS (Zheng and Wang 1999; Zheng et al. 2001; Zheng 2006) for groundwater transport.

Model development also includes a process of model evaluation whereby the characteristics of the model (e.g., model assumptions, discretization, boundary conditions, etc.) are evaluated and modified to better represent what is known about the site and to eliminate or reduce model errors (e.g., mass balance errors, unrealistic heads, etc.). Model evaluation was primarily carried out within the GMS software.

Parameter estimation and uncertainty calculation are more amenable than model development to the application of generalizable procedures. Nonetheless, there are many subjective considerations that arise in their implementation, as discussed in the guidelines of Hill and Tiedeman (2007). Parameter estimation and uncertainty calculations can also be computationally demanding, which sometimes generates a tension between completing these tasks and increasing the complexity of a model.

A number of software tools were used in the application described in the following chapter to carry out parameter estimation and uncertainty calculations. Both PEST (Doherty 2004) and UCODE (Poeter et al. 2005) were used to estimate parameters and parameter uncertainties (as linear confidence intervals and parameter covariances). These codes also provide the model selection criteria values, although for reasons explained in Appendix A, these values were computed separately using a spreadsheet.

Predictive uncertainties were evaluated using utility software associated with PEST and UCODE. As described in Doherty (2010) a variety of utilities are distributed with PEST that implement the predictive error methods of Moore and Doherty (2005). For the application here, the utility “predunc6” was used. For UCODE, the LINEAR_UNCERTAINTY companion code (Poeter et al. 2005) was used to compute predictive uncertainty.

Poeter and Hill (2007) document MMA, a code that uses output produced by UCODE and LINEAR_UNCERTAINTY to compute model probabilities and model-averaged predicted values. Because MMA does not directly read PEST output, and for reasons related to the computation of model selection criteria (see Appendix A), model probabilities and model-averaged predicted values were calculated in a spreadsheet for this report.

3.2.2 Software Capabilities and Limitations

Some of the capabilities and limitations of the software used in the application described in the following chapter are summarized here. Those features of the software most relevant to the analysis of model and parameter uncertainty are listed here.

GMS

Capabilities

- The GMS Map module facilitates alternative conceptual model development.
- PEST is integrated.
- A Monte Carlo simulation capability is integrated.

Limitations

- PEST is only implemented for use with MODFLOW.
- The set of MODFLOW parameters that can be estimated with PEST in GMS is limited.

- ParallelPEST, the multi-core/multi-processor version of PEST is not implemented in the federal agency distribution of GMS v. 7.1.
- The use of an HDF file for storing model input makes it more difficult to work with files outside of GMS.
- There are limited Monte Carlo simulation options (e.g., correlations between parameters is not implemented).

PEST

Capabilities

- Nonlinear regression uses the Levenberg-Marquardt method.
- Singular value decomposition and regularization techniques for highly-parameterized systems are available.
- Global optimization methods are implemented.
- A large number of utilities are available for file preparation and manipulation, groundwater-specific applications, and predictive error and uncertainty analysis.
- Model selection criteria values are calculated.

Limitations

- The large number of utilities and extensive capabilities can be overwhelming; documentation is currently not tightly integrated.
- Predictive uncertainty is not well-integrated with the basic operation of PEST.
- KIC values don't consider the impact of parameter transformation on the parameter covariance term in Eq. (21) (see Appendix A).

UCODE

Capabilities

- Nonlinear regression uses the Levenberg-Marquardt method.
- Utilities for residual analysis, model linearity evaluation, and linear uncertainty estimates are tightly integrated.
- Utilities are available for analysis of highly nonlinear models.
- Model selection criteria values are calculated.
- Results are readable by MMA for multi-model analysis.

Limitations

- A limited set of methods is currently implemented.
- KIC values don't consider the impact of parameter transformation on the parameter covariance term in Eq. (21) (see Appendix A).

4 EXAMPLE APPLICATION

This chapter presents an example application of the uncertainty methodology presented above. The example is for groundwater analyses related to the safety review of a nuclear power plant application, such as might be carried out in review of the Final Safety Analysis Report (FSAR) Section 2.4.12. The example uses publically available information from the Bellefonte Nuclear Power Plant Units 3 and 4 Combined Operating License (COL) application, namely, the FSAR and the Environmental Report (ER) submitted as part of the application.

The objectives of the example are to demonstrate the application of the uncertainty methodology to a relevant site and to illustrate the type of results that can be expected. We also show what is required to evaluate uncertainties using existing software tools and we comment on areas for potential improvement. The example uses a set of groundwater models. No groundwater model was submitted as part of the Bellefonte application and no model is referred to in FSAR 2.4.12. The groundwater models developed for this example and described below are solely the product of the coauthors of this report. Their use here implies neither suitability of the models for use in an actual review of the Bellefonte application nor approval by the NRC staff for such a purpose.

While the uncertainty methodology described above addresses the joint consideration of parameter, model, and scenario uncertainties, the implementation described here is limited to the consideration of parameter and model uncertainties. Including alternative scenarios requires additional simulation in the predictive period and averaging across scenarios [see Eqs. (17) and (18)], but does not require any other calculations since the scenario probabilities are subjective, prior values. See Meyer et al. (2007) for additional discussion.

4.1 **Building the Groundwater Model**

The site of the proposed Bellefonte Nuclear Power Plant Units 3 and 4 is located along the Tennessee River near Scottsboro, Alabama, in Jackson County (referred to hereafter as the Bellefonte site). The site description and available data are documented in the COL application located on the NRC website (<http://www.nrc.gov/reactors/new-reactors/col/bellefonte.html>): specifically, the FSAR, Rev. 1, and the ER, Rev. 1. The proposed Units 3 and 4 are located adjacent to existing Units 1 and 2 reactor buildings, which were partially constructed in the 1980s, but never completed. The location of the site is shown in Figure 6.

The first question to ask when preparing to build a groundwater model is, "What will this model be used for?" Identifying the purpose of the model and the kinds of questions that model simulations will be expected to address is important for defining the overall model configuration. If a model is used for regional-scale assessments, then the inclusion of local-scale specifics will be less important. If the model is for designing an in-situ remediation system, then a fine-scale model resolution may be needed for describing the flow field specifics and for solute transport. For a groundwater review following SRP Sections 2.4.12 and 2.4.13 (NRC 2007), the model will be used to evaluate groundwater heads, transport pathways, and possibly contaminant concentrations. This example emphasizes the use of a model to estimate the maximum post-construction groundwater heads in the power block area.

The process of building a groundwater model is depicted in Figure 7. Initially, one must determine the objectives of the modeling and assemble the set of data that will be used to

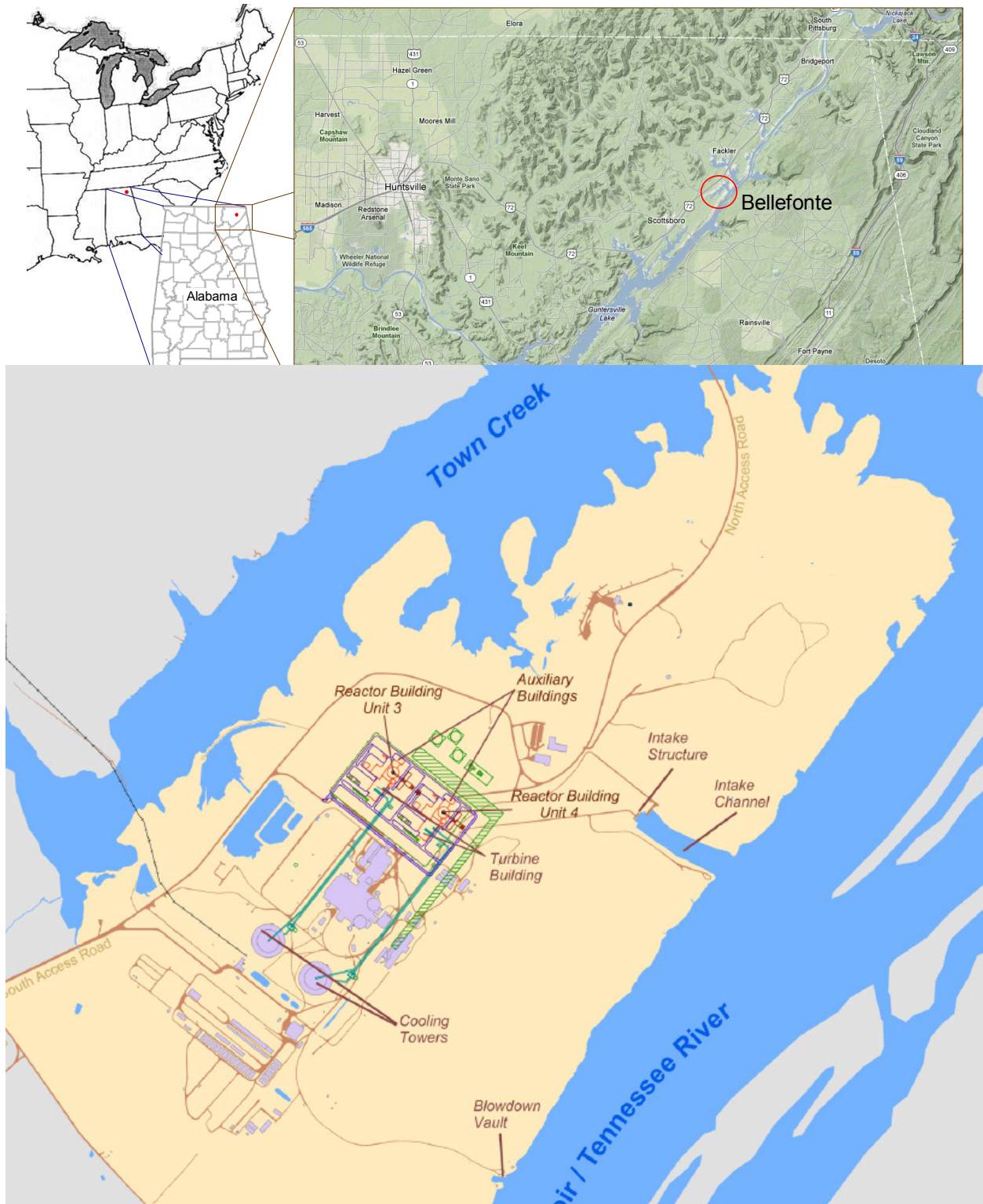


Figure 6. Location of the Bellefonte site. Lower image taken from FSAR Figure 2.1-201 (TVA 2009).

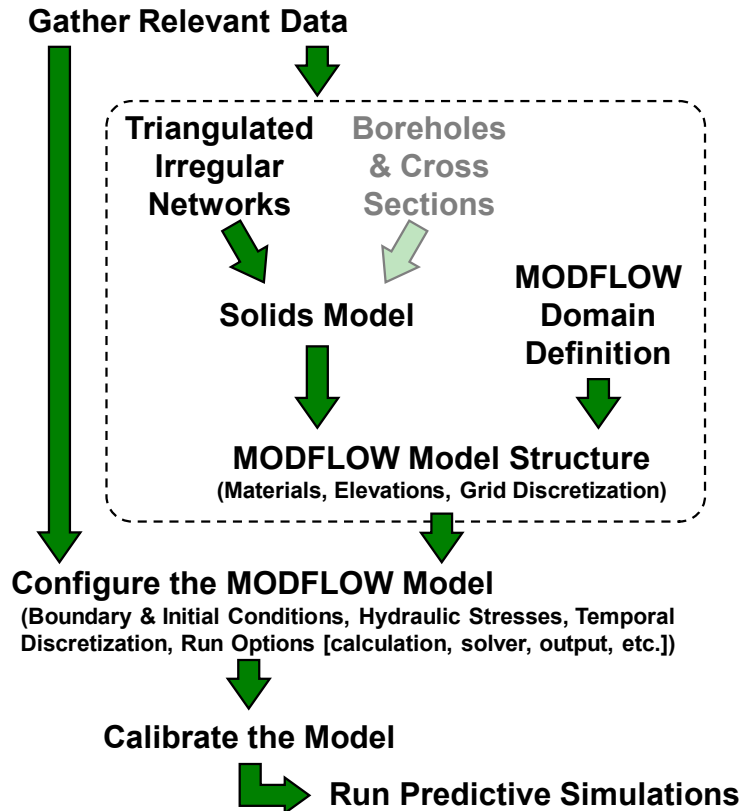


Figure 7. Steps in building a MODFLOW groundwater model

construct the model. A basic conceptual site model is developed from the data. The model framework (lateral grid, layers, domain extent, etc.) is defined based on knowledge of hydrogeology and the modeling objectives. Once the framework is determined, the groundwater model parameters and boundary conditions can be specified. The groundwater model then requires calibration with either trial and error adjustment of parameter values or an automated optimization process. For this example, automated calibration using least squares regression was used to provide the required parameter uncertainty estimates. The calibrated model can then be used in predictive simulations, typically after making adjustments (e.g., to reflect post-construction conditions). The process of implementing each of these steps with respect to modeling the Bellefonte site is described in subsequent sections of this report.

4.1.1 Gather Relevant Data

The first step in building and configuring a numerical model for simulating groundwater flow with MODFLOW is to gather the relevant site-specific data. Figure 8 depicts the types of data that go into defining a groundwater flow model. Many of the necessary data are quantitative (elevations, distances, flow rates, aquifer properties, etc.), but some of the input is qualitative.

The nature of the model (lateral grid resolution, number of model layers, domain extent, temporal nature, etc.) must be balanced between meeting the objectives of the modeling, the computational constraints associated with the simulations (i.e., memory, run time) and the resolution of the available data. The extent of the model domain may also be influenced by the locations of natural boundary conditions. Keeping this in mind, the data elements of Figure 8 were gathered and examined for the Bellefonte site.

4.1.1.1 Site Locale and Topology

Photographic images provide a basis of reference for locating geographic features and buildings. Digital orthographic quarter quad (DOQQ) imagery from 2006 was downloaded from the Alabama State Water Program (ASWP 2006) website for the following named quads (with quarter quad indicated):

- Henagar (NW and SW)
- Hollywood (NW, NE, SW, and SE)
- Stevenson (SW)
- Wannville (SW and SE)

The DOQQ imagery (Figure 9) was provided in the Universal Transverse Mercator (UTM) projection for zone 16 relative to the North American Datum of 1983 (NAD83) in units of meters. The State Plane Coordinate System (SPCS) for Alabama East (Zone 101) relative to NAD83 in units of feet was selected for this work, so Global Mapper was used to transform the imagery to the SPCS prior to exporting a zone around the Bellefonte Nuclear Plant. The export process creates a world file with a file extension of *.jgw corresponding to the current coordinate system (combination of projection, datum, and units). The exported image was read into GMS, which used the world file to automatically register the image to the appropriate coordinates. Images are found listed in the Images module of GMS. Note that multiple images can be loaded into GMS and are treated as layered images with the first image loaded at the back and the most recent image loaded on top. The georeferenced DOQQ provides a basis for registering non-georeferenced image files (e.g., maps copied from PDF documents) in that coordinates of specific features (e.g., buildings, road inter-sections) can be determined and mapped to specific pixels of the non-georeferenced image. This approach was used to register several images (e.g., hydraulic head contours, construction diagrams) in GMS.

A USGS topographic map (digital raster graphic [DRG]; Figure 10) of the Hollywood quad, georeferenced to the Universal Transverse Mercator (UTM) projection relative to the North American Datum of 1927 (NAD27) in units of meters, was also downloaded from the ASWP website. Topographic maps provide additional detail about surface features, including streams, lakes/ponds, and topography. However, the topography information is not in a format conducive to applying in a numerical model.

Digital elevation model (DEM) data are a representation of topographic elevations as an array of numbers, and thus are well suited for use in numerical models. USGS 1/3 arc-second (10 m) DEM data were retrieved from the AlabamaView website (USGS 2009). The DEM data were loaded into Global Mapper (Figure 11) and were automatically converted from a UTM projection relative to the World Geodetic System of 1984 (WGS84) in units of meters to the same coordinate system as the DOQQ imagery.

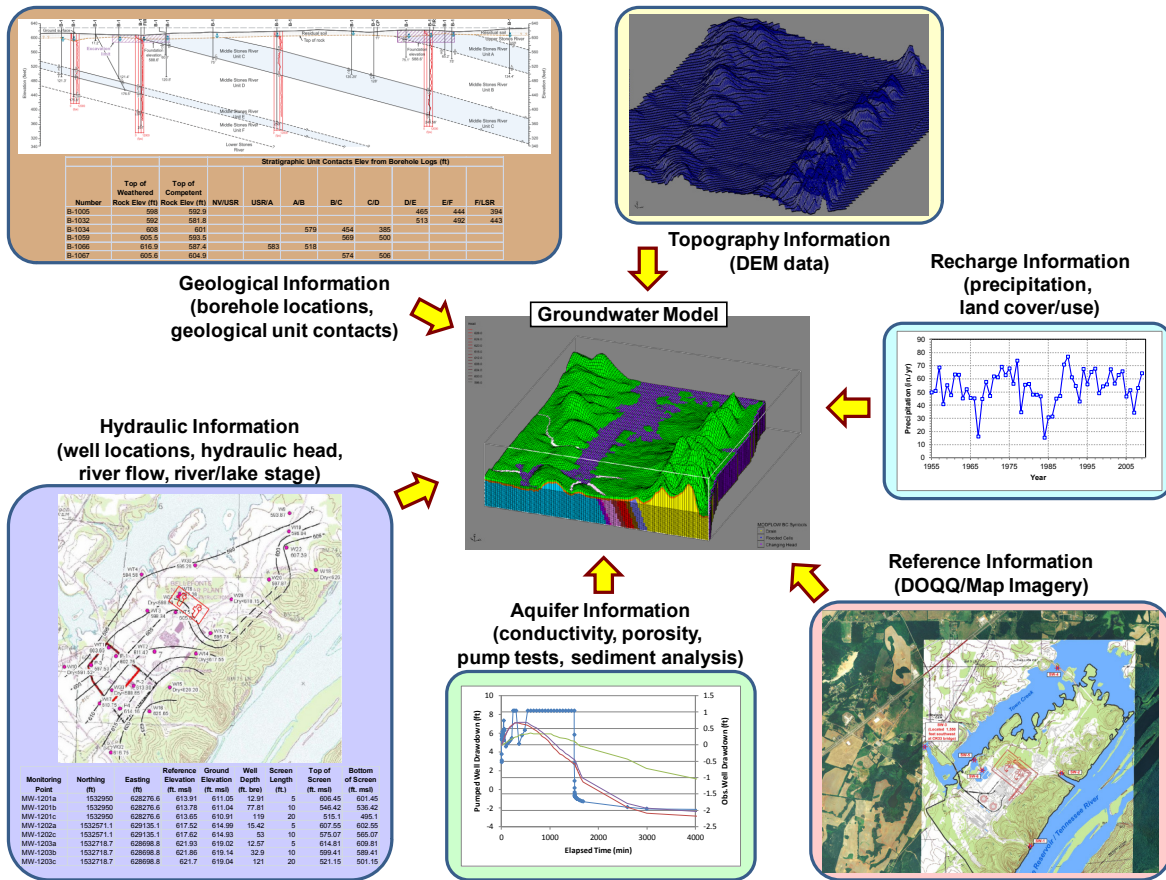


Figure 8. Depiction of data inputs used to configure a three-dimensional MODFLOW model for simulating groundwater flow in the subsurface



Figure 9. DOQQ imagery for the Bellefonte site vicinity. Coordinates are SPCS Alabama East, in feet

4.1.1.2 Site Hydrogeology

Site hydrogeology is a key component for a groundwater flow model in that it delineates geological features and hydraulic units for groundwater movement. The hydrogeologic setting of the Bellefonte site is the Valley and Ridge aquifer system in the southern portion of the Sequatchie Valley, a northeast trending, eroded anticline (Miller 1990). The thrust faulting and folding that produced the anticline resulted in fracturing of the sedimentary rock formations and led to the erosion of the overlying sandstone-shale units and karst formation in the underlying limestone units. A conceptual depiction of the hydrogeology of the Sequatchie Valley is shown in Figure 12, taken from Miller (1990). A geologic map of the region surrounding the Bellefonte site and a representative cross-section taken south of the site, both shown in Figure 13, illustrate the location of the site on the southeasterly dipping side of the Sequatchie anticline. The Sequatchie fault is far enough to the northwest to be outside the area of interest.

The relevant formation descriptions from Irvin and Dinterman (2009) are:

- Nashville Group: partly argillaceous wackestone/packstone with interbedded lime mudstone. Some intervals are abundantly fossiliferous.
- Stones River Group: Lower part is partly argillaceous lime mudstone and wackestone that is locally fossiliferous. Upper part is thin- to thick-bedded, fossiliferous limestone with rare very fine grained calcareous sandstone. Laminated bentonitic shale is near the upper contact. At the base, locally, is sandy chert conglomerate (Pond Spring Formation).
- Knox Group—finely crystalline, siliceous dolomite and minor locally silty limestone. At the surface, the Knox weathers to residuum with abundant, predominantly dense chert that generally preserves primary sedimentary features.

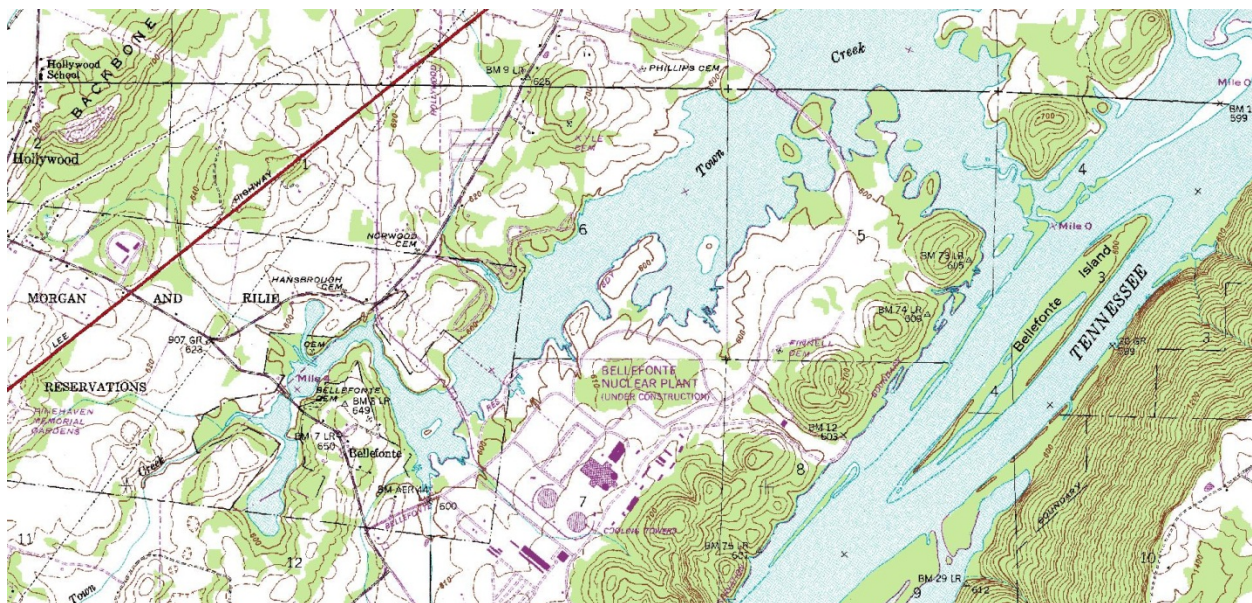


Figure 10. Topographic map for the Bellefonte site vicinity

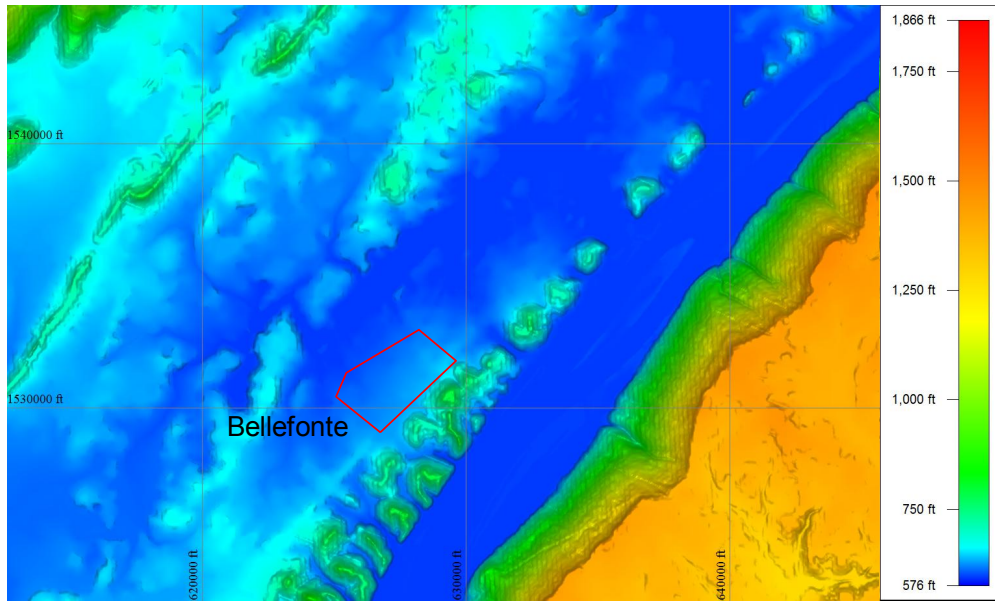


Figure 11. DEM data in the vicinity of the Bellefonte site (as depicted in Global Mapper)

Figure 99. The arrows show the movement of water in the folded and faulted rocks of the Valley and Ridge physiographic province. Shale confining beds divert water to ridge faces where it emerges as springs. Most of the water in the limestone moves through large solution openings.

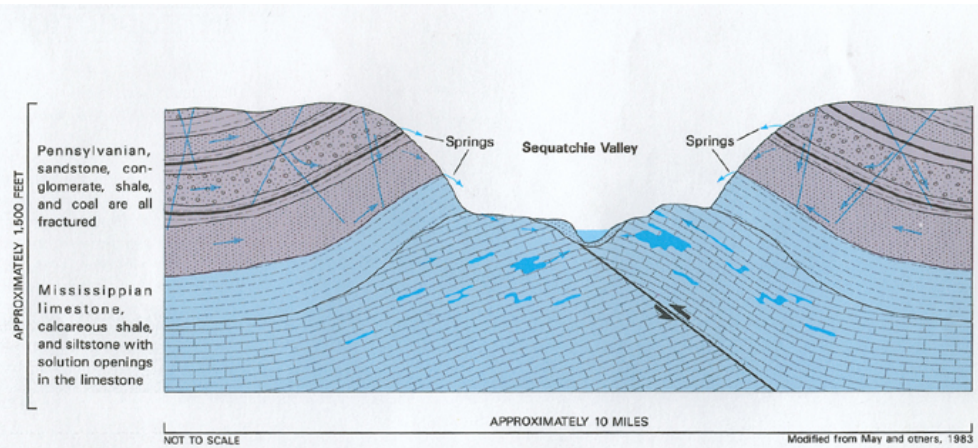


Figure 12. Conceptual depiction of hydrogeology in a cross-section of the Sequatchie Valley, the location of the Bellefonte site (from Miller 1990)

Additional information pertaining to the geology of the site is contained in TVA (2009). FSAR Figures 2.5-307 and 2.5-308 show photos of the inclined geology taken during construction of Bellefonte Units 1 and 2 (not shown here). FSAR Figures 2.5-339 to 2.5-341 show cross sections of interpreted geologic bedding planes through the location proposed for Units 3 and 4 (part of Figure 2.5-339 is shown in Figure 14 below). In a cross section perpendicular to a strike of N45°E, FSAR Fig. 2.5-306 shows the stratigraphic contacts between the Lower Stones River, Middle Stones River (which has multiple subunits termed A through F), and Upper Stones River units. For this work, contacts were based on the borehole logs in FSAR Appendix 2BB (listed in Table B.1 of Appendix B of this report). Elevations of the top of the weathered rock come from the Standard Penetration Test (SPT) borehole data; top of competent rock was based on the Rock Quality Designation (RQD) and borehole log notes on rock weathering.

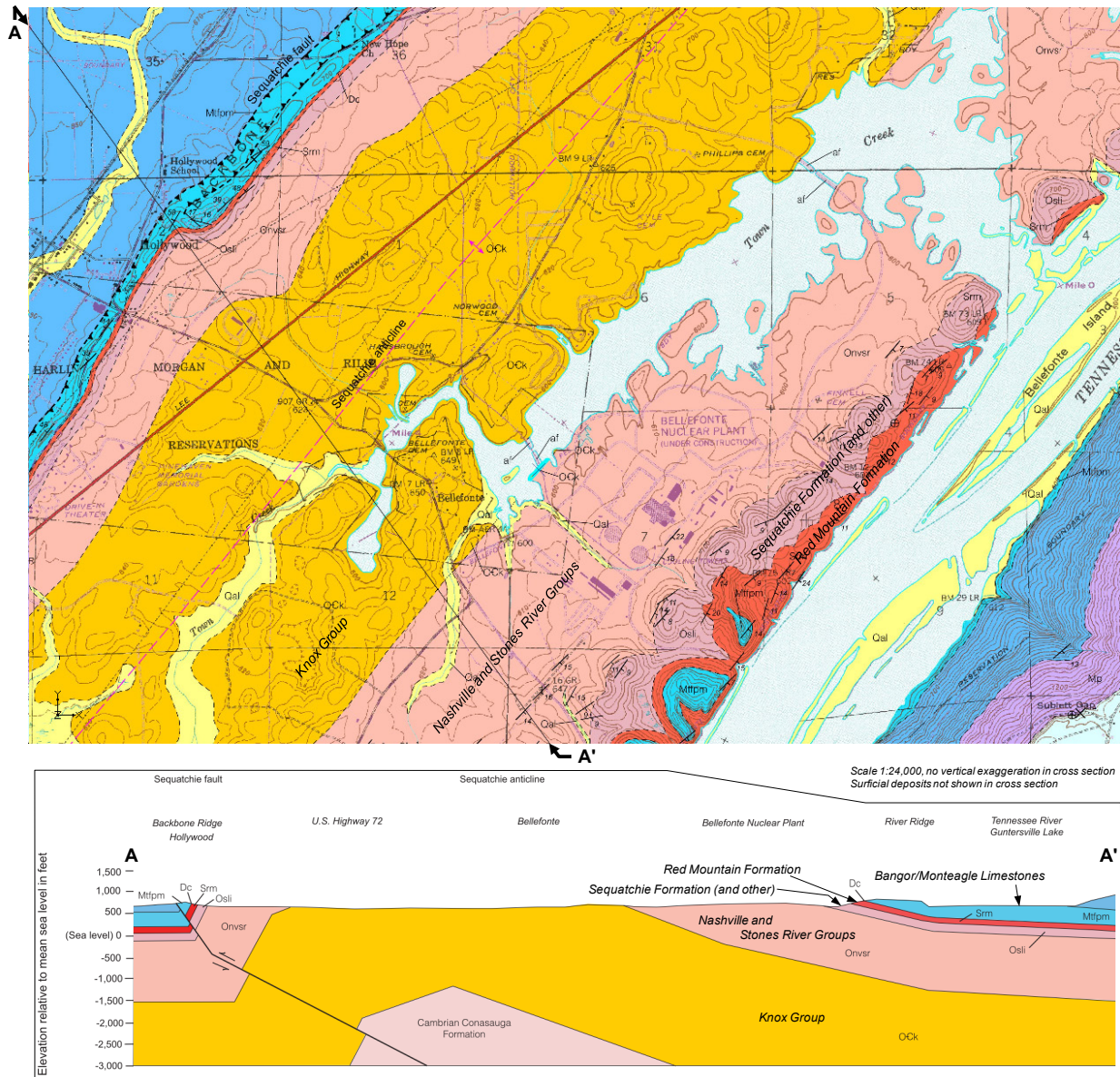


Figure 13. Geological units in the vicinity of the Bellefonte site. Adapted from Irvin and Dinterman (2009).

4.1.1.3 Aquifer Properties

The key aquifer property for modeling groundwater flow is the hydraulic conductivity of the subsurface materials. Table 1 lists data as reported in TVA (2009) for the Bellefonte Units 1 and 2 site and from site investigation tests conducted in 2006 for Units 3 and 4. Average values (both mean and geometric mean) were calculated for that data. The materials of interest are Soil, Weathered Rock, and Competent Rock (i.e., bedrock, in the form of the Nashville, Upper Stones River, Middle Stones River, and Lower Stones River units).

To simulate solute transport, the porosity of the subsurface materials (Table 2) and adsorption-related properties are required. Potential radionuclide contaminants and their linear equilibrium

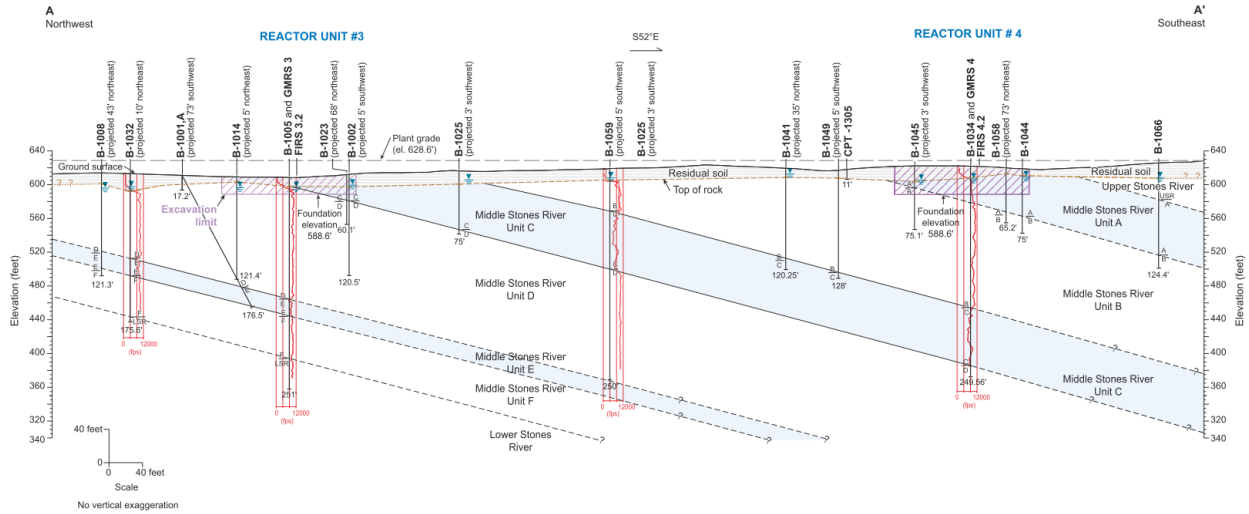


Figure 14. A geologic cross-section through Units 3 and 4 showing rock units (taken from FSAR Figure 2.5-339, TVA 2009)

Table 1. Hydraulic conductivity (K_s) for subsurface materials near the Bellefonte site. Minimum and maximum values reported in TVA (2009); midpoints and averages were calculated

Material	Min. K_s (cm/s)	Max. K_s (cm/s)	Midpoint of Range (cm/s [ft/d])	Geometric Mean of Max./Min. (cm/s [ft/d])	Data Source
Soil	1.00E-08	1.00E-06	5.05 E-07 [1.43 E-3]	1.00 E-07 [2.83 E-4]	FSAR for Bellefonte Units 1 and 2
Bedrock	4.00E-06	3.80E-03	1.90 E-03 [5.39]	1.23 E-04 [0.349]	FSAR for Bellefonte Units 1 and 2, borehole packer tests
	2.50E-05	4.20E-03	2.11 E-03 [5.99]	3.24 E-04 [0.919]	Units 3 and 4, 2006 site investigation, borehole packer tests
	6.11E-07	3.95E-03	1.98 E-03 [5.60]	4.91 E-05 [0.139]	Units 3 and 4, 2006 site investigation, MW-1203b pump test
Bedrock (All Data)			2.00 E-03 [5.66]	1.25 E-04 [0.355]	Mean/Geometric Mean of all six Max./Min. values for Bedrock
Weathered Rock			9.99 E-04 [2.83]	3.54 E-06 [0.010]	Mean/Geometric Mean of the Soil and Bedrock (All Data) Averages

Table 2. Porosity for subsurface materials in the vicinity of the Bellefonte site

Material	Interval Below Bedrock Surface	Void Ratio	Total Porosity	Data Source
Soil	—	—	0.45	TVA (2009)
Bedrock	—	—	0.005	TVA (2009)
Bedrock	0-5 ft	0.01378	0.0136	Void ratios computed from information in Attachment A of Request for Additional Information (RAI) Response (ML082070075 ^a) on cavity and total core lengths; porosities computed from void ratios
	5-10 ft	0.02712	0.0264	
	10-20 ft	0.01504	0.0148	
	20-30 ft	0.00191	0.00191	

^aAvailable at <http://adams.nrc.gov/wba/>

partitioning coefficients (K_d) are described in FSAR Section 2.4.13 (TVA 2009). The average dry bulk density (ρ_b) of the soil is given in FSAR Section 2.4.12 (TVA 2009) as 90 lb/ft³ (1.44 g/cm³), which can be used with the K_d and porosity values to calculate the retardation factor for solute transport.

4.1.1.4 Precipitation and Land Usage

Historical precipitation data (PRCP) were retrieved (from <http://www1.ncdc.noaa.gov/pub/data/ghcn/daily/>, or alternatively, from www.ncdc.noaa.gov/cdoweb/search#t=secondTabLink) for the Scottsboro, Alabama Global Historical Climatology Network (GHCN) (Menne et al. 2012) station USC00017304 (U.S. Cooperative Network [COOP] station 017304), which is part of the U.S. Historical Climatology Network (HCN) and is located at latitude 34.6736° and longitude -86.0536° and an elevation of 187.5 m above sea level. The average annual total precipitation for the period from 1955 to 2009 is 53.4 in./yr (Figure 15).

FSAR Section 2.4.12.1.2 (TVA 2009) states that precipitation at the Bellefonte site “averages about 50 in. per year” and that “approximately 8 in. of this precipitation is estimated to enter groundwater storage.” The average precipitation per year is consistent with that calculated from the Scottsboro COOP station 017304 data.

Land use can be inferred from the satellite imagery (Section 4.1.1.1).

4.1.1.5 Hydraulic Information

A variety of hydraulic information for a site can be used to define boundary conditions or calibration targets. Where there are induced stresses, such as pumping wells or injection wells, the flow rate and time frames of the hydraulic stresses must be assembled. Similarly, river flow data (i.e., from river gages) are important for defining boundary conditions and/or for use as a flow calibration target. Certain rivers/streams or surface features may act as drains, resulting in loss of groundwater from the subsurface to the surface water (i.e., gaining streams, potentially a seasonal effect). Bodies of water often represent constant head boundary conditions (although the constant head may vary seasonally, which is a time-varying constant head). The regional hydraulic head distribution may also be used as a constant head boundary condition. Hydraulic head data from monitoring wells can be used to help establish boundary conditions, but are most often used as calibration target data. For the Bellefonte site, the hydraulic information of

interest pertains to gaining streams, constant hydraulic head regions, and observed monitoring well hydraulic head data.

The major surface water features at the Bellefonte site are Town Creek and the Tennessee River (Figure 6, Figure 10). Town Creek actually starts as a river/stream, but the portion most relevant to this work is essentially a lake (backwater of the Tennessee River) on the northwest side of the Bellefonte site. The Tennessee River runs along the southeast side of the Bellefonte site and constitutes, at this location, the Guntersville Reservoir. Figure 16 shows locations of surface water gaging locations on both Town Creek and the Tennessee River. Data are available in FSAR Table 2.4.12-204 for monthly observed surface water elevations from June 2006 through May 2007. Average stage elevations based on this data for SW-1, SW-2, SW-3, and SW-4 are listed in Table 3 (SW-5 and SW-6 represent on-site ponds, not Town Creek). The overall stage elevation for Town Creek and the Tennessee river is 594.5 ft, which is essentially constant over a seasonal cycle.

Examining the topographic map of the Bellefonte vicinity (Figure 17), five streams are observed to discharge into Town Creek. Elevations of these streams were estimated from the topographic map and were used to define drainage features in the groundwater model.

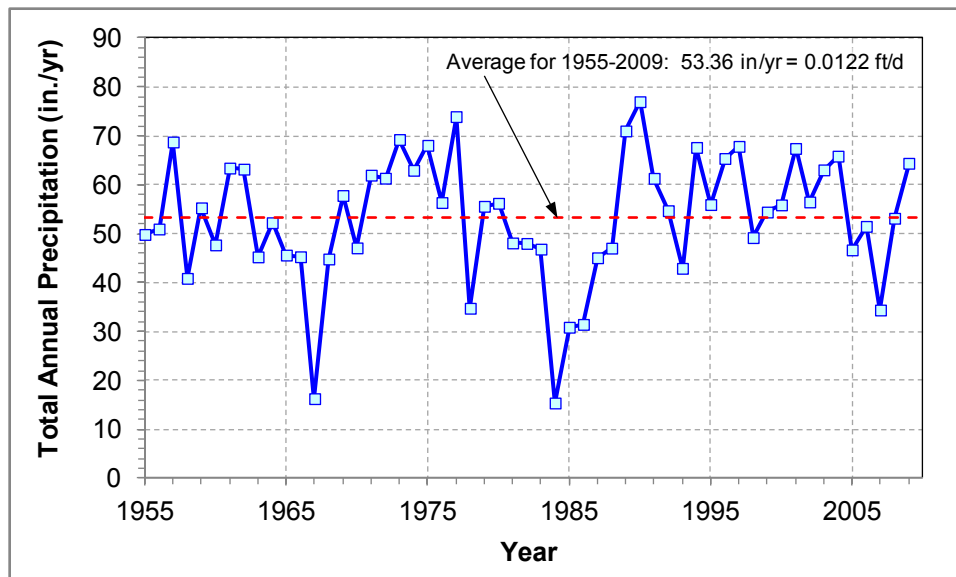


Figure 15. Total annual precipitation at COOP station 017304 in Scottsboro, Alabama from 1955 through 2009. The dashed line is the annual average over this time frame.

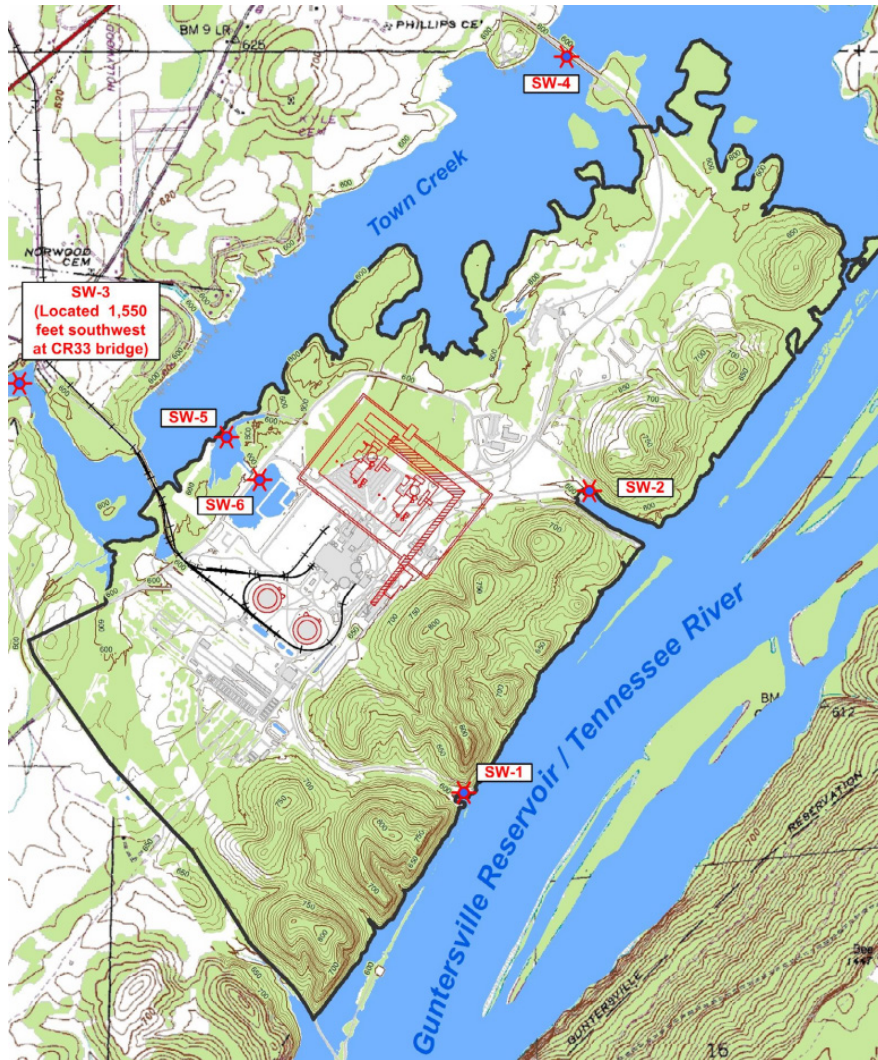


Figure 16. Locations of surface water gaging locations. This figure shows a portion of FSAR Figure 2.4.12-213 (TVA 2009).

Table 3. Average stage observed at surface water measurement locations

Surface Water Gage Location	Average Stage (ft) for June 2006-May 2007 Data ^a
SW-1	594.5
SW-2	594.4
SW-3	594.6
SW-4	594.6

^a Based on data in FSAR Table 2.4.12-204. The standard deviation for stage data at each location is about 0.3 to 0.4 ft.

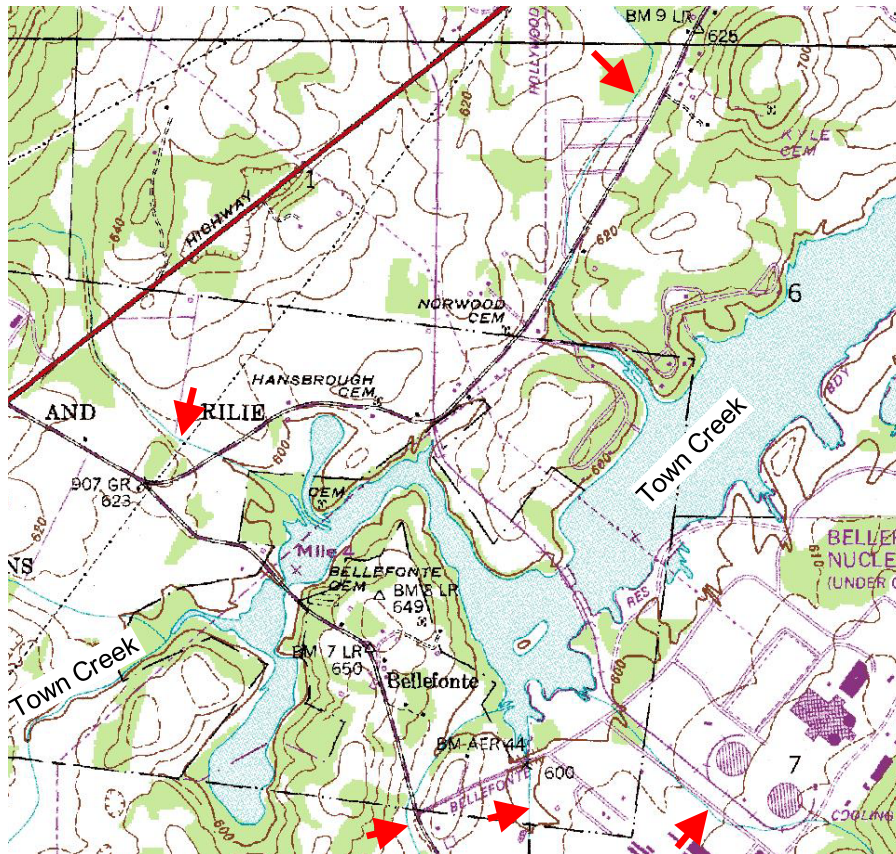


Figure 17. Locations of streams that discharge into “Town Creek” (marked by the arrows)

Three data sets of observed groundwater hydraulic heads at monitoring wells were used for model calibration and to assist with boundary condition definition. These data sets included data from 1961 (FSAR Figure 2.4.12-204), from September 2005 (FSAR Figure 2.4.12-210), and from monthly observations (plus two extra events) between June 2006 and May 2007 (FSAR Table 2.4.12-204, TVA 2009). Bedrock wells that exhibited a slow response during development and wells listed as “dry” in FSAR Table 2.4.12-204 were excluded. Figure 18 shows a composite of portions of FSAR Figures 2.4.12-204 and 2.4.12-210, which indicate flow towards Town Creek. The 2006-2007 data are shown as a portion of FSAR Figure 2.4.12-215 (Figure 19), also showing groundwater flow from the Bellefonte site to Town Creek. The groundwater head data used in the calibration process are listed in Table B.3 in Appendix B for these three data sets.

Because of the well locations, some of the data from 1961 were also used to define the boundary conditions along the northwest side of the model.

4.1.1.6 Conceptual Model Based on the Data

According to the conceptual model presented in FSAR Section 2.5 (TVA 2009), groundwater flow occurs in three stratigraphic regions: the overburden (residual soil), the epikarst zone (upper weathered rock), and the karst zone (bedrock). In this model, flow is predominately downward in the overburden with horizontal flow occurring in the epikarst and through solutionally enlarged joints and bedding plane fractures in the karst zone. Karst features

identified in the site investigation were soft zones and cavities in soil, cavities in boreholes, and an irregular rock surface. A conceptual depiction of the karst environment is shown in Figure 20. The occurrence of observed cavities (those greater than 0.1 ft in thickness) decreased with depth. Most cavities were observed within 10 to 20 ft. of the top of rock. The deepest cavity was observed at 63 ft. below ground surface. Many of the cavities were soil-filled, which was attributed to the argillaceous character of the limestone. Thin shale layers observed in the boreholes were also stated to be a lithologic control on the flow of groundwater.

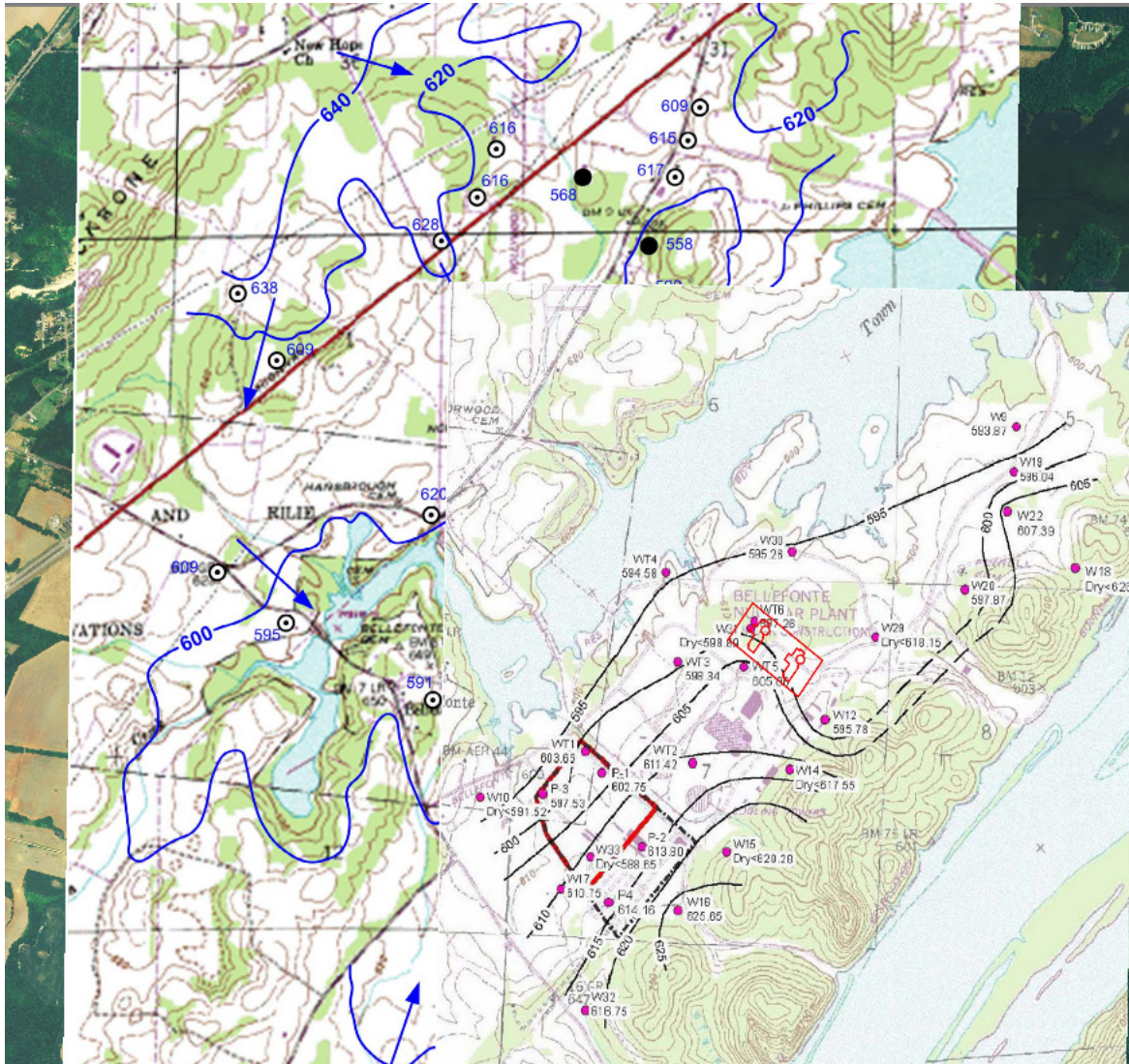


Figure 18. Hydraulic head data and interpreted contours for the 1961 data (blue contours at west and north sides) and the September 2005 data (black contours in southeast quadrant), all overlay on the Bellefonte area imagery

Under the conceptual model of groundwater flow presented in FSAR Section 2.4.12 (TVA 2009), during normal (dry) conditions, lateral groundwater flow is primarily through the fractures and joints of the partially-filled epikarst region. During periods of significant recharge (following heavy or frequent rainfall events), the epikarst fills and significant lateral flow takes place in the overburden soils. Flow in the karst bedrock zone is generally small. Groundwater occurrence in

wells was inconsistent across the site, with dry wells or wells with minimal flow observed in each of the zones depicted in Figure 20.

Bedrock stratigraphy consists of basically parallel inclined units along a strike of nominally N45°E with a dip of about 15°SE. Units progress with depth (and from southeast to northwest) in the sequence of Nashville (NV), Upper Stones River (USR), Middle Stones River (MSR) subunits A through F, and Lower Stones River (LSR). While the elevated River Ridge hills to the southeast are comprised of Sequatchie, Red Mountain, and other limestones and shale, these units are represented here as Nashville material. This approach is reasonable because there is little basis for distinguishing properties between these River Ridge units, the groundwater flow of interest at the site is expected to be towards Town Creek, and representing the groundwater table in a layered hill provides challenges in model configuration (discussed in Section 4.1.2).

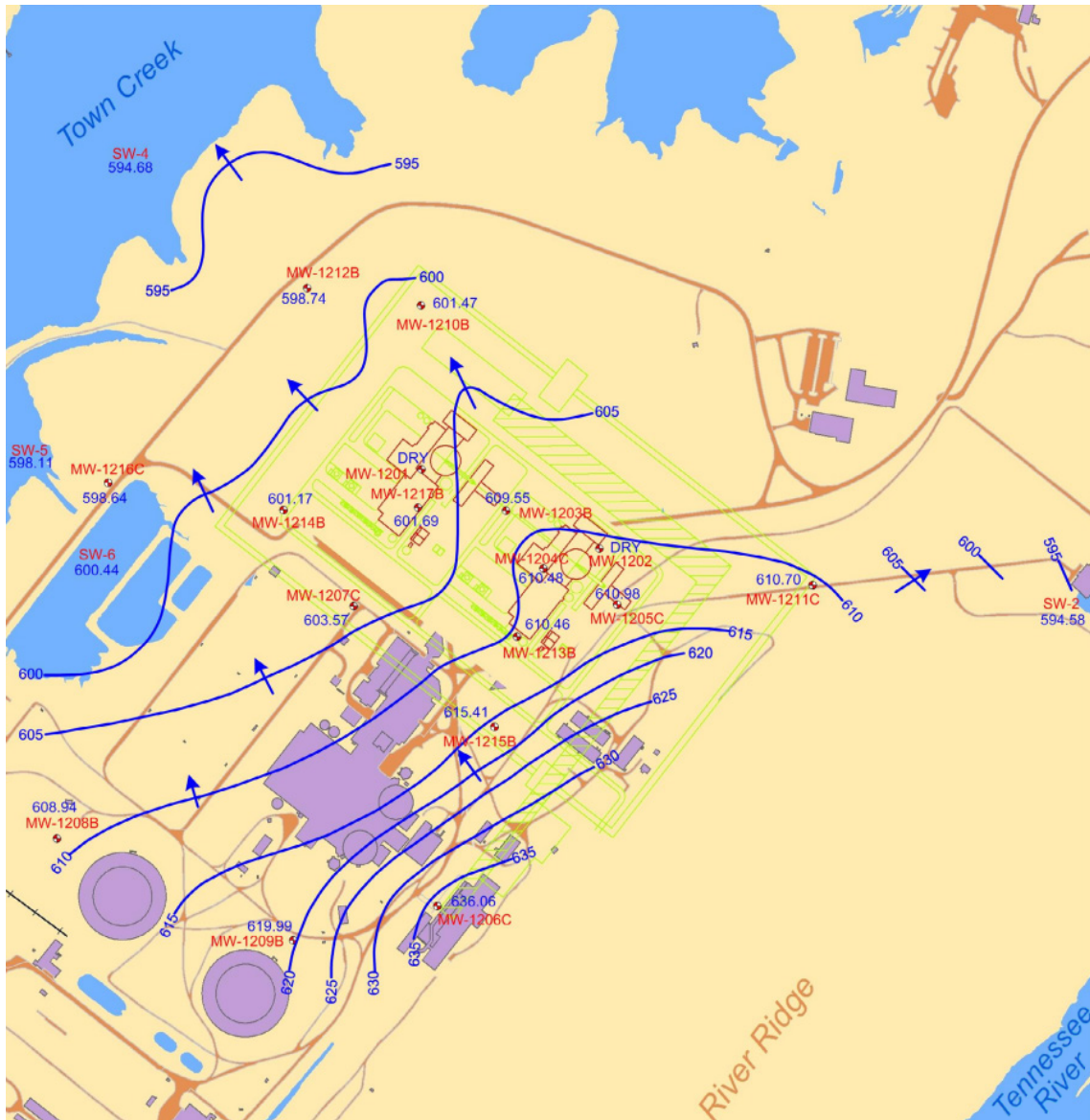


Figure 19. Example of recent hydraulic head contours interpreted from November 2006 groundwater head data

Groundwater flow is expected to be sensitive to recharge and site topography and thus would be expected to flow towards Town Creek (from both the northwest and southeast) except for the southeast side of the River Ridge hills, where groundwater would flow towards the Tennessee River. The Tennessee River and Town Creek are natural hydraulic boundaries. However, the Sequatchie anticline was selected as the boundary location to the northwest instead of Town Creek to allow the model to address potential interaction between the site and groundwater users on the northwest side of Town Creek.

Because of the regulation of the reservoir (Tennessee River), elevations in the reservoir and Town Creek are fairly constant in time. As a result, temporal variation in groundwater heads is primarily due to variation in recharge. Groundwater heads would be expected to vary with seasonal changes in recharge; such variation can be seen in some of the historical data (FSAR Figure 2.4.12-211, TVA 2009), but is not clearly evident in the monthly data collected more recently (FSAR Figure 2.4.12-218, TVA 2009) due to the short period of data collection.

Groundwater heads also respond to precipitation events. A rapid response to a precipitation event was observed between September 21st and 26th, 2006 in many of the monitoring wells at the site. Figure 21, the head response in well MW-1202a, screened in the soil unit, is typical. About 10 cm (4 in) of precipitation were recorded at Scottsboro, Alabama between September 22nd and 24th, and the observed groundwater head increased about 5 ft (1.5 m) between September 21st and the 26th. For evaluating the maximum groundwater head around the power block, these data indicate that it is important to evaluate the unsteady behavior of the flow. Completing such an evaluation using the existing data would be difficult, however. Better aquifer pump test data, on-site precipitation data, and more frequent groundwater head measurements would be required. For this example, however, there is no opportunity to obtain this data (a situation often encountered in practice, as discussed above). As a result, a steady-state groundwater flow model was developed for this example. The uncertainty in the maximum groundwater head induced by this steady-state assumption was evaluated qualitatively, as described below in the section on predictive modeling.

4.1.2 Define the Geological/Model Structure

After the necessary data are gathered, the next step in building a model for groundwater simulation is to define the geological structure and the model grid structure.

4.1.2.1 Groundwater Model Domain

Based on the modeling objectives and the conceptual model, an initial model grid was selected with the properties shown in Table 4. The uniformly spaced model grid was aligned nominally orthogonal to the strike of the bedrock units, at a 45° rotation (Figure 22), with boundaries at the Tennessee River, the Sequatchie anticline, and covering most of the extent of Town Creek to the northeast and southwest. This placed the location of Bellefonte Units 3 and 4 nominally in the middle of the model domain. The vertical origin was (somewhat arbitrarily) selected at an elevation of 450 ft. The vertical distribution of layers was determined later in the process, but this depth was believed to be sufficiently large, while allowing fine enough vertical resolution in the grid. The selected number of grid cells in the three directions resulted in a total grid cell count of about a half million, which is reasonably detailed, while still allowing feasible simulation run times. This initial definition of the model domain provides a basis for building the geological model structure in terms of lateral and vertical extents.

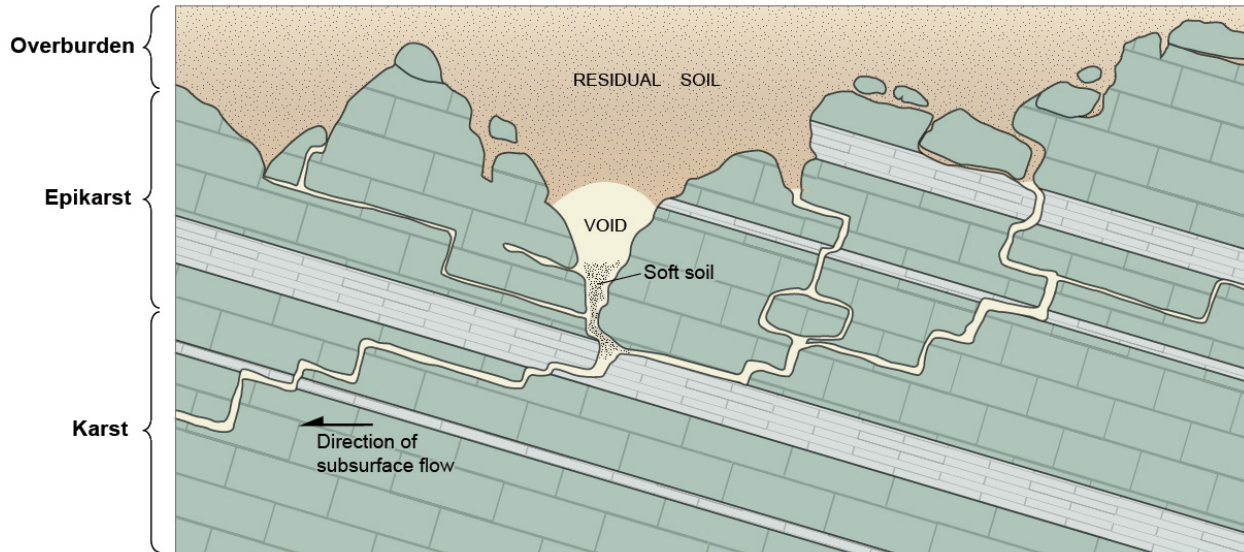


Figure 20. Conceptual model of karst development at the Bellefonte site (from FSAR Figure 2.5-304, TVA 2009)

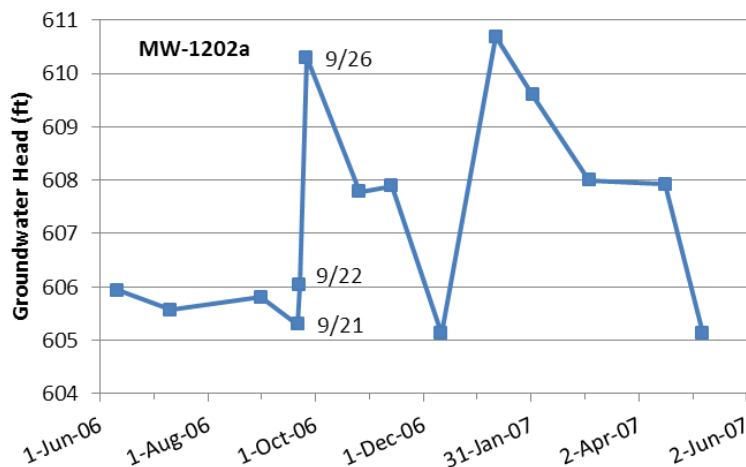


Figure 21. Groundwater head response to a precipitation event: about 10 cm (4 in) of precipitation were recorded at Scottsboro, Alabama from 9/22/06 to 9/24/06 (Scottsboro 2 NE Experimental Station, downloaded 8/27/10 from <http://www.ncdc.noaa.gov>). Groundwater head data from FSAR Table 2.4.12-204 for monitoring well MW-1202a screened in the soil unit (TVA 2009).

Table 4. Initial model grid description

Grid Information	Units	X direction (columns)	Y direction (rows)	Z direction (layers)
Number of Cells	—	135	120	31
Total Grid Length	ft	13500	12000	148
Grid Cell Size (i.e., width, thickness)	ft	100	100	4.8
Origin Coordinates ^{a,b}	ft	625800.0	1525300.0	450.0

^a State Plane Coordinate System (Alabama East), NAD83 for lateral coordinates. Vertical elevations are relative to NAVD88.

^b Angle of rotation for the model grid = 45°.

4.1.2.2 Define Hydrogeological Units as Materials

Given the conceptual model of the site lithology/stratigraphy, a set of materials was defined in GMS (Figure 23). When materials are used, the properties for each material (e.g., hydraulic conductivity, porosity) and the zones where each material is present are specified. Working with the model is easier in that property values can readily be changed at a material level rather than on a grid cell-by-cell level. GMS translates the material properties into parameter values for each grid cell when creating the input files used by the MODFLOW code.

4.1.2.3 Build a Solids Model

There are two typical approaches to start the process of defining the geological structure of a site. One approach is to enter lithologic/stratigraphic contact information from borehole logs as “borehole data,” which can be organized in Excel then placed in an ASCII text file. It is often convenient to define a “dummy” stratigraphic material as the bottom-most material and to have a uniform bottom elevation (rather than the varying actual borehole bottom elevations). The borehole data text file can be imported into GMS via the file import wizard and the data sent to the GMS Boreholes module. Depending on the density and location of borehole data, it may be necessary to add “control point” boreholes (i.e., estimated/extrapolated lithology) such that the boreholes extend at least to the boundaries of the groundwater model domain (if not beyond). Once in GMS, the boreholes need to be connected by creating cross sections between pairs of boreholes. The cross sections should be created around the groundwater model domain boundaries and in multiple (preferably orthogonal) directions within the groundwater model domain. Creating borehole cross sections involves matching up stratigraphic units and estimating how a unit that is present in one borehole but not the other “pinches out” between the two locations. GMS is particular in requiring no unmatched stratigraphic units and interpretation of a given cross section is challenging at times. However, once all the cross sections are defined, the “horizons -> solids” command can be applied to have GMS interpolate the contacts across all the cross sections and automatically create a solids model from these interpolations.



Figure 22. Extent of the groundwater simulation model grid relative to key features. The grid origin is located in the lower left corner of the model at the bottom of the domain.

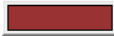
Soil		MSR_C	
WeRo		MSR_D	
NV		MSR_E	
USR		MSR_F	
MSR_A		LSR	
MSR_B		dummy	

Figure 23. Material designations (and corresponding colors) used in GMS to represent the stratigraphic units of the subsurface (Section 4.1.1.6). The “dummy” material was used to facilitate work in GMS, but was not applied in the groundwater model.

The second approach to defining the geological structure involves working with scatter data sets and triangulated irregular networks (TINs) to form a solids model. This approach offers more flexibility at the expense of being more involved. In this approach, the user defines relevant surfaces, such as ground surface and contacts between units, based on the gathered data and conceptual model. Because the data density was low outside of the Bellefonte site and there exists a good conceptual model, this second approach was applied in this work.

The USGS DEM (Figure 11) data were exported from Global Mapper as a set of coordinate points (X, Y, elevation) for an area encompassing the model domain. The exported DEM data were opened in GMS as a tab-delimited text file with a header row, which was designated as a 2D Scatter Point data set in the file import wizard (thus the data showed up in the 2D Scatter Data module of GMS). The scatter data set was converted to a TIN with the GMS “Scatter Points -> TIN” command. This DEM TIN thus represents the ground surface elevations across the model domain (Figure 24). However, the DEM was refined by manually deleting scatter data points within the boundaries of available well data near the Bellefonte site and points representing the ground surface elevation at those wells were inserted. Although coarser, site-specific well data on ground surface elevations were deemed to be more useful than the generic DEM data. The resultant impact to the ground surface elevation TIN produced from the modified scatter data is shown in Figure 25.

Little information on the vertical extent of the Soil and Weathered Rock (WeRo) materials is available outside of the borehole data at the Bellefonte site. Thus, an average thickness for each of these two units was applied uniformly where borehole data did not exist. Based on the borehole data (Table B.1), the average thickness of the Soil is 13.0 ft and the average thickness of the Weathered Rock material is 10.2 ft. The ground surface TIN was duplicated and translated downward vertically by 13 ft and by 23.2 ft to create TINs for the bottom of the Soil and Weathered Rock units, respectively (Figure 25). These three TINs (DEM, Soil, Weathered Rock) were placed together in a folder of the GMS TIN module and the “Horizons -> Solids” command was applied on that folder using the DEM TIN as the topmost elevation and the Weathered Rock TIN as the bottommost elevation. The resulting solids model for these two materials is shown in Figure 26.

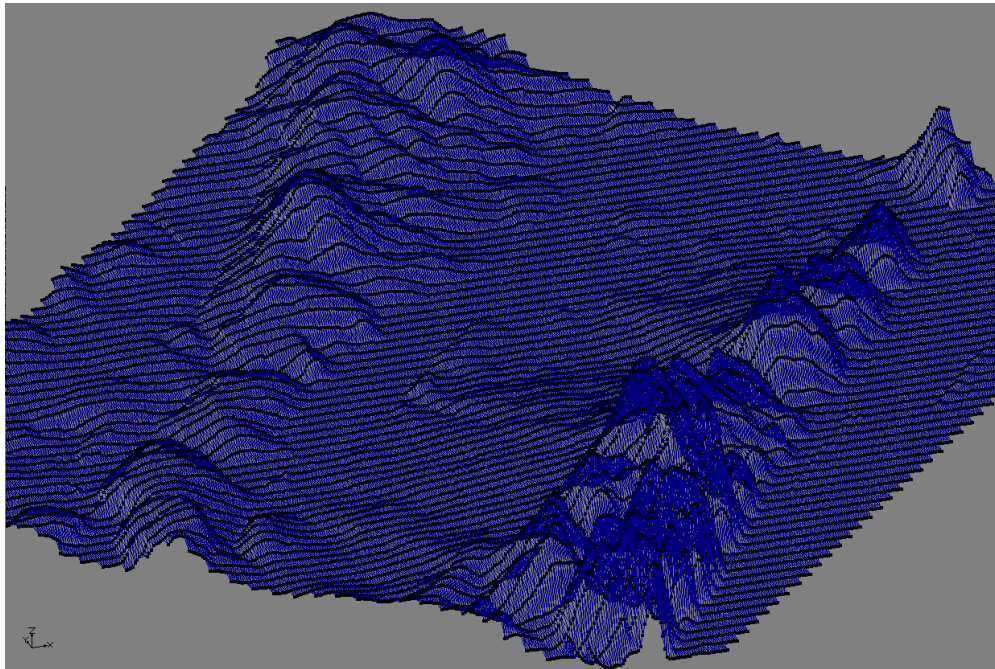


Figure 24. DEM data in the vicinity of the Bellefonte site, looking nominally to the NNE. A 10X vertical exaggeration is applied

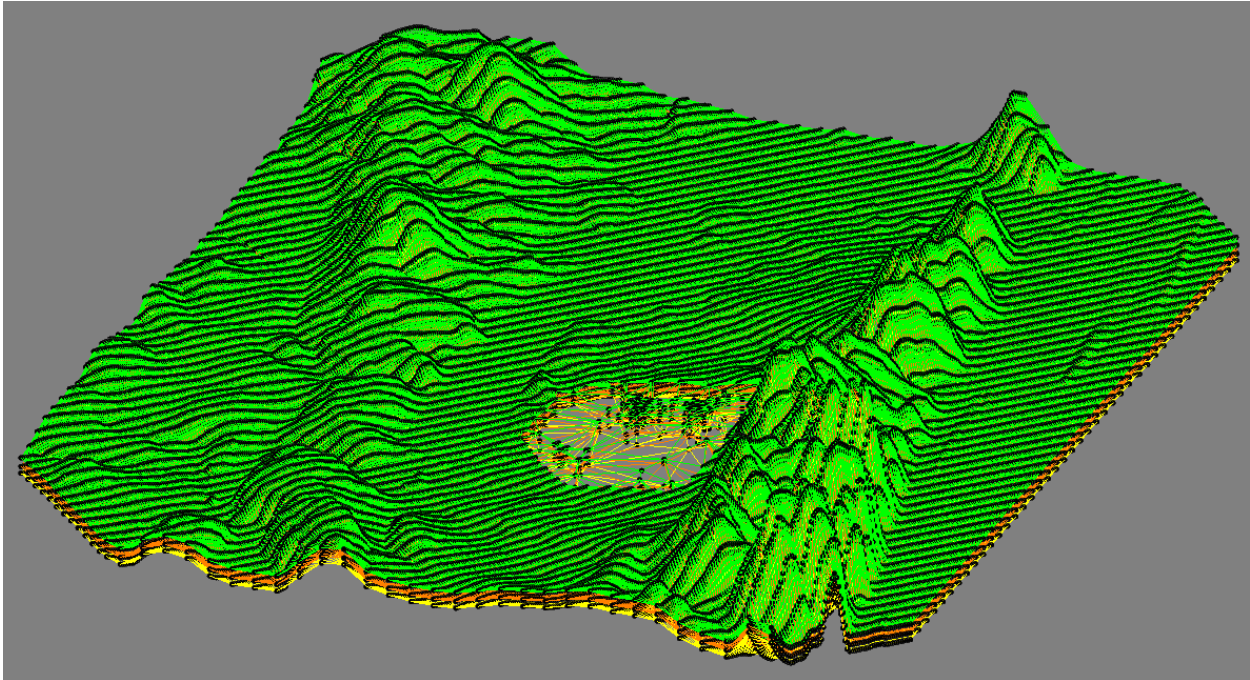


Figure 25. Set of TINs defining the Soil (between green ground surface and orange) and the Weathered Rock (between orange and yellow). The zone of low data density represents where ground surface elevations from wells at the Bellefonte site were used in place of the DEM data. The orange and yellow TINs are offset from ground surface by the nominal thickness of each material. View is nominally to the NNE with a 10X vertical exaggeration.

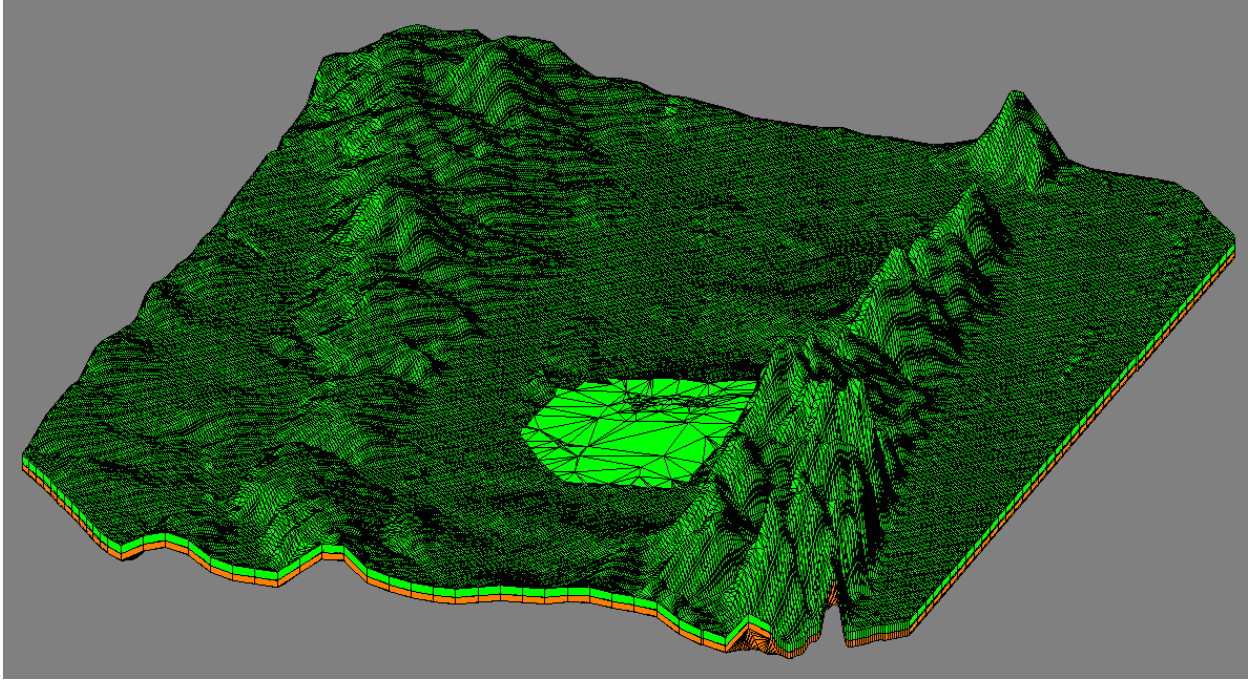


Figure 26. Solids models for the Soil and Weathered Rock (WeRo) materials based on a uniform thickness of each material from ground surface. View is nominally to the NNE with a 10X vertical exaggeration.

The borehole data (Table B.1) for the USR, MSR, and LSR bedrock units were read into GMS as separate 2D scatter data sets (x, y, height) and then converted to individual TINs as described above. Examination of these TINs (Figure 27) in three-dimensions reveals that they are nearly parallel planes. However, if each contact data set is fit to a plane and those planes are extended, it is seen that some of them intersect. Because the existing data are of limited spatial extent and need to be extrapolated (such that the TINs extend somewhat beyond the groundwater model domain) and because the contacts lay in nearly parallel planes, it was decided to use parallel planes to represent the contacts. The plane equations for the seven sets of contact data were averaged to arrive at a consistent plane equation, with an appropriate offset to the average center of each data set. The Nashville/USR contact consisted of a single data point, so the plane equation was applied through that point. The resulting set of TINs is shown in Figure 27. Flat TINs above and below the model domain extents were added and the entire set of 10 TINs was processed with the GMS “Horizons -> Solids” command to obtain a set of 9 solids (Figure 28).

Although the bedrock units have been defined along their contacts, additional solids are required to represent bedrock throughout the rest of the groundwater model domain. GMS allows the user to define “prisms” for solids with a drawn plan-view shape and specified top/bottom elevations. Prisms were drawn to represent the LSR and NV units to the northwest and southeast, respectively. This gave a set of solids representing the bedrock units (Figure 29) that then needed to be merged with the Soil and Weathered Rock solids. The GMS Solids module has an undocumented feature for performing set operations (union, difference, intersection) on two selected solids. Thus, a solid can be defined (using the prism tool or from TINs) to act as a clipping solid when performing a difference operation. The Weathered Rock TIN was used with a flat TIN of arbitrary high elevation to create a solid having the Weathered Rock solid bottom elevation. This clipping solid (Figure 29) was then differenced with each of the bedrock unit solids to produce solids that mesh precisely with the overlying weathered rock solid (Figure 30). Clipping solids were also used around the sides and the bottom to trim the solids to match the groundwater model domain, which resulted in the final set of solids shown in Figure 31.

4.1.2.4 Map the Geological Structure to a MODFLOW Domain

At this point the conceptual model, solids model, and initial model grid definition need to be brought together to map the hydrogeology to the MODFLOW groundwater model. Particular attention must be given to the expected water table elevation across the model domain; it is preferred to avoid grid cells going dry during the simulation, if possible.

GMS offers several approaches for mapping the solids model to the MODFLOW model grid, depending on which groundwater flow package is being used in MODFLOW: BCF/LPF or HUF. The Layer Property Flow (LPF) package is used most often in MODFLOW groundwater models; BCF (Block-Centered Flow) is essentially an older version of LPF and can be handled in a similar fashion. The GMS “Solids -> MODFLOW” command applies to the LPF package and can be done in three ways:

- **Boundary Matching.** Gives a deformed grid that matches the boundaries of the solids model; may result in very thin layers in places; cells have aquifer properties of the material intersecting the grid cell center.
- **Grid Overlay.** Gives a (potentially deformed) grid with uniform vertical cell thickness across all layers for any given vertical column of cells; cells have aquifer properties of the material intersecting the grid cell center.

- **Grid Overlay with K Equivalent.** Gives a (potentially deformed) grid with uniform vertical thickness for any given vertical column of cells across all layers; aquifer properties are specific to each grid cell (i.e., uncoupled from material definitions) and are effective values based on the proportions of materials intersecting the cell.

The choice of one of these three methods depends on the nature of the model and the modeling objectives.

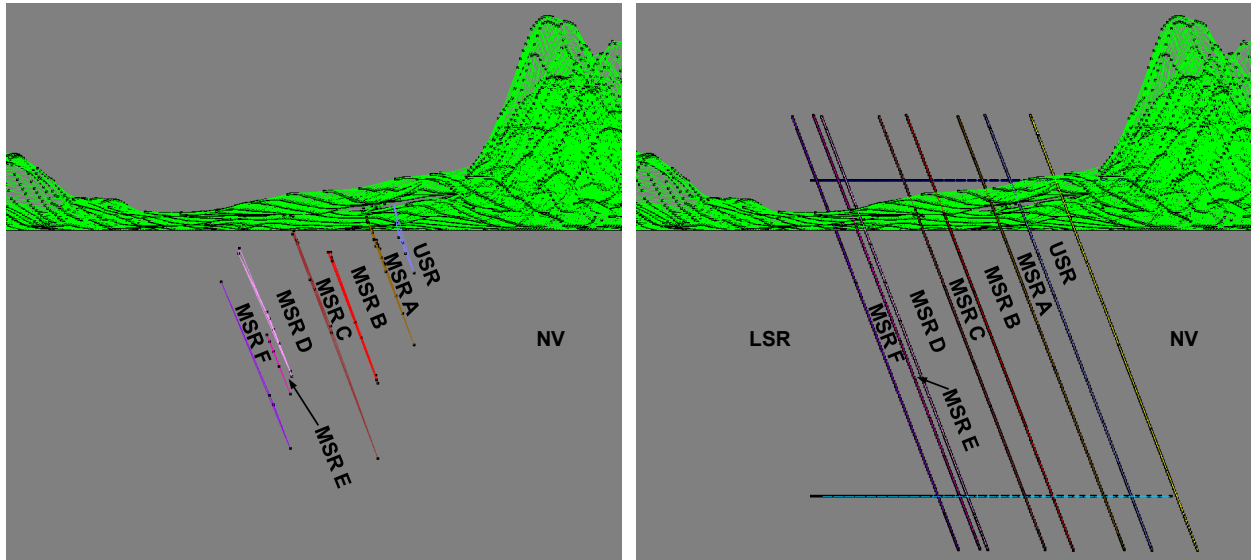


Figure 27. Examination of TINs representing the contacts between bedrock units. The left image depicts the TINs based on borehole data for contacts between the units, while the right image shows the parallel planes used to represent the unit contacts. The view is along a strike of 42.5° with a 10X vertical exaggeration.

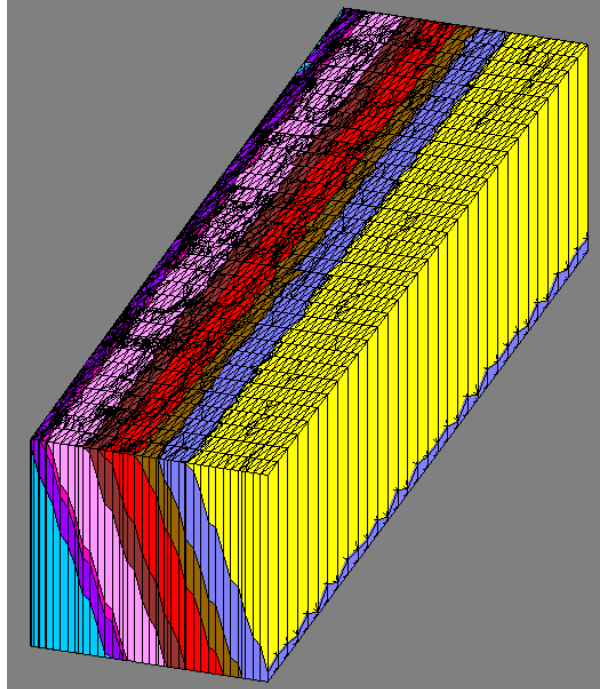


Figure 28. Solids representing the USR, the MSR units A to F, and the contacts with the NV and LSR units. View is nominally to the NNE with a 10X vertical exaggeration.

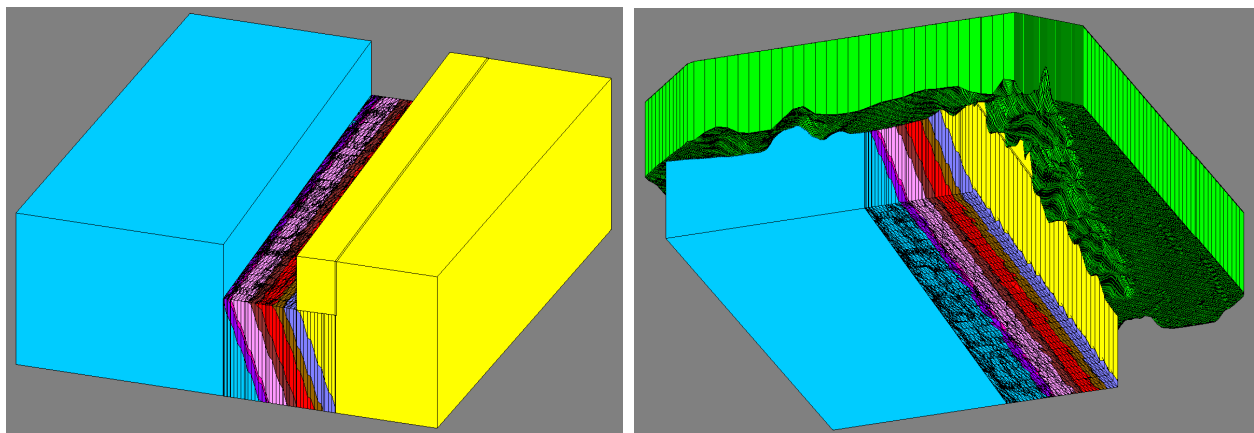


Figure 29. View of solids used to fill in space such that the groundwater model domain is encompassed (left) and the solid used for clipping the top of the solids representing the bedrock units (right). The rightmost block representing the NV unit has been hidden in the right image so that the variation of the clipping solid surface is visible. Note that although the clipping solid is green, it does not represent Soil. The view is nominally to the NNE with a 10X vertical exaggeration but with 25° (left) and -25° (right) dip viewing angles.

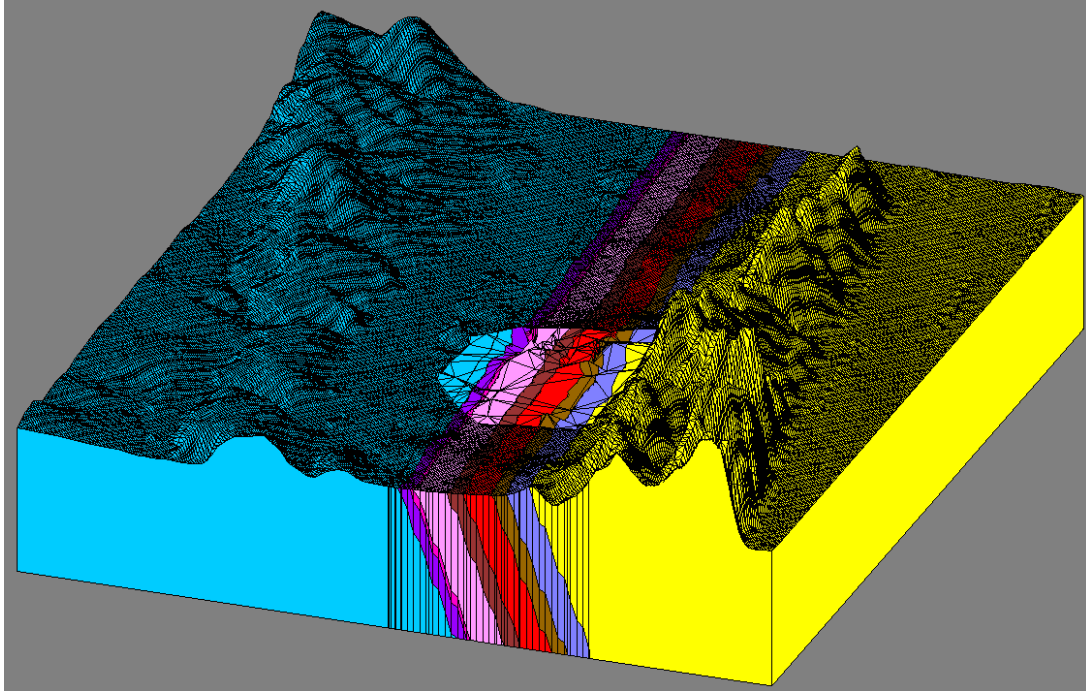


Figure 30. Solids representing bedrock stratigraphic units after being clipped so the top elevation matches with the bottom elevation of the Weathered Rock (WeRo) solid. View is nominally to the NNE with a 10X vertical exaggeration.

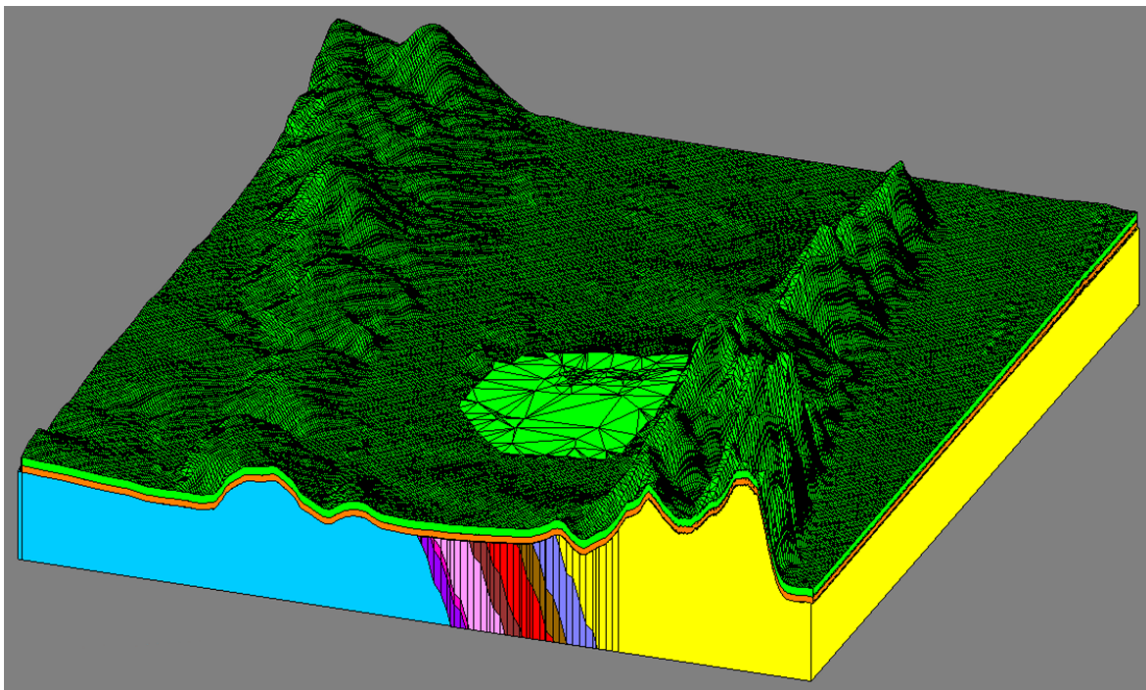


Figure 31. Final set of solids representing all materials and trimmed to the lateral and bottom extent of the groundwater flow model domain. View is nominally to the NNE with a 10X vertical exaggeration.

GMS also includes a “Solids -> HUF” command, which is applicable when the MODFLOW model uses the Hydrogeologic-Unit Flow (HUF) package. This process translates the solids models of hydrogeological units to appropriate HUF package definitions, retaining the elevations of the solids but not altering the MODFLOW grid. Thus, a given model grid layer could contain more than one hydrogeological unit. This approach requires that the user has chosen a meaningful grid definition (including the top elevation of the top layer), since the grid is not deformed to match the solids model. Additionally, the user must take care to avoid misleading images in GMS, because the HUF hydrogeological units do not affect the material definitions of the grid cells (i.e., displaying the materials assigned to each grid cell doesn't reflect the hydrogeological units of the HUF package).

For the model of the Bellefonte site, there are boundary conditions for Town Creek and the Tennessee River at an elevation of 594.5 ft (Section 4.1.1.5). Thus, it is expected that the water table will progress from some elevation around 630 ft in the River Ridge hills and hills northwest of Town Creek down to 594.5 ft.

An attempt to apply the GMS “Solids -> MODFLOW” command for the LPF package using the Boundary Matching option failed, either because the hydrogeological units are not horizontal layers or because of slight irregularities in the matching of surfaces between hydrogeological units. When the mapping to the LPF package is applied with either Grid Overlay option, the originally orthogonal grid becomes deformed as shown in Figure 32. This provides a good match to the solids model, but the water table will cut through multiple layers and the simulation will have dry cells (which may require the option of cell rewetting). It is challenging for most (if not all) MODFLOW solvers to converge to a solution even when grid cells that go dry are allowed to rewet (hence the preference for a model configuration that avoids dry cells).

To use the LPF package in MODFLOW and avoid dry cells, a single layer should contain the water table, but this cannot be accomplished with the mapping to the initial grid definition (Table 4). To obtain a single layer containing the water table, the solids model would have to be split, each portion mapped to a separate grid, then the grids manually combined. Selecting an elevation of 594 ft as the plane to slice the solids model into two pieces leaves ½ ft below the presumed lowest elevation of the water table (i.e., Town Creek/Tennessee River). The upper portion of this sliced solids model can be mapped to a 1-layer groundwater flow model grid. This will incorporate the topography and (when using the Grid Overlay method) assign the material for each grid cell based on the material at the center of the grid cell. The bottom half of the sliced model can be mapped to a 30-layer groundwater flow model grid, which will result in an orthogonal grid. Both of these MODFLOW groundwater models then need to be exported as “Native Text” (from the MODFLOW menu). To merge the files, data from the one-layer model need to be manually copied from the *.mfs, *.lpf, *.dis, and *.ba6 files (assuming that MODFLOW 2000 is being used) to the corresponding files for the 30-layer model (with appropriate adjustments to indices). The merged “native text” files can be loaded into GMS. The resulting MODFLOW groundwater model grid is shown in Figure 33. This approach is complicated, requiring a reasonable knowledge of MODFLOW input files, and the top layer material designations should be assessed to ensure that the appropriate material type (i.e., the dominant material through which groundwater flows) is represented.

The alternative to the above-described manipulations is to use the HUF package instead of the LPF (or BCF) package. When using the HUF package, a single model layer can be used for the water table, while the hydrogeological units defined in the solids model are applied for calculating groundwater flow. The initial model grid definition (Table 4) needs to be modified to apply the topography of the top of the solids model (i.e., the ground surface shown in Figure 25) to the top elevation of the uppermost grid layer. Then the GMS “Solids -> HUF” command can

be applied to map the solids onto the MODFLOW groundwater model. Selected cross sections depicting the hydrogeological units in the MODFLOW model grid are shown in Figure 34.

The HUF package was used because it not only affords a straightforward method of mapping the hydrogeological units to the MODFLOW model, but also because it facilitates modeling of alternative conceptual representations of the site. For the HUF package, the representation of the soil and rock units, derived from geotechnical borehole data and physically reasonable assumptions (as represented by the solids model), is independent of the grid discretization. Thus, changing the conceptual model can easily be done by either altering the solids model and re-mapping it to the MODFLOW model or by simply altering material parameter values. For example, to combine the soil and weathered rock units into a single unit entails nothing more than assigning identical values for the materials properties. Use of the HUF package also avoids potential anomalies in hydraulic head results that may occur with the LPF approach (Figure 33) that stem from assigning material properties using a categorization approach based on the material present at the center of a grid cell. The HUF package accounts for all units present within a grid cell (e.g., transmissivity is a sum of unit conductivities weighted by thickness of units within the cell).

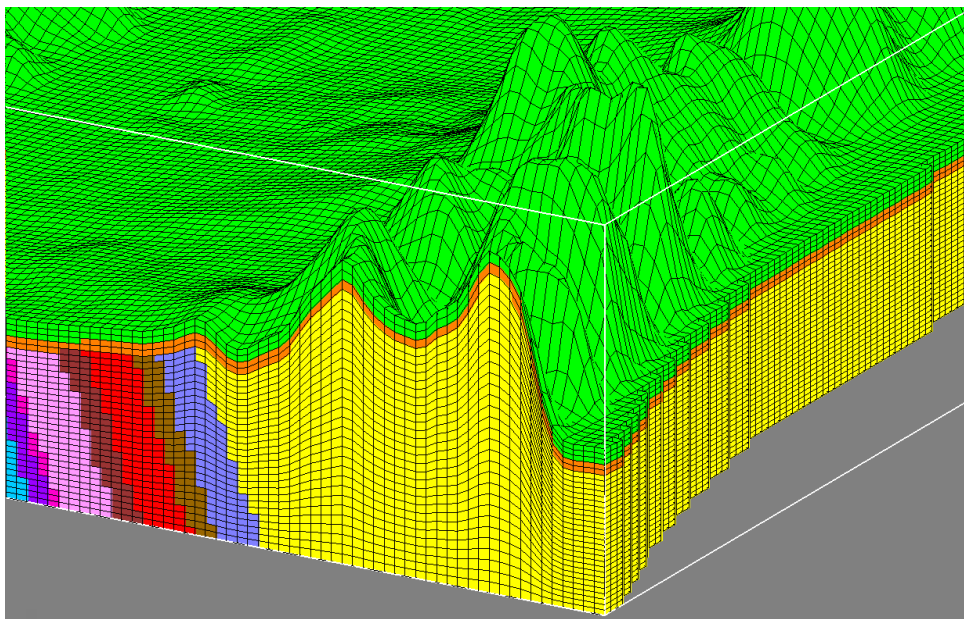


Figure 32. Deformation of an originally orthogonal model grid after mapping the solids model (Figure 31) to the MODFLOW LPF package using the Grid Overlay option. The grid layers follow the topography (using equal grid cell thickness for all layers in a given vertical column of grid cells). The water table would cut through multiple layers. View is nominally to the NNE with a 10X vertical exaggeration.

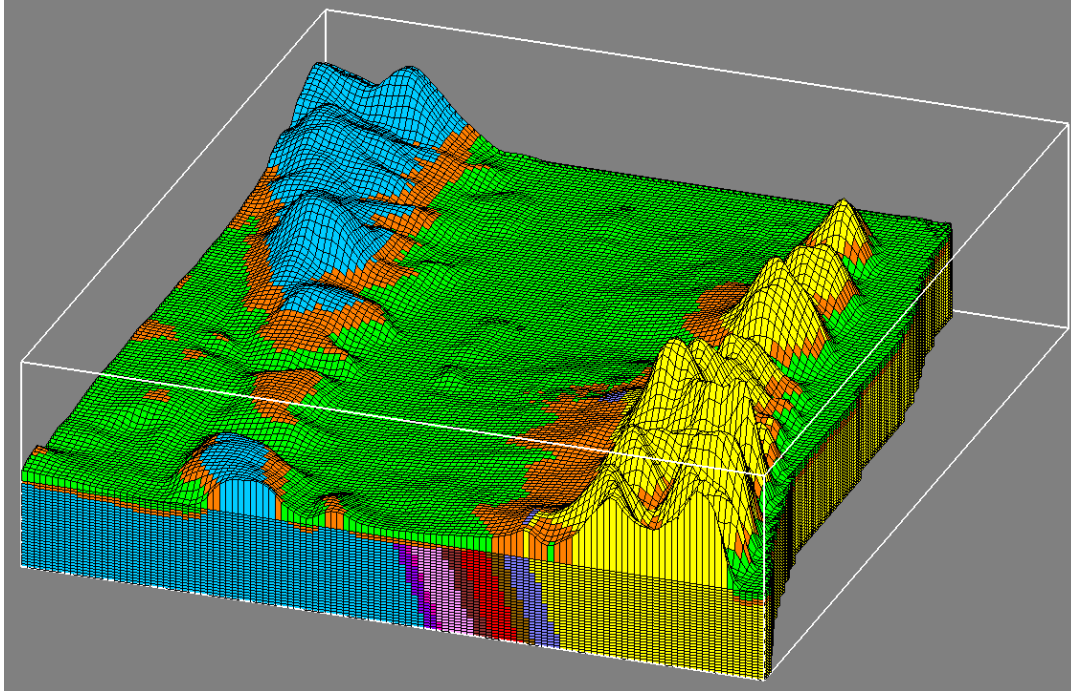


Figure 33. MODFLOW model grid for the LPF package, showing the materials (hydrogeological units) applied to the grid cells. This model was created by splitting the solids model into two portions, mapping (using the Grid Overlay option) to two model grids, and then merging both grids into a single model grid. Grid cells beyond the shoreline of the Tennessee River have been inactivated. View is nominally to the NNE with a 10X vertical exaggeration.

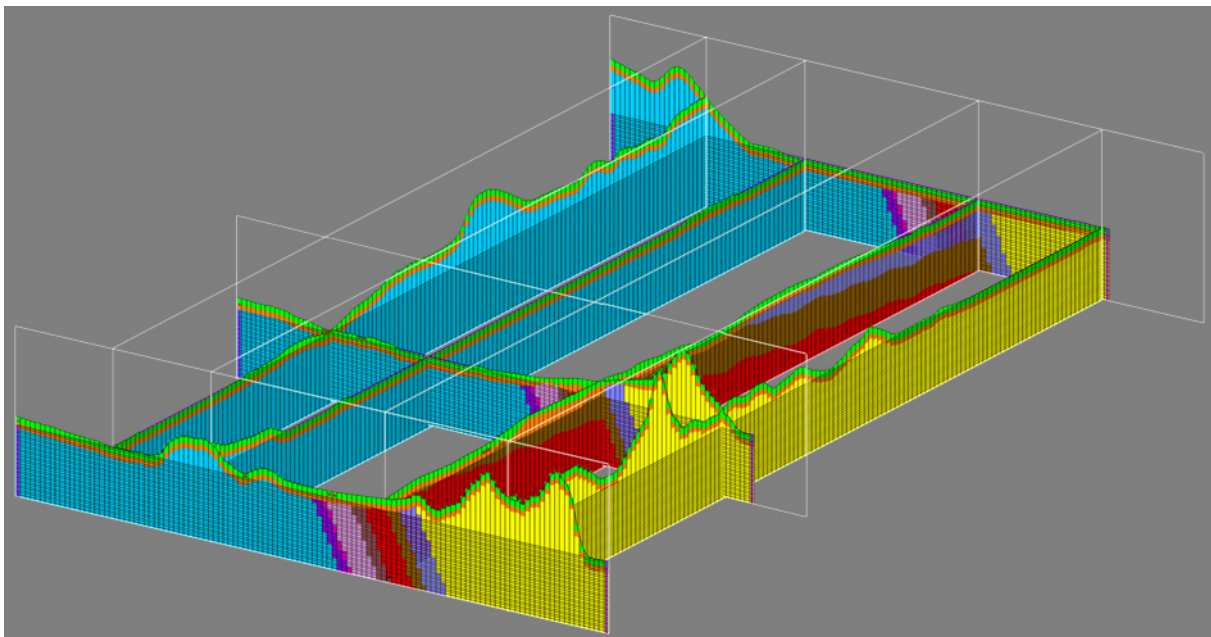


Figure 34. Fence diagram of MODFLOW model grid for the HUF package, showing the hydrogeological units applied to the grid cells along selected cross sections. View is nominally to the NNE with a 10X vertical exaggeration.

4.1.3 Configure the MODFLOW Model

With the groundwater flow model material types and grid structure defined, the temporal nature, boundary conditions, and initial conditions can be defined to complete the model configuration.

4.1.3.1 Temporal Nature of the Model

There are two choices for the temporal nature of a MODFLOW groundwater model: steady state or transient. A steady state model represents a set of constant conditions whereas a transient model will include variations in boundary conditions (e.g., river stage, recharge, pumping at wells, etc.) over time. For the Bellefonte site, there are no induced hydraulic stresses (e.g., wells) and the conceptual model (Section 4.1.1.6) assumed steady-state flow due to limitations in the data available to support a time-dependent numerical model.

4.1.3.2 Boundary Conditions on Sides of Model Domain

Grid cells on the southeast side of the model domain were inactivated such that the boundary followed the Tennessee River shoreline. This “downgradient” boundary was set to a constant hydraulic head of 594.5 ft to represent the river.

Constant head boundary conditions were assigned to the “upgradient” boundary at the northwest side of the model domain based on professional judgment in approximating interpolation of the 1961 data (Figure 35), ignoring wells impacted by pumping. The northwest model boundary nominally follows the Sequatchie anticline and a “valley” in the hydraulic head, except the northwest corner where the topography and groundwater hydraulic head rise. The set of boundary condition hydraulic head values for the northwest side is shown in Figure 36. Between specified points the boundary conditions are set by linear interpolation.

The northeast and southwest sides of the model domain are left as no-flow boundary conditions to match the conceptual model.

4.1.3.3 Boundary Conditions for Surface Water Features

Boundary conditions were set in layer 1 for surface water features inside the groundwater model domain. The entirety of Town Creek and inlet for the nuclear plant water intake were set to the same constant head as the Tennessee River (594.5 ft). The five streams identified as draining into Town Creek were represented as drain boundary conditions, which allow withdrawal of water from the model domain when the groundwater hydraulic head is above the bottom elevation of the drain. The bottom elevation of each drain was specified at the head (or model boundary) for each stream and was linearly interpolated to the elevation of Town Creek (594.5 ft) along the line representing the path of the stream. The conductance (i.e., proportionality factor for flow through the bottom of the drain that accounts for hydraulic conductivity and drain dimensions) of each drain was given a large value of 100 ft²/d per ft, and GMS calculated the length of the stream through each grid cell. The stream paths and the drain elevations at the head of each stream are shown in Figure 36.

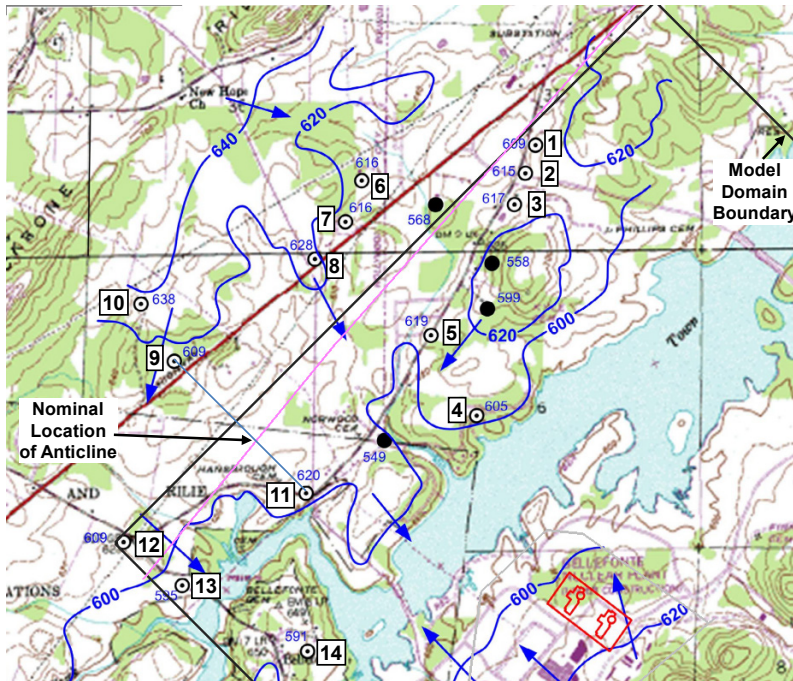


Figure 35. Hydraulic head data from 1961 relative to the model domain boundary. Data from numbered wells were used to define the boundary conditions along the northwest side. Filled circles indicate wells impacted by pumping and thus not used in this analysis.

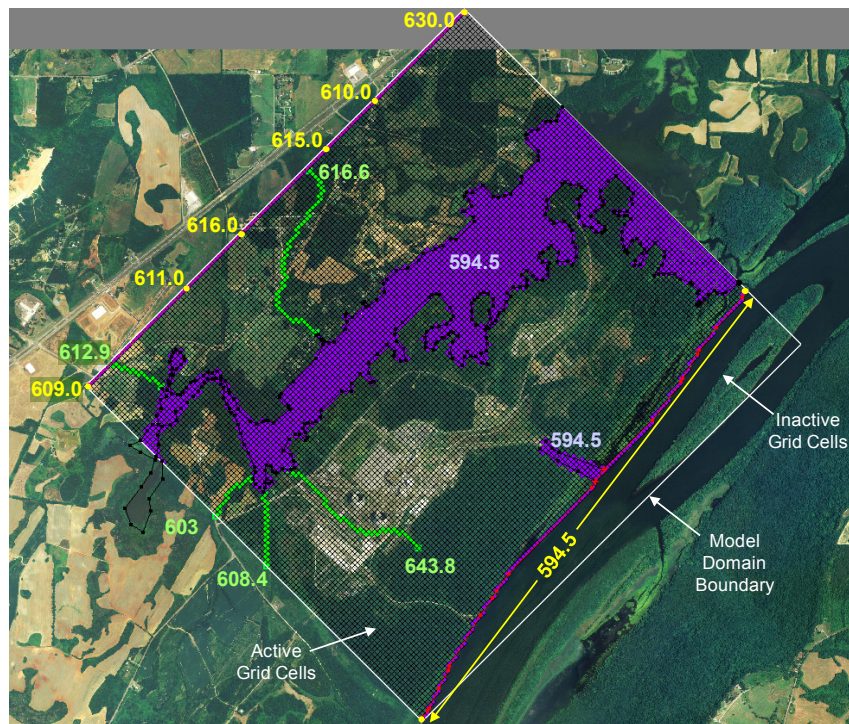


Figure 36. Boundary conditions for the groundwater model. Internal boundary conditions (green drain and purple constant head) apply to layer 1, others (yellow) to all layers.

4.1.3.4 Recharge Boundary Conditions

The plan view of the model domain was divided into several zones for specifying the recharge (from precipitation) based on nominal land usage. The zones, shown in Figure 37, included:

- The northwest portion of the model, a mixture of forest, farmland, and sparse residential development,
- The lowlands on the southeast side of Town Creek, consisting of forest and wetlands,
- The developed area encompassing the existing Bellefonte Nuclear Plant and associated facilities, and
- The River Ridge highlands along the Tennessee River, primarily forest with a few clearings.

No recharge was applied over the area of Town Creek itself. The initial recharge rate was taken to be 8 in/yr (0.00182 ft/d) based on TVA (2009).

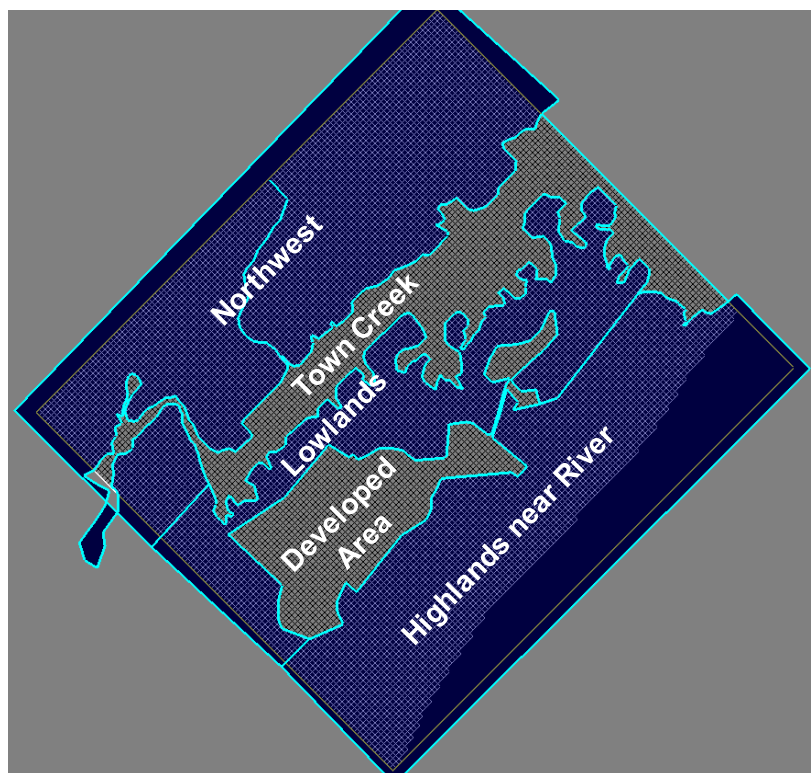


Figure 37. Zones for the recharge boundary conditions

4.1.3.5 Initial Conditions

Initial conditions for a MODFLOW model consist of the hydraulic heads for each active grid cell. Where constant head boundary conditions are specified, the boundary condition is taken as the initial condition. For a purely transient simulation, a good set of initial conditions is critical to obtaining meaningful results. For a steady state simulation, the closer the initial conditions are to the solution, the more easily the solver will converge. However, it is reasonable to begin a steady state simulation with initial conditions that are relatively far from the final solution. One approach is to guess the water table based on observed data. Another approach is to set the initial hydraulic heads to some high value and let the heads settle down to the converged

solution. Reasonable high values would be ground surface or some constant value that is above the expected water table across the model domain. For this work, an initial hydraulic head of 750 ft was specified for all grid cells that did not have a constant head boundary condition. Once a reasonable head solution was obtained, this solution was used as the initial condition for subsequent simulations.

4.1.3.6 Configured Model

The boundary and initial conditions described above were applied to the MODFLOW groundwater model grid/hydrogeological structure defined based on using the HUF package. The resulting model, showing materials and boundary conditions (except recharge), is presented in Figure 38. Alternative models were formulated from this initial model configuration to represent model uncertainties.

4.2 Model Calibration

Groundwater flow model calibration is the process of adjusting model parameters to obtain a hydraulic head distribution that best matches the observed values for hydraulic head and (if available) the observed discharge of ground or surface water. There are two basic approaches to calibration: directed trial and error or automated parameter estimation. The trial and error approach involves manual adjustment of parameter values based on the conceptual model and knowledge of the site data. Automated parameter estimation is a process using optimization techniques (e.g., the Levenberg-Marquardt algorithm) to find the hydraulic head solution with the minimum error in the calibration targets, and was used here.

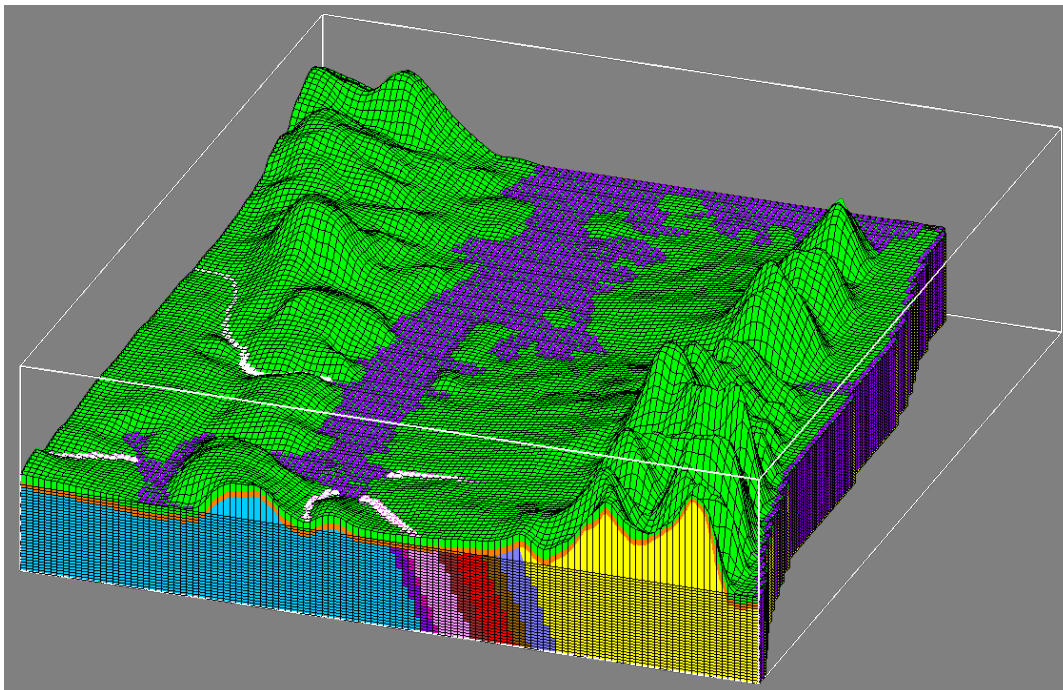


Figure 38. MODFLOW groundwater model for the Bellefonte site as configured with the hydrogeological units (HUF package), constant head boundary conditions (purple points), and drains (white points)

4.2.1 Define Calibration Targets

The three data sets of observed hydraulic heads at monitoring wells discussed in Section 4.1.1.5 were used for hydraulic head calibration targets. Despite the age of the 1961 observations relative to the other data sets, the older data set provided important information at points in the northwest area of the model domain at a distance from the actual Bellefonte site. The September 2005 data provided information across much of the area between Town Creek and the reservoir. The June 2006 through May 2007 data set, which primarily includes locations in the vicinity of the proposed reactors, was split into two groups (Soil and Bedrock) for display purposes. To reflect the steady-state flow assumption, the average head values for the 2006/2007 period were used as the calibration targets. The average range in head over the observation time period was 5.3 ft (1.6 m) for the soil wells and 5.7 ft (1.7 m) for the bedrock wells (see Figure 21 for an example).

Calibration weights were based on assumed error intervals for the head observations of ± 5 ft for the 1961 data, ± 2 ft for the September 2005 data, and ± 1 ft for the June 2006 to May 2007 data. These assumed errors reflect the differences in time of the observations and the relative uncertainty in the 1961 measurements. Better estimates of observation errors could be obtained with more information about the head measurements. Observation standard deviations were computed by assuming normally distributed head errors and that the error intervals represented 95% confidence values. Calibration weights were then entered as the inverse of the head observation standard deviations. Values are given in Table 5.

Table 5. Head observation error intervals, standard deviations, and calibration weights

Dataset	95% Interval (ft)	Std. Dev. (ft)	Weight (ft ⁻¹)
1961	5	2.55	0.39
2005	2	1.02	0.98
2006-07	1	0.51	1.96

Locations of the head data points used as calibration targets are shown in Figure 39; head values are listed in Table B.3 of Appendix B. There are no flow calibration targets for this site. The implications of this are discussed in Section 4.2.4.

4.2.2 Define Parameters for Estimation

The parameters selected for estimation during calibration were the horizontal hydraulic conductivity of each material type and the recharge. For calibration purposes, the bedrock units identified at the site were divided into two groups, with each unit in a group assigned the same parameter values. One group included the bedrock units characterized as prominently silty/argillaceous limestone: the Middle Stones River subunits A, C, and E (shaded in Figure 14). The other group included all other bedrock units. In addition to these two bedrock groups, parameters were estimated for the soil material and for the weathered rock material. For each material type, vertical hydraulic conductivity was tied to the estimated value of the horizontal hydraulic conductivity and assumed to be a factor of 10 smaller (i.e., anisotropy ratio of 10). Initial parameter values were based on the geometric mean values provided in Table 1 and the average recharge discussed in Section 4.1.3.4. Calibrated values were determined to be insensitive to the initial parameter values. Minimum and maximum parameter limits were set sufficiently small/large such that they did not restrict the final estimated parameter values.

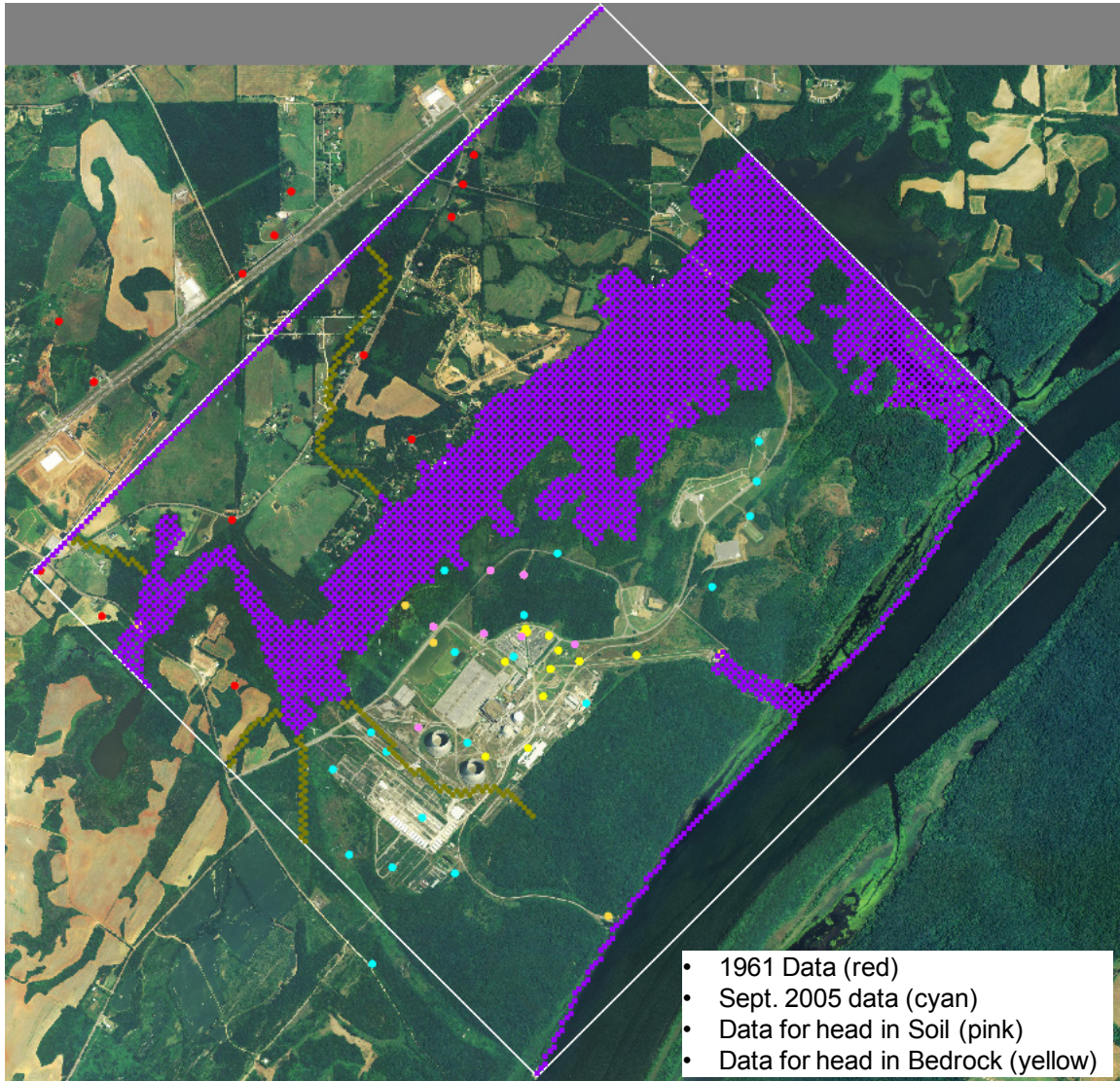


Figure 39. Locations of hydraulic head calibration targets for the four groups of data. Points outside the model domain boundary were not included as calibration targets.

4.2.3 Calibration Results

An initial calibration was carried out to evaluate the ability of the calibration code to produce a reasonable solution. To improve the robustness of the parameter estimation, all recharge zones except Town Creek were grouped together and given the same recharge rate. Calibration was completed using PEST with the PEST input files constructed by GMS. Hydraulic head results for the optimal solution returned by PEST are shown in Figure 40. Flooded cells indicate locations where the hydraulic head of the groundwater exceeded the ground surface elevation, which are interpreted here to represent expected conditions (e.g., along the Tennessee River), and artifacts of the resolution of the ground elevation data or minor errors in the assigned drain elevations. Flooded cells could also indicate problems with the model configuration, such as streams that should have been included or drain conductances that should be increased.

Head residuals (the difference between the observed value and the simulation result) are shown in Figures 41 to 44. The residuals in these figures are shown as colored circles where the area of each circle is proportional to the magnitude of the residual. Positive residuals (blue) indicate a simulation result that is lower than the observed hydraulic head; negative residuals (pink) indicate a simulation result higher than the observed head. The majority of the residuals in the area of the proposed reactors were negative, except for the soil wells shown in Figure 44. The four soil wells with the largest positive residuals were all indicated to be nonresponsive in FSAR Table 2.4.12-204, which suggests that these residuals should be discounted when evaluating the model.

Different scales are used for the display of residuals in Figure 41 to Figure 44 so that they are not directly comparable. It can be seen, however, that the residuals frequently are larger in magnitude than the estimated error intervals of the head observations. In fact, the least squares standard error for the calibration [$\hat{\sigma}_{LS}$, see discussion after Eq. (14)] was 8.0, indicating that the fit is inconsistent with the observation weighting (Hill and Tiedeman 2007). This may indicate some structural errors in the model. Additional discussion of the residuals can be found in Section 4.4.1.



Figure 40. Hydraulic head contours (every 2 feet) resulting from the initial PEST calibration

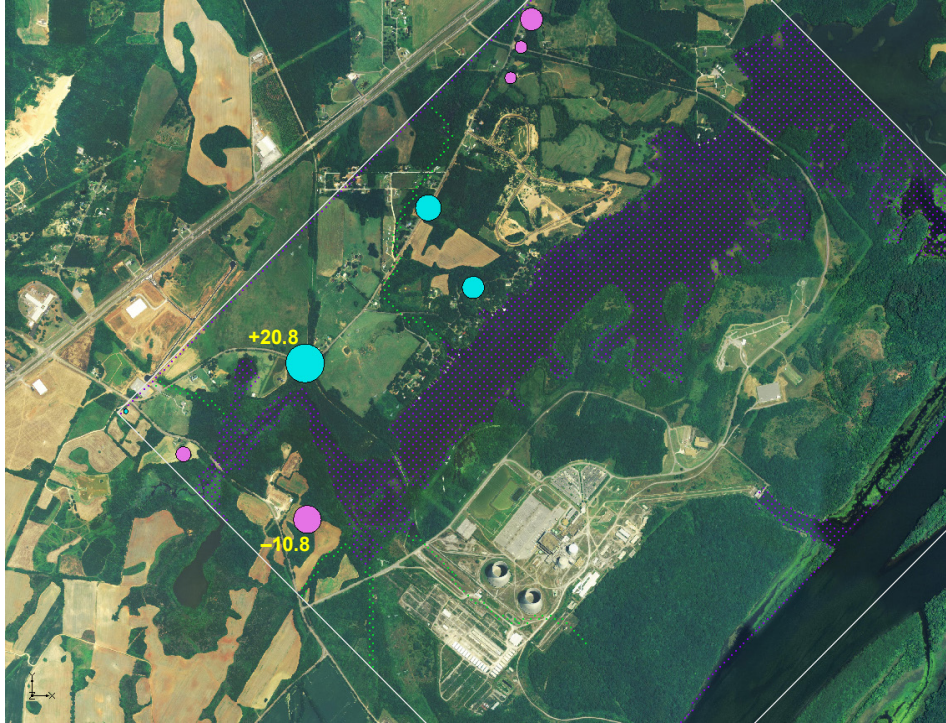


Figure 41. Unweighted residuals (observed minus simulated, in feet) for the 1961 data. Positive (blue) and negative (pink) residual magnitudes are proportional to symbol size.



Figure 42. Unweighted residuals (observed minus simulated, in feet) for the September 2005 data. Positive (blue) and negative (pink) residual magnitudes are proportional to symbol size.

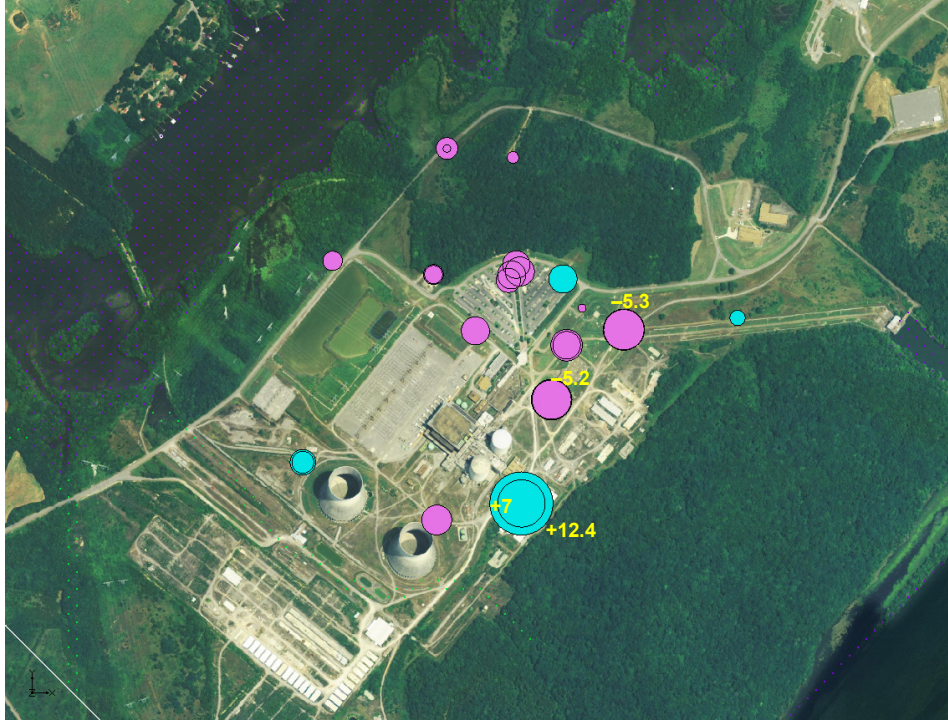


Figure 43. Unweighted residuals (observed minus simulated, in feet) for the average 2006/2007 “Bedrock” data. Positive (blue) and negative (pink) residual magnitudes are proportional to symbol size.



Figure 44. Unweighted residuals (observed minus simulated, in feet) for the average 2006/2007 “Soil” data. Positive (blue) and negative (pink) residual magnitudes are proportional to symbol size.

4.2.4 Define Prior Parameter Information

At the Bellefonte site, the data available for use in calibration are limited to hydraulic heads at wells. This is an issue because the groundwater flow at the site is governed by the amount of recharge and the hydraulic conductivity. Recharge and hydraulic conductivity will be positively correlated in any calibration carried out using heads alone as the basis for the parameter estimation. This is illustrated for the Bellefonte site model in Figure 45 which shows calibrated values of hydraulic conductivity when recharge was fixed at three values (4, 8, and 12 in/yr). (This is for a model with a single hydraulic conductivity parameter for all hydrogeologic units.) The calibrated hydraulic conductivity value depends linearly on the value of recharge. The 95% confidence limits shown on the figure indicate that hydraulic conductivity can be fit with little uncertainty when the recharge is known. However, no unique solution can be determined when both hydraulic conductivity and recharge are estimated using head data only.

Ideally, there would be some flow observations at the site that would constrain the parameters and allow a unique solution. At the Bellefonte site, however, there are no significant streams on site at which flows could be measured. The boundaries of Town Creek and the reservoir are relatively constant due to the reservoir control and are not responsive to groundwater conditions. Flow parameters could also be constrained by transport observations (e.g., results of a tracer test), but such data are not available at the Bellefonte site and are typically not collected during site characterization for a nuclear power plant.

In the absence of flow observations, prior information on the values of hydraulic conductivity and recharge were used to constrain the calibration. This required prior information equations to be used in the objective function with suitable weights representing the errors in the prior estimates. Hill and Tiedeman (2007) recommend caution in using prior information (Chapter 11, Guideline 5), preferring instead to initially estimate parameters without any prior information to understand the information that is directly available from the observations alone. For the Bellefonte site, that approach requires that either the recharge or the hydraulic conductivity be estimated, but not both due to the correlation. Fixing a parameter during the calibration is equivalent to applying a prior estimate with an infinite weight. This will cause the uncertainty of the fitted parameter to be underestimated. Thus prior information was applied to both the hydraulic conductivity and the recharge.

The optimization balances (via user-supplied weights) the prior information and the head observations to provide unique estimates and uncertainties that reflect the combination of head data and prior information. Figure 45 shows the solution for the homogeneous model when prior information on recharge and hydraulic conductivity were included. The 95% confidence intervals on the parameter estimates reflect the parameter correlation and the relatively large standard deviations (small weights) used for the prior information. The large magnitude of the confidence intervals indicates that, although the prior information has provided unique parameter estimates, other combinations of parameter values are almost equally likely.

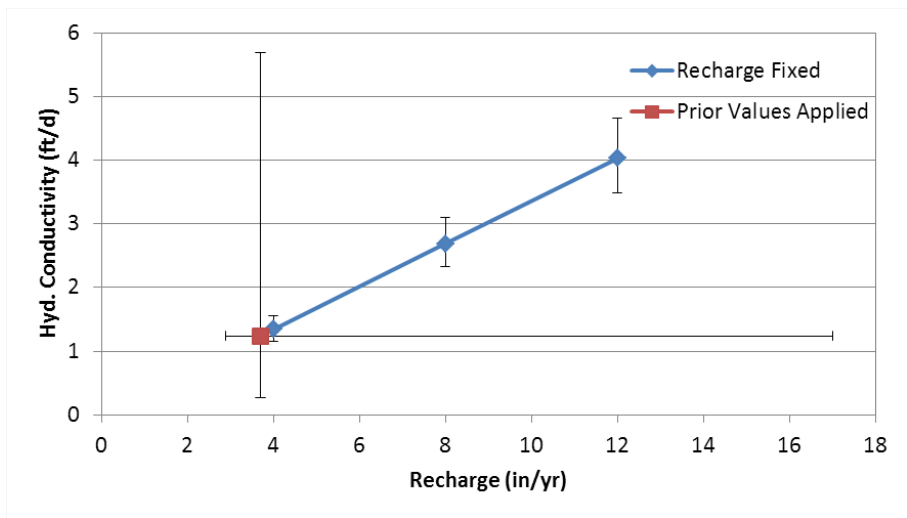


Figure 45. Correlation between hydraulic conductivity and recharge prevents unique parameter estimates unless one value is fixed (e.g., recharge here) or prior values of parameters are applied. Here the prior mean recharge was 8 in/yr; the prior mean hydraulic conductivity was 0.438 ft/d.

At the Bellefonte site, prior information for the hydraulic conductivity (as provided in the FSAR) included a range for the hydraulic conductivity of the soil and a range for the bedrock plus a single point on the cumulative distribution function for the bedrock pressure test data. That is, the application did not provide the set of hydraulic conductivity measurements, but a summary of those measurements consisting of the minimum and maximum values measured and a statement that a specific percentage of measured values were less than a specified value. In an actual review, the full set of actual measurements would be obtained through a request for additional information. Statistical analysis of these data could then be completed to develop the prior information mean and weight. For this example, however, an assumption was made that the hydraulic conductivity followed a lognormal distribution and that the ranges provided represented 95% probability intervals. From this assumption the parameters of the hydraulic conductivity distribution for each dataset listed in Table 1 were determined. The mean value was used as the prior estimate and the inverse of the standard deviation was used as the prior equation weight. Results for the bedrock datasets were arbitrarily assigned to the three hydrogeologic parameter groups: Unit 3 and 4 packer test data to the weathered rock, Unit 1 and 2 packer test data to the silty limestone units, and Unit 3 and 4 pump test data to the remaining rock units.

Prior information for the Bellefonte site recharge included only a point estimate (8 in/yr). It was assumed that this represented the geometric mean of a lognormal distribution, and that there was a $\frac{1}{2} \times 95\%$ probability that the recharge was between 4 and 8 in/yr. From these assumptions a weight for the prior equation was determined. Prior parameter distributions are shown in Figure 46.

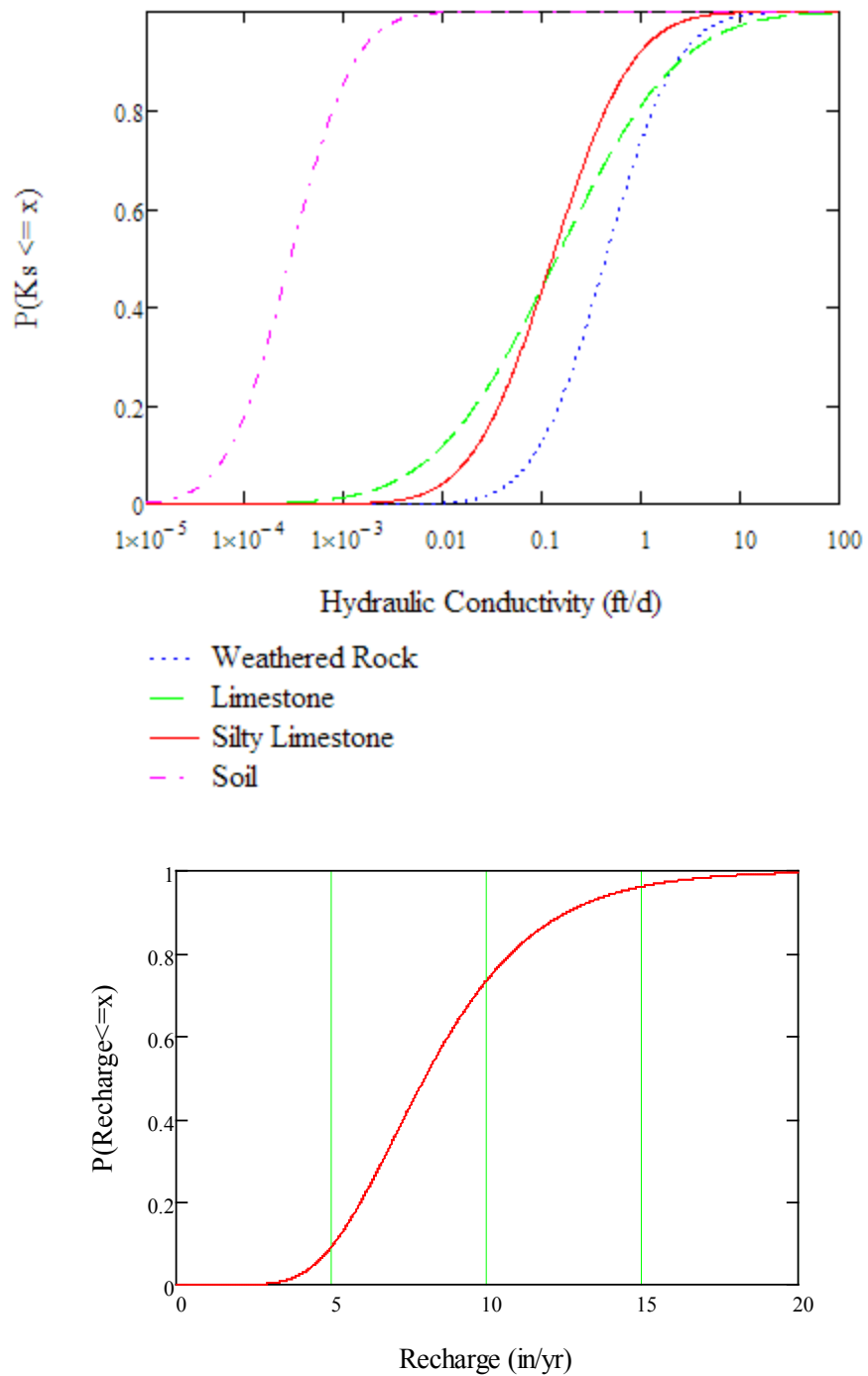


Figure 46. Prior parameter distributions derived from data and assumptions discussed in the text: horizontal hydraulic conductivity (top) and recharge (bottom)

As discussed by Ye et al. (2008), when prior parameter estimates are available, they can be incorporated in the calibration dataset (Cooley 1983; Carrera and Neuman 1986) and the observation weight matrix. Use of prior parameter estimates is implemented in both PEST and UCODE. The uncertainty methodology described in Section 3.1 requires that the same set of

data be applied to the calibration of each alternative model. This condition will not hold, however, when prior parameter estimates are included in the least squares objective function for alternative models with differing numbers of estimated parameters. This can have a significant impact on the calculation of model selection criteria such as AIC and KIC. Resolution of this issue has not been addressed in the literature. Possible approaches are to:

- Calculate the model selection criteria using only the system state observations (groundwater head in this example). In this option, the prior parameter estimates are used in the calibration, but not in the calculation of $\hat{\sigma}_{ML}^2$ in Eqs. (20) and (21).
- Include prior parameter estimates only for parameters common to all the alternative models.
- Include extra prior parameter equations in those models with fewer estimated parameters so that the effective number of prior data contributing to the objective function in each model is the same.

For this example, the last option was used. It was implemented by increasing the weight of a prior estimate, to provide the effect of adding one or more duplicate prior data. For example, a model with one recharge parameter for each recharge zone identified in Figure 37 would have four prior parameter estimates. An alternative model with a single parameter characterizing recharge across the domain would have one prior parameter estimate. By increasing the weight of this single prior estimate by a factor of four (the weight being the inverse variance of the estimate) the effective number of prior recharge estimates contributing to the objective function was increased to four. (In PEST and UCODE the prior weights are entered as the inverse standard deviation; these were increased by a factor of two to get the equivalent result.)

4.3 Alternative Models Evaluated for the Bellefonte Site

The uncertainty methodology represents model uncertainty using a set of alternative models. For this example application, the conceptual issues considered were the degree of karst development, the importance of the argillaceous bedrock layers, the depth of active flow, and the variation in recharge. Since no karst-specific flow features (e.g., springs or large conduits) were identified in the site characterization, a distinct weathered rock layer is the only model element representing karst development. Similarly, the importance of the argillaceous layers is incorporated in the model through their explicit representation as separate hydrogeologic units. Variation in recharge is represented through the use of multiple recharge zones.

The alternative models were formed by considering combinations of alternatives for three aspects of site conceptualization and parameterization. These three aspects were the representation of the individual hydrogeologic units, the recharge, and the depth of active flow. The hydrogeologic units (via their respective hydraulic conductivity values) and the recharge were expected to control groundwater flow at the site. The depth of significant porosity development (through weathering and cavity formation) is a key aspect of the conceptual model of groundwater flow described above.

4.3.1 Hydrogeologic Unit Representation

The following options were considered for the representation of the identified hydrogeologic units.

1. A homogeneous domain in which all units had the same properties.
2. A two-zone domain in which the upper zone included the soil and weathered rock units and the lower zone included the other rock units.

3. A three-zone domain in which the upper zone included the soil and weathered rock units and the remaining rock units were represented by one of two sets of properties, those for the limestone units (NV/USR, MSR-B, MSR-D, MSR-F, and LSR) and those for the silty/argillaceous limestone units (MSR-A, MSR-C, and MSR-E).
4. A four-zone domain in which the soil and weathered rock units were represented distinctly and the remaining rock units were represented as in option 3.

Alternatives were implemented in GMS by modifying parameters of the hydrogeologic units on the Materials page.

4.3.2 Recharge Representation

Two options were considered for recharge.

1. Recharge was homogeneous across the site.
2. Recharge was varied across four zones representing (a) the surface across Town Creek, (b) the vegetated lowlands on the plant side of Town Creek, (c) the area developed for the plant with minimal vegetation, and (d) the uplands between the plant and the river.

Alternatives were implemented in GMS by changing the recharge zone assignments in the Map module.

4.3.3 Depth of Active Flow

Two options were considered for the depth of active flow.

1. A deep domain extending to an elevation of 450 ft. msl (the existing 31 layer MODFLOW model).
2. A shallow domain extending to an elevation of about 541.52 ft. msl. This depth is 54 ft. below the elevation of the river and Town Creek.

The shallow domain option represents a case in which the significant rock porosity is limited to the upper portion of the rock units. This conceptualization was implemented in the MODFLOW groundwater model by inactivating all but the top 12 layers. All head observation points are located in the top 12 model layers except for MW-1204c, which has a screen mid-point elevation of 509.35 ft.msl. Because the multi-model comparison requires that all models use the same data, the elevation of the MW-1204c observation point was set to 542 ft. msl to include this data point in the active model domain for this conceptualization. This was not anticipated to significantly affect the model comparison since it involved a single observation's contribution to the regression objective function, the vertical variation in head at that depth was small in the deep domain models (particularly for the more homogeneous models), and the residual for the MW-1204c observation was relatively small in the deep domain models.

4.3.4 Alternative Model Designations

There are 16 possible combinations of the three conceptual model aspects described above, leading to 16 alternative models. Each of the alternative models was designated by a six-character name in the form of H?R?D?, where the ? characters were replaced by the option numbers as listed above. For example, model H4R2D1 was the model with four hydrogeologic zones, four zones of recharge, and a deep domain.

4.4 Calibration Implementation

The primary calibrations completed for the example were conducted using GMS and PEST. Because the implementation of PEST within GMS has some limitations, the PEST input files were generated from within GMS, but the actual execution of PEST was completed as a stand-alone code (i.e., from the Windows OS environment). The basic steps required to complete the calibrations were as follows.

1. Develop the groundwater flow model within GMS. Enter key values (usually negative numbers) for those parameters to be estimated using PEST. In the example, key values were entered in the Map module for the recharge zones and in the Materials window for the hydraulic conductivity.
2. Enter parameter information in the GMS-MODFLOW-Parameter window. This includes the initial parameter values, minimum and maximum values, selections for the log transformation option, and designating tied values, among other options.
3. Execute a forward run of MODFLOW from GMS and evaluate the flow solution for the initial parameter values.
4. Generate the PEST input files (control, template, and instruction files) by executing a parameter estimation run of MODFLOW from within GMS. Terminate this run after initiation is complete and PEST execution begins.
5. Using a text editor, modify the PEST control file (*.pst) generated by GMS to include the prior information equations.
6. Execute PEST. In the example, Parallel PEST was executed from the Windows OS using a custom script file.
7. Import the optimal parameters determined from the PEST execution (the *.par file) back into GMS from the GMS-MODFLOW-Parameters window.
8. Execute a forward run of MODFLOW from GMS using the optimal parameter values and evaluate the results.

Because the calibration is executed from outside GMS, a similar set of steps could be completed using UCODE instead of PEST. This would require a couple of extra steps, however, to translate PEST input files to the UCODE format and to get the optimal parameters back into a GMS-readable file.

4.4.1 Model Evaluation

Two of the calibration steps above involve evaluating the model results, once with the initial parameter values to ensure that the calibration begins at a reasonable solution and once with the optimal parameter values to ensure that the results are acceptable. GMS was used in a visual evaluation of heads (Figure 40) and in evaluating flow pathways computed using MODPATH as shown in Figure 47 (model H4R1D1) for a plan view and across-section through the Units 3 and 4 reactor areas. All pathways terminate in Town Creek and some extend to a significant depth (note 10x vertical exaggeration). This suggests that the depth of the flow domain has a significant impact on flow pathways and potentially travel times.

Some model evaluations were more appropriately completed outside the GMS environment because GMS has limited statistical analysis and graphing capabilities. These evaluations were completed using custom spreadsheets (see Figure C-1 of Appendix C for an example). Text file output from PEST was either copied or imported into the spreadsheets. Output used included the list of measured values, simulated equivalents, calibration weights, and calculated residuals. Estimated parameter values, 95% linear confidence limits, and the reported parameter

estimation covariance matrix were also included in the spreadsheets. A statistical evaluation of the residuals was completed using the integrated spreadsheet graphics capabilities.

Results were evaluated for each of the alternative models discussed above. The standard error of regression varied from 7.9 to 10.8 with the results shown below being typical for the majority of the alternative models. There were only small differences in the head residuals between the deep and the shallow domain models.

Several of the plots used for model evaluation are shown in Figure 48 for the H4R1D1 model, including plots of measured heads and weighted residuals versus the simulated (modeled) equivalent heads, a boxplot of weighted residuals, and a quantile-quantile plot of weighted residuals (constructed following Helsel and Hirsch [2002]). These plots were used to evaluate the quality of the model fit and randomness of the residuals to determine whether the predicted values and predictive uncertainty could be accurate. The magnitudes of the unweighted head residuals were generally less than 10 feet, although these exceeded 20 feet in the extreme cases. Residuals appeared to increase with the magnitude of measured heads, indicating a possible structural error in the model. The quantile-quantile plot indicates that the weighted residuals are not normally distributed and suggests that the distribution is influenced by a number of outliers. The boxplot in Figure 48 shows that five of these outliers are positive (i.e., the simulated equivalents were less than the measured heads), with a single negative outlier.

Three of the positive outliers were measured in observation wells completed in the soil zone and located near each other between the proposed units (see Figure 44). According to footnotes in FSAR Table 2.4.12-204 (TVA 2009), these wells exhibited a slow response during monitoring; observed heads may be unrepresentative of actual conditions. They were nonetheless included in the calibration because the data suggested that they were somewhat responsive to site conditions and it was desired to have relatively shallow head observations in the calibration.

The remaining two positive outliers were from bedrock wells that were part of a multi-level cluster located near the base of River Ridge (see Figure 43). The large negative outlier was also from a well located near the base of River Ridge (see Figure 42). These outliers suggest that either there are unknown errors in the observed data, or, more likely, that structural errors in the model result in a poor representation of the high groundwater ridge coincident with River Ridge (see Figure 47).

Model fit was inconsistent with the assumed head observation errors as reflected in the large standard error of the regression. This was interpreted to indicate that model errors were significant. With the six outliers removed, however, the weighted residuals satisfied conditions of normality, as determined by the correlation coefficient between the ordered weighted residuals and the standard normal quantiles (Figure 48). This suggests that a number of sources may be contributing to the model error and that predicted values and predictive uncertainties derived from the model may be accurate (Hill and Tiedeman 2007; Hill et al. 1998), at least in the areas of the model domain not associated with the outliers.

Parameter estimates and their uncertainties were evaluated by examining composite sensitivities (printed in the output files) and by comparison with prior estimates. Estimated parameter values were reasonably close to initial values except for the hydraulic conductivity of the soil material, which was generally estimated to be about four orders of magnitude greater than the initial value of 3.5×10^{-4} ft/d. The discrepancy between the estimated value and the prior information indicates either that there is a significant structural error in the model, or that the prior information for the soil hydraulic conductivity does not represent conditions at the site. Hydraulic heads collected at the site prior to and shortly after a significant rainfall (discussed in

Section 4.1.1.6 with respect to Figure 21) indicated a widespread and rapid response of groundwater head to the precipitation. This suggests that the range given for the hydraulic conductivity of the soil in TVA (2009) is unrepresentative of actual site conditions and that the estimates from the calibration may be more reasonable.

Parameter estimates from the calibrations and 95% confidence intervals are shown in Figure 49. In this figure, the hydraulic conductivity parameters are shown as hk_11 to hk_14 and the recharge parameters as rch_31 to rch_34. As a result of the way the various alternative models represented the hydraulic conductivity and recharge zones, a given parameter did not always represent the same region of the model. For example, all models names beginning with "H1" were homogeneous and the hk_11 parameter represented the entire domain. For the remaining models, the materials represented by the hydraulic conductivity parameters are given in Table 6. For the recharge parameters, the models with "R1" in the name had a single recharge zone represented by the parameter rch_34. For the "R2" models, the four recharge zones were represented by the four parameters: rch_34 for the surface across Town Creek, rch_33 for the vegetated lowlands on the plant side of Town Creek, rch_32 for the area developed for the plant, and rch_31 for the River Ridge uplands.

In general, the parameter results shown in Figure 49 indicate that the estimates were fairly stable across the alternative models. For a given parameter, differences in values estimated for the alternative models generally varied by less than one order of magnitude. Parameter confidence intervals were two orders of magnitude in nearly every cases and were significantly larger for many of the parameters. These large parameter uncertainties are indicative of a low composite sensitivity (e.g., the measured heads were much more sensitive to hk_11 than to hk_14). Composite sensitivities (Hill and Tiedeman 2007) for model H4R2D1 are shown graphically in Figure 50.

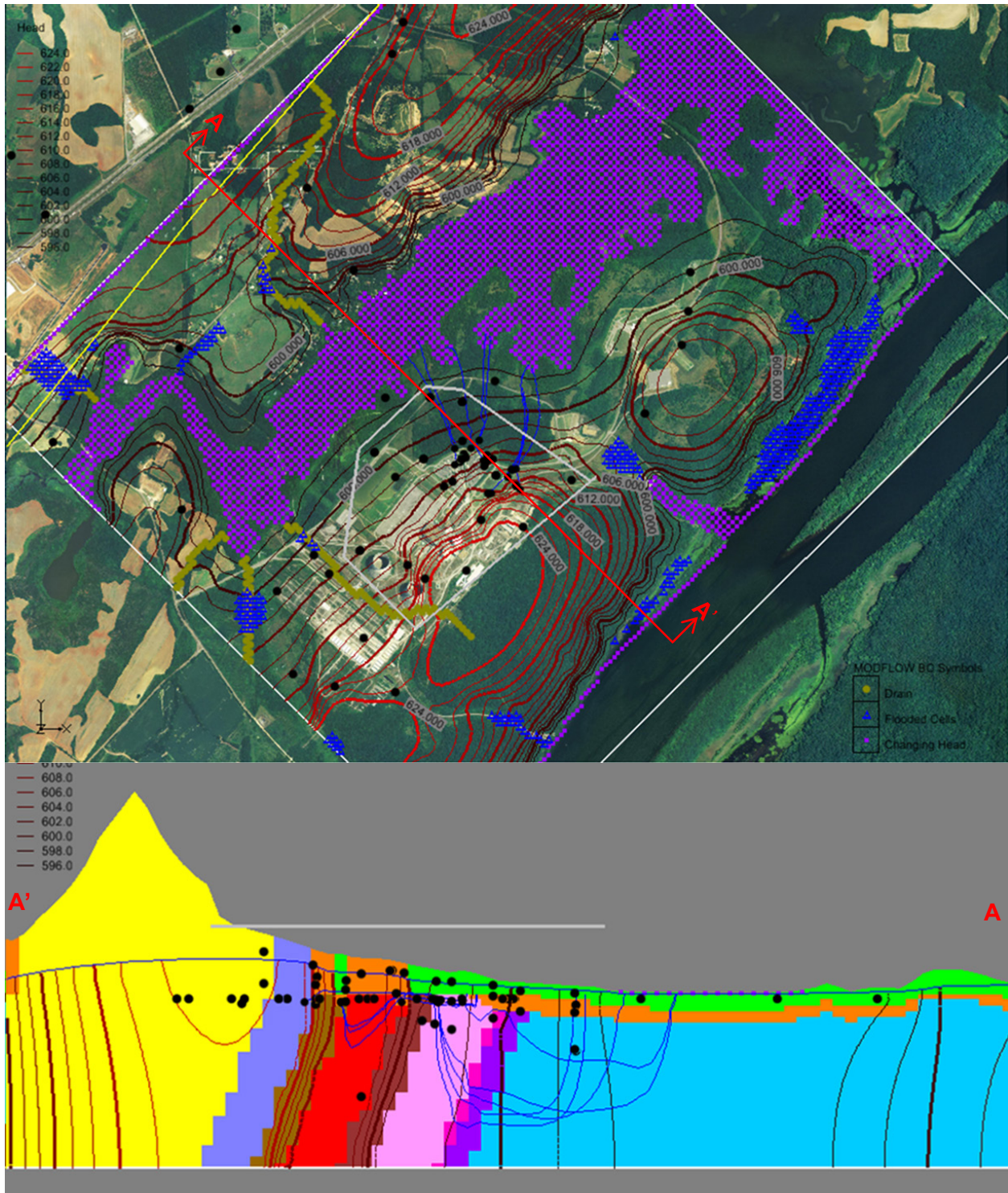


Figure 47. Pathlines from points around the Units 3 and 4 reactor buildings computed in GMS using MODPATH: plan view (top) and cross-section through the reactor building areas (bottom, 10x vertical exaggeration)

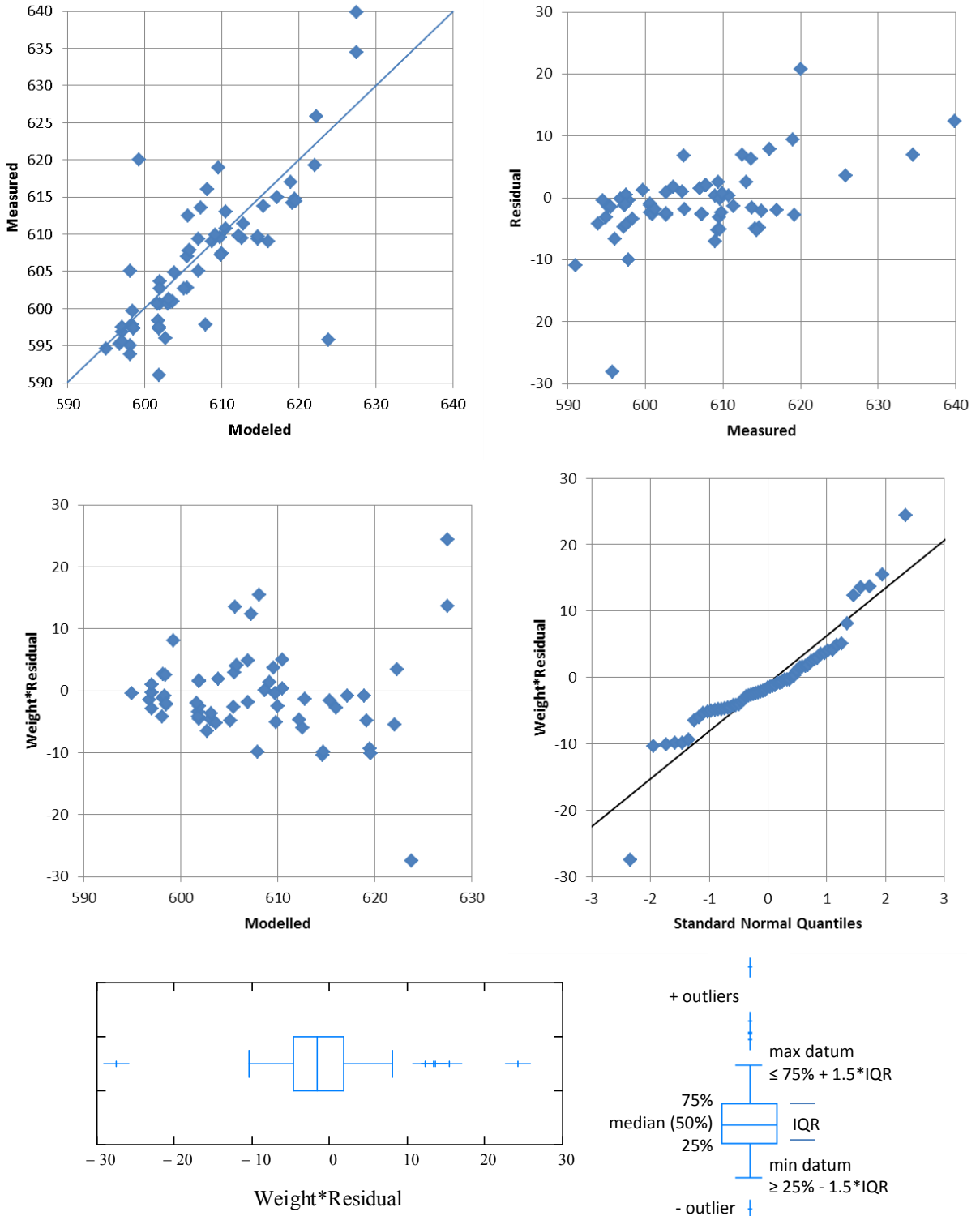


Figure 48. Graphical evaluation of residuals for model H4R1D1: observed vs. simulated heads (feet) (top left), unweighted residuals vs. observed heads (top right), weighted residuals vs. simulated heads (middle left), quantile-quantile plot of weighted residuals (middle right), and boxplot of weighted residuals (bottom, with explanatory legend)

Table 6. Materials represented by hydraulic conductivity parameters in alternative models

Model Name	Parameter			
	hk_11	hk_12	hk_13	hk_14
H1...	entire domain	n/a	n/a	n/a
H2...	soil & weathered rock	n/a	all limestone units	n/a
H3...	soil & weathered rock	n/a	limestone	silty limestone
H4...	soil	weathered rock	limestone	silty limestone

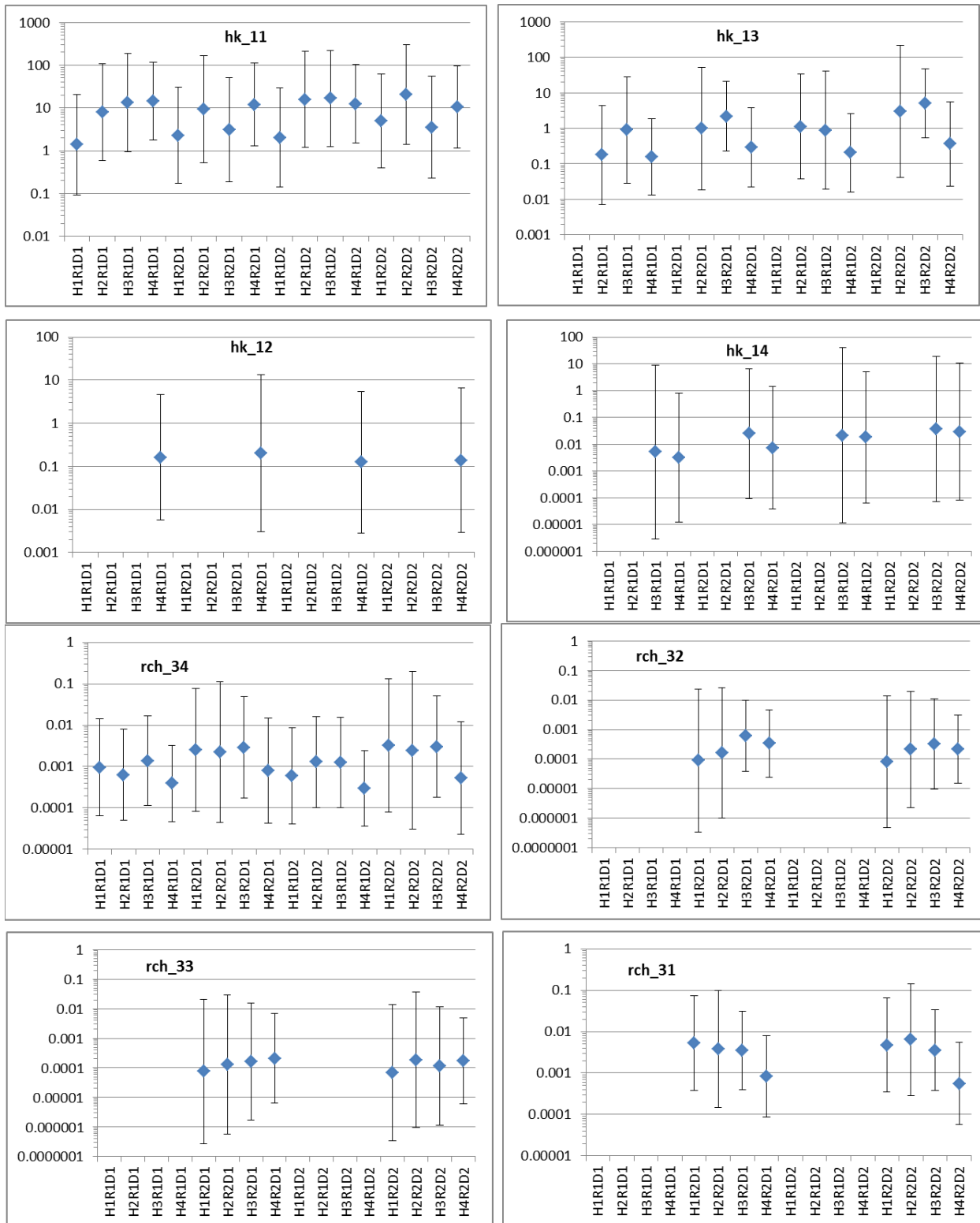


Figure 49. Parameter estimates and 95% confidence intervals for hydraulic conductivity (top, ft/d) and recharge (bottom, ft/d). See text for explanation of parameters.

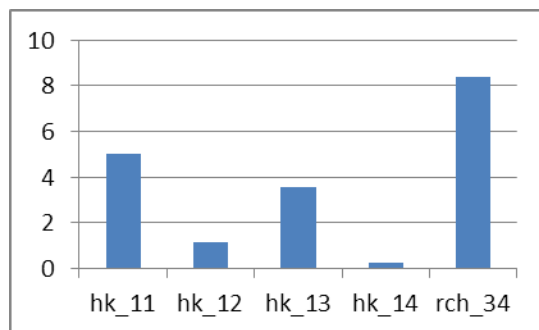


Figure 50. Composite sensitivities for model H4R1D1 at the final parameter values as computed following Hill and Tiedeman (2007)

4.5 Alternative Model Probabilities

As discussed previously, the values for *KIC* reported by PEST and UCODE do not take into account the possible log transformation of parameters, which will affect the *KIC* values as described in Appendix A. Because of this the model selection criteria were computed within a spreadsheet to account for the log transformation of parameters (Figure C-1 of Appendix C). The model probabilities follow directly from the model selection criteria and were calculated in the same spreadsheet (Figure C-2 of Appendix C).

The model selection criteria for each of the alternative models are shown in Table 7. These values provide a balance between model fit and model complexity. The resulting model probabilities are also provided in the table and shown graphically in Figure 51. For comparison, values of the weighted sum of squared residuals, a measure of fit only, are provided in Table 7 and shown in Figure 51.

The use of *AICc* resulted in three models with significant probability. Two of these models were those with four hydraulic conductivity zones and one recharge zone (H4R1D1 and H4R1D2). The former used the deep domain and was somewhat preferred by *AICc*, while the latter used the shallow domain. The other model with significant probability assigned by *AICc* was the best-fitting model with the minimum SSWR (H3R2D1). This model lumped the soil and weathered rock materials together and had four recharge zones. One other model (H3R2D2) was assigned a relatively small, but noticeable probability (5%).

When using *KIC*, H4R1D1 and H4R1D2 were preferred, similar to *AICc*, but *KIC* preferred the shallow domain model by a probability ratio of almost four to one. No other models received significant probabilities. This result is consistent with some other comparisons of model selection criteria in the literature, which have found that the use of *KIC* can tend to emphasize a smaller number of models than *AICc* (e.g., Singh et al. 2010).

Table 7. Model selection criteria values and model probabilities for alternative models

Model	N_z	P_k	SSWR	AICc	KIC	$-\ln \sum_k^{ML} $	Model Probability	
							AICc	KIC
H1R1D1	71	2	8010.42	341.89	349.90	9.51	0.00%	0.00%
H2R1D1	71	3	6026.49	323.93	328.31	5.71	0.00%	0.01%
H3R1D1	71	4	5590.22	320.92	323.02	3.33	0.01%	0.20%
H4R1D1	71	5	4244.35	303.75	313.78	11.22	39.59%	20.25%
H1R2D1	71	5	5137.42	317.31	354.44	38.32	0.05%	0.00%
H2R2D1	71	6	4932.50	316.88	344.02	28.37	0.06%	0.00%
H3R2D1	71	7	4021.04	304.92	337.15	33.58	22.03%	0.00%
H4R2D1	71	8	4176.33	310.24	349.18	40.49	1.54%	0.00%
H1R1D2	71	2	7767.93	339.71	347.91	9.71	0.00%	0.00%
H2R1D2	71	3	6056.45	324.29	321.71	-1.25	0.00%	0.38%
H3R1D2	71	4	5725.10	322.61	321.30	-0.08	0.00%	0.47%
H4R1D2	71	5	4276.54	304.29	311.07	7.97	30.28%	78.68%
H1R2D2	71	5	5227.29	318.54	354.05	36.70	0.02%	0.00%
H2R2D2	71	6	4941.69	317.02	337.98	22.20	0.05%	0.00%
H3R2D2	71	7	4184.85	307.76	337.38	30.98	5.34%	0.00%
H4R2D2	71	8	4222.75	311.03	349.85	40.38	1.04%	0.00%

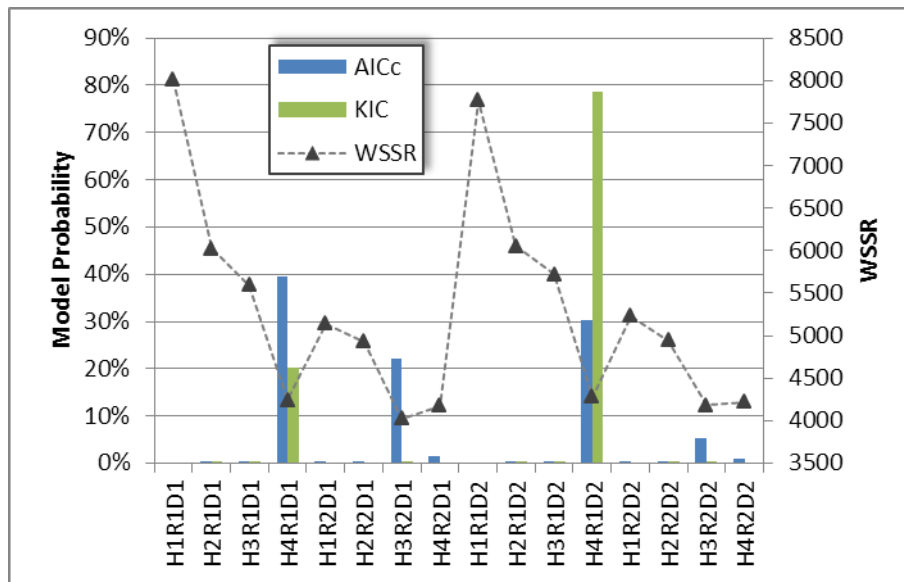


Figure 51. Model probabilities computed with AICc and KIC, and the weighted sum of squared residuals for the alternative models

4.6 Predictive Modeling

Having characterized parameter uncertainty in the history-matching period and having obtained model probabilities for the alternative models, these results were used with a predictive model to

estimate predictive uncertainties. This required modification of the basic model, used in the calibration discussed above, to reflect the conditions of the predictive period. For this example, involving review of a nuclear power plant application, that involved modifying the model to represent the groundwater conditions after the plant has been constructed. These modifications included structural changes in the models (excavations, topography), modification of parameter values (recharge), and the addition of new parameters (to represent the fill material not present in the history-matching models). In many cases, an entirely new model may also be required to simulate desired regulatory outcomes. For example, while an evaluation of contaminant transport was not considered in the history matching period, it may be required in the post-construction period.

4.6.1 Modifications for Post-Construction Conditions

The primary changes from construction of Units 3 and 4 that would be expected to affect groundwater at the Bellefonte site are the removal of existing subsurface materials in the excavations of building foundations, the placement of engineered fill materials within the excavation and around building foundations, surface grading that affects the site topography, and land use changes that affect recharge.

The FSAR (TVA 2009) contains several figures (2.5-347, 2.5-348a, and 2.5-348b) that identify the extent of the excavations for Units 3 and 4. Based on this information, and considering constraints of the groundwater model grid cell size, the lateral extent of the reactor building foundations (Category 1 Structure Excavation) and the surrounding fill material were identified in the groundwater model, as shown in Figure 52. The vertical extent of the building foundations is down to an elevation of 588.6 ft, which puts it into model grid layer 3 (which actually extends to an elevation of 584.9 ft). The building foundation zone was set to inactive grid cells (thus no-flow boundary conditions). The backfill material around the foundations was assumed to encompass layers 1 and 2 (from ground surface to 589.7 ft elevation). A new "Fill" material was defined to represent the backfill, with a horizontal hydraulic conductivity of 2.83 ft/d (10^{-3} cm/s).

The construction plan for Units 3 and 4 includes modifications to the land use and topography, denoted in Figure 52 (see FSAR Figure 2.5-362 for details). Site plans for buildings, parking lots, and other developed areas are also apparent, which means that the land use will alter. Thus, the recharge zones required modification in the newly developed area, as shown in Figure 53. The major buildings and parking lots are distinguished as zones of zero recharge (Figure 54). Recharge must be set in MODFLOW to apply to Layer 1 only, otherwise recharge might inappropriately be applied in lower layers due to inactive grid cells.

Changes to topography included a cut from part of the hillside to the southeast and fill across the reactor area to flatten the site, with a gradual slope away from the power block buildings to promote drainage. Several approaches can be used to implement the revised topography contours (Figure 52) in the MODFLOW groundwater model. If the MODFLOW model was using material definitions with the LPF package, then the changes could be implemented by drawing arcs/polygons representing the elevation contours in a GMS Map module coverage, and mapping the coverage to layer 1 of the MODFLOW grid. This would provide the correct topography and would not change the material designations, which should be appropriate given the original approach to mapping the solids model to the top layer (but an assessment to confirm the material designations would be appropriate).

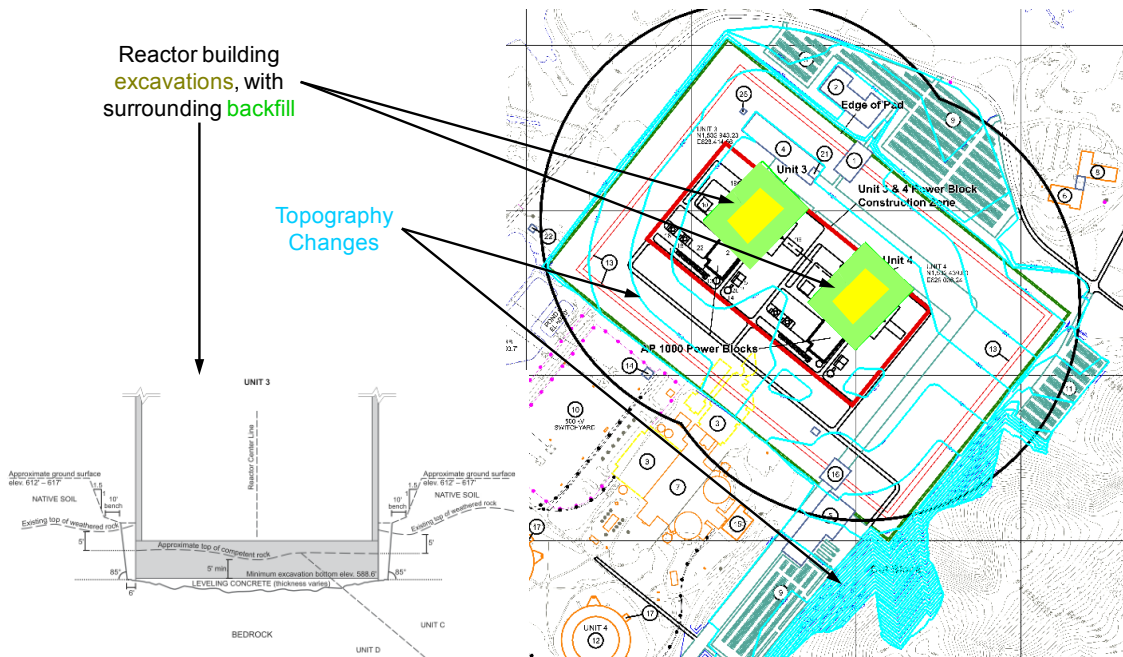


Figure 52. Figures depicting the depth of the reactor building excavation (left), changes in topography, the locations of reactor buildings, and the groundwater model grid zones representing fill material and reactor building excavations (right). Figures adapted from FSAR Figure 2.5-348a and Figure 2.5-362.

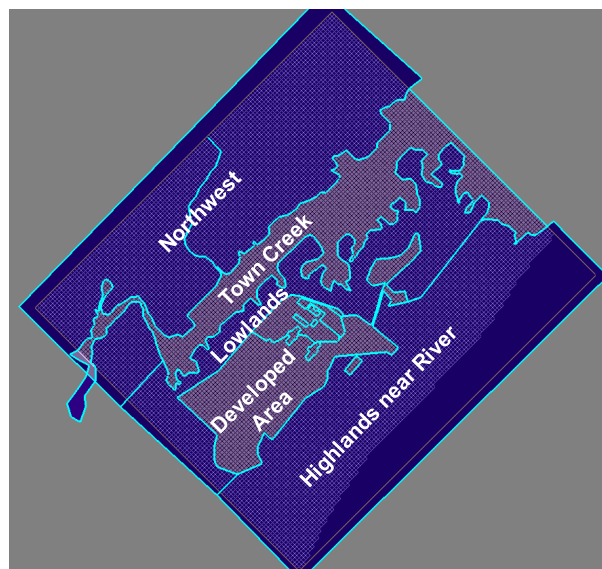


Figure 53. Refined recharge zones for the post-construction scenario. A portion of the Lowlands zone was incorporated into the northern corner of the Developed Area zone.

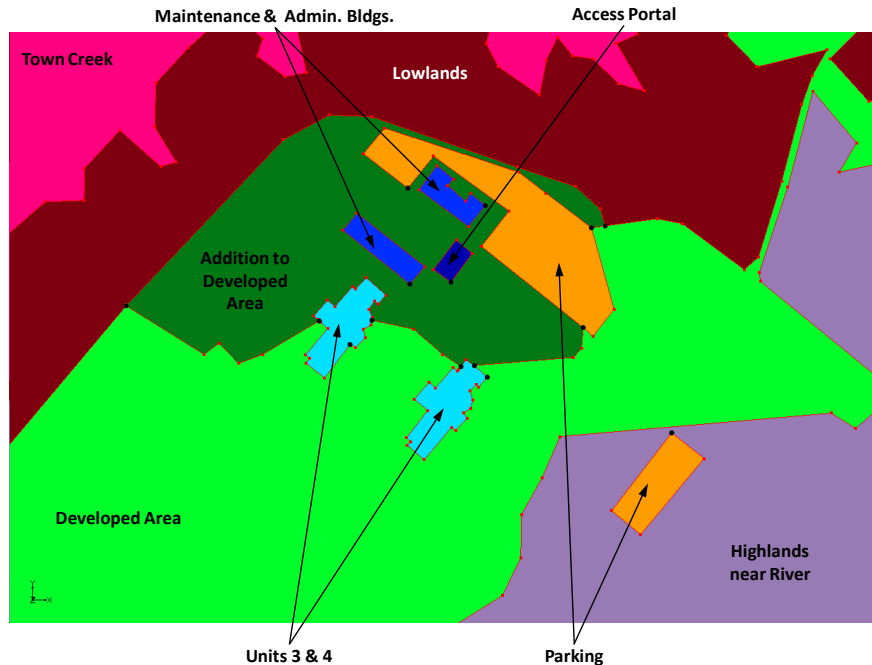


Figure 54. Details of the post-construction recharge zones around Units 3 and 4. Reactor and other significant buildings and the main parking areas are set to zero recharge. Note that the colors are simply used to distinguish zones and are unrelated to materials.

When using the HUF package for the MODFLOW groundwater model, the process is complicated by the uncoupled nature of the HUF hydrogeological units and the model grid elevations, so a multi-step approach is required. One approach is to define the new topography elevations as a scatter data set, Map module points/arcs, or directly as a TIN. The goal is to define a TIN that represents the post-construction ground surface elevations. This TIN can be used with flat planes above and below to create solids for clipping/filling the existing solids model (Section 4.1.2.3, Figure 31). The adjusted solids model can then be mapped to the HUF package of the MODFLOW groundwater model as described in Section 4.1.2.4. A second approach, applied in this example, is to manipulate the HUF package data arrays for potentially affected units and the grid elevation data arrays. Data arrays for grid layer elevations (i.e., the top elevation of layer 1) and for the HUF unit top elevations and thicknesses can be exported to the GMS 2D Grid module. Data arrays can be manipulated directly in GMS using the GMS Data Calculator. The Data Calculator could be used to merge the Soil unit top elevation with the new topography (i.e., mapped to the MODFLOW grid as described above for the LPF package). That said, it may be more efficient to copy the data arrays into an external spreadsheet, perform manipulation/calculations in the spreadsheet, then copy the adjusted arrays back to GMS. The adjusted data arrays should be transferred (internally using the “2D Grid -> Layer” command or by pasting data from an external source) to the hydrogeological unit definitions for the HUF package. Note that both top elevations and thicknesses of the hydrogeological units must be adjusted. The fill material (discussed above) must be added as a new HUF hydrogeological unit. The resulting changes for the post construction model topography are depicted in Figure 55.

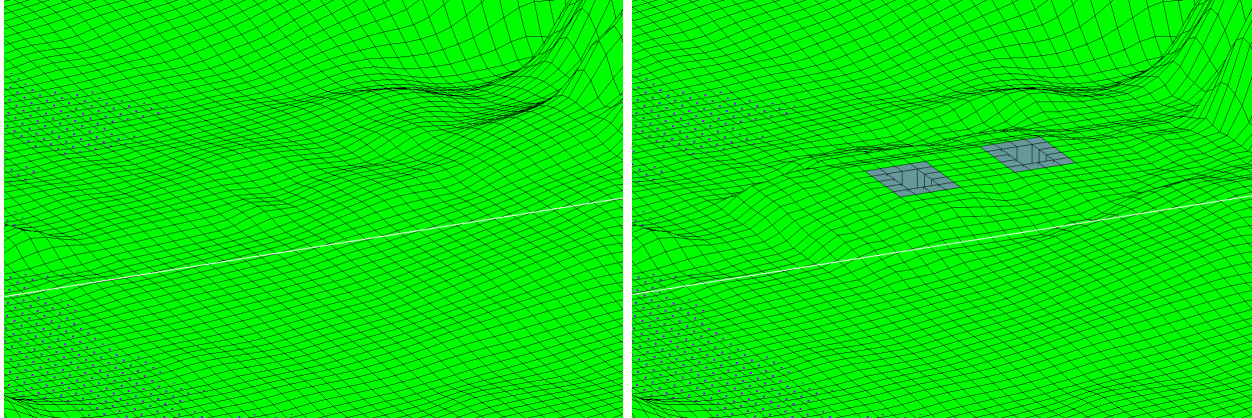


Figure 55. Pre-construction topography and materials (left) and modifications to represent the post-construction scenario (right) in the vicinity of Units 3 and 4. The topography was flattened at the site and the Category 1 building foundations were represented by inactive grid cells surrounded by fill material. View is nominally to the ENE with a 10X vertical exaggeration.

4.6.2 Post-Construction Model Results

Simulations were conducted with the post-construction groundwater model configuration to assess the impact of the topographic and subsurface changes on the hydraulic heads and the groundwater flow directions. Figure 56 shows the resulting hydraulic head contours for the post-construction H4R1D1 simulation (compare to the pre-construction results in Figure 40). Figure 57 shows a zoomed view and compares pre-construction results to post-construction results. The differences are small and are localized around the Bellefonte site. The significance of the differences with respect to estimating maximum groundwater head (and its uncertainty) is evaluated in the following section.

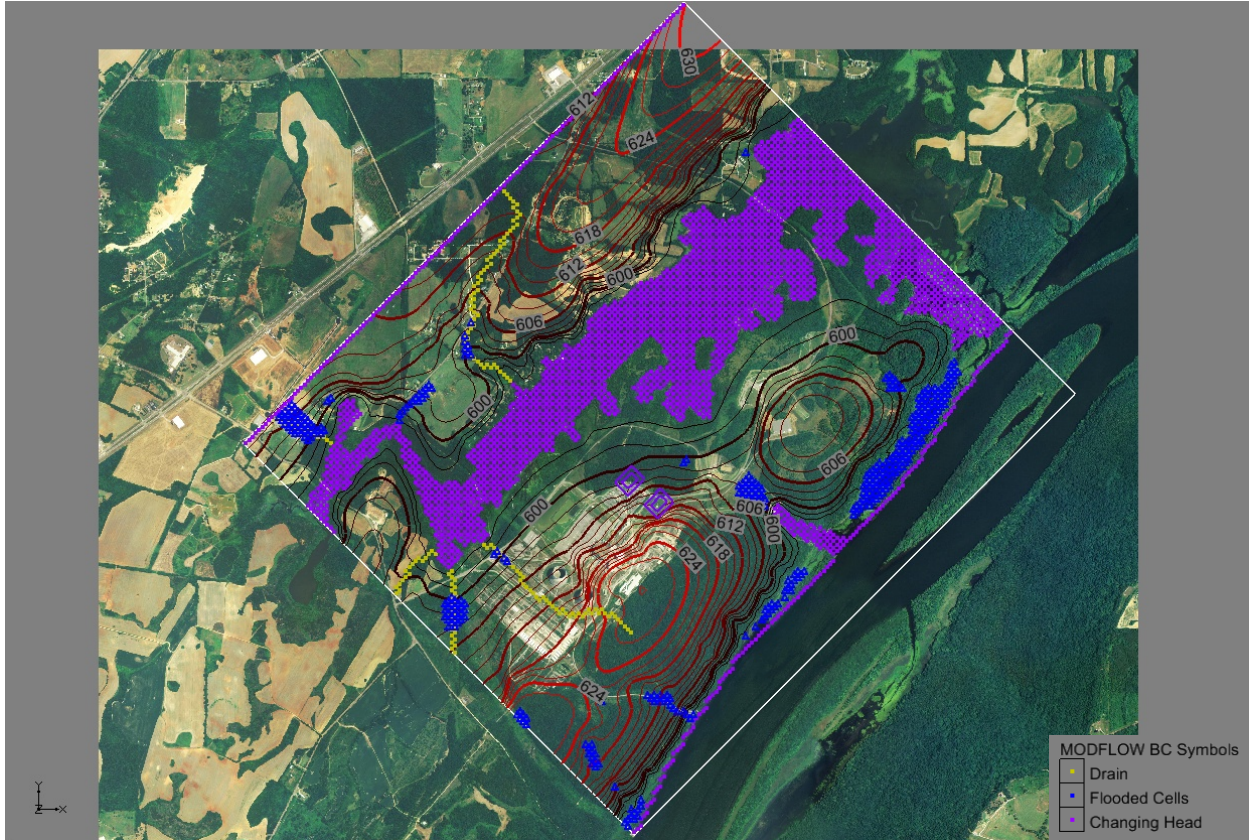


Figure 56. Hydraulic head contours for model H4R1D1 with the post-construction model configuration modifications. The purple rectangles indicate the location of Units 3 and 4, where inactive cells represent building foundations and fill material surrounds the foundations.

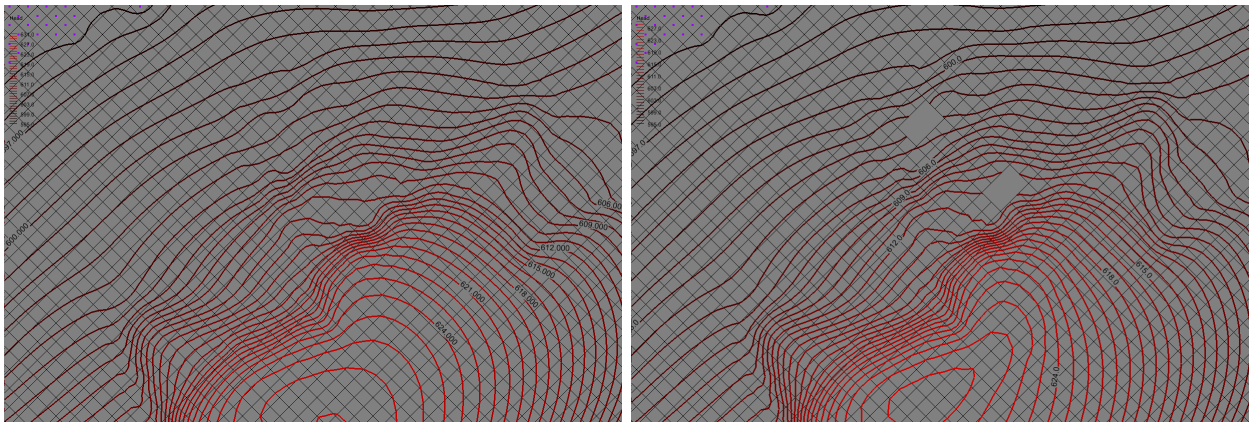


Figure 57. Comparison of pre-construction (left) and post-construction scenario hydraulic head contours for model H4R1D1. Contour intervals are 1 ft.

4.6.3 Predictive Uncertainty

Predictive uncertainties for this example were estimated using linear methods to calculate the mean and variance of the predicted values resulting from parameter uncertainties. As discussed

in Section 3.2, GMS has a Monte Carlo simulation capability, but it was not used due to the computational requirements of Monte Carlo simulation and the limitations of the GMS implementation (a limited set of applicable parameters, limited distribution types, and no parameter correlations). The linear uncertainty estimates used here [Eq. (12)] are computationally quick, requiring only the parameter covariance (available from the calibration of the history-matching model) and prediction sensitivities computed with the post-construction predictive model.

4.6.3.1 *Software Used in Estimating Predictive Uncertainty*

The PEST `predunc6` utility implements the methods of Moore and Doherty (2005). The utility calculates the parameter covariance matrix using observation weights from a PEST control file and the Jacobian matrix file associated with that control file. Both of these files have to reflect the calibration conditions. Prediction sensitivities are read by `predunc6` from a separate Jacobian file produced by a PEST execution under the predictive conditions. One of the requirements of `predunc6` is that the parameter sets for all three files (calibration control file, calibration Jacobian file, and prediction Jacobian file) must be consistent. This means that the predictive conditions can't include parameters that are not also included in the calibration. As discussed above, this condition is likely to be violated for a nuclear power plant application due to the introduction of new materials (e.g., excavation fill) and simulation requirements (e.g., contaminant transport) under post-construction conditions. This limits the applicability of `predunc6`.

It is also worth noting that one of the inputs required by the `predunc6` utility is the prior parameter covariance [the $C(p)$ matrix in the PEST documentation] supplied by the user. A result equivalent to Eq. (12) will be returned by `predunc6` when the prior parameter variances are much larger than the parameter estimation variances resulting from the calibration [i.e., when the diagonal elements of $C(p)$ are sufficiently large].

Predictive uncertainty results presented below were computed using the UCODE `Linear_Uncertainty` utility. This utility reads the parameter covariance matrix directly from UCODE calibration results. Because the calibration was completed using PEST, this required translating the PEST control file from the calibration to a UCODE input file and executing a UCODE sensitivity run at the optimal parameter values. This produced the needed UCODE parameter covariance matrix for the calibration (pre-construction) model. A UCODE sensitivity run was also completed with the post-construction model to generate the prediction sensitivities. For this example, the UCODE input file for the post-construction predictive sensitivity run was translated from a PEST control file generated in GMS. UCODE can easily accommodate parameters in the predictive model that were not used in the calibration model. It does this by supplementing the parameter covariance matrix read from the calibration output with the variances of any additional parameters used in the prediction sensitivity run. UCODE uses prior information contained in the input file for the prediction sensitivity run to determine the variances of the additional parameters.

There are some limitations of GMS when working with predicted quantities for which uncertainties are desired. When working within GMS, contributions to uncertainty are limited to parameters that are allowed in MODFLOW as designated parameters (i.e., that can be specified with key values). Similarly, predicted values must be quantities that can be specified as observations in MODFLOW. In particular, results from other codes available in GMS (e.g., MODPATH and MT3DMS) can't be used with PEST and therefore can't be easily used to calculate predictive uncertainty. Using models prepared within GMS, but working outside GMS to estimate predictive uncertainty, one could use any model parameter as a contributor to

uncertainty and any results as a predicted value. However, this would require the user to access the parameter input files and model output files to create the needed template and instruction files by hand instead of relying on GMS to do so.

4.6.3.2 Predictive Uncertainty Results

For this example, the predicted quantities were groundwater heads at three locations at the corners of each proposed reactor unit. These locations are indicated on Figure 58 as the yellow dots. Note that the desired predicted heads are within the fill material (colored gray in the figure) adjacent to the buildings. These locations are appropriate for estimating maximum groundwater levels required as part of a review under SRP 2.4.12. Based on the head contours shown in Figure 58, the predicted head at the location indicated by the arrow will be the largest of the six predicted values.

The assumption of steady-state flow with the use of average observed heads as calibration targets for the history-matching models is non-conservative when the modeling objective is to estimate maximum groundwater head. The average observed heads used as calibration targets were about two to three feet (0.6 to 0.9 m) less than the maximum observed heads for the 2006/2007 observation period. The results from the calibration, however, indicated that the simulated heads were generally larger than the average observed heads by about the same amount, at least in the area of the desired predicted head; Table 8 provides results for several wells in this area.

In this case, the errors in the model fortuitously provide an unquantified degree of conservatism countering the steady-state assumption. To account for an additional quantifiable degree of conservatism, the upper limit of an estimated 95% confidence interval (with an exceedance probability of 2.5%) for the predicted head was evaluated. This value could be compared to the design limit in a safety evaluation. If the limit was exceeded or if the margin was small, a more reliable analysis could be carried out by obtaining additional site data and completing an unsteady flow analysis.

For the estimation of predictive head uncertainty, the hydraulic conductivity and recharge uncertainties from the calibration were included (through the parameter estimation covariance). Two sets of prediction sensitivity runs were completed. In one, no additional post-construction parameters contributed to the predictive uncertainty. In the second, the hydraulic conductivity of the fill material contributed to the predictive variance through the use of a prior parameter equation in the UCODE input file. The fill hydraulic conductivity was assumed to be lognormally distributed with a geometric mean value of 2.8 ft/d (10^{-3} cm/s) and a 95% probability interval of plus and minus one order of magnitude from the mean. The resulting distribution is shown in Figure 59. Predictive uncertainties for each of the alternative models with significant model probabilities were computed with the UCODE Linear_Uncertainty utility. Model averaged predictive uncertainties were calculated in Excel (see Figure C-3 in Appendix C).

Predicted heads at the location indicated with the arrow in Figure 58 and the prediction uncertainties are shown in Figure 60. In this figure the top of the colored bars are the predicted head values for the four alternative models assigned a probability of at least 5% by either the *AICc* or *KIC* model selection criterion. Models H4R1D1 and H4R1D2 predict similar values indicating that the depth of flow has little impact on the head near the reactor units. As noted previously, the depth of flow may have a much greater impact on a different predicted quantity, for example travel time from the reactor area to Town Creek. H3R2D1 and H3R2D2 also have similar predicted head values. However, these models with three hydraulic conductivity zones and four recharge zones predict a head more than two feet higher than models with four

hydraulic conductivity zones and one recharge zone. The model-averaged predicted values are shown for model probabilities calculated from both *AICc* and *KIC*. Because H3R2D1 and H3R2D2 were given negligible probabilities by *KIC*, the larger predicted values do not contribute to the *KIC* model-averaged predicted head. This is not the case for the *AICc* model-averaged head since the two H3 models have a combined 27% probability.

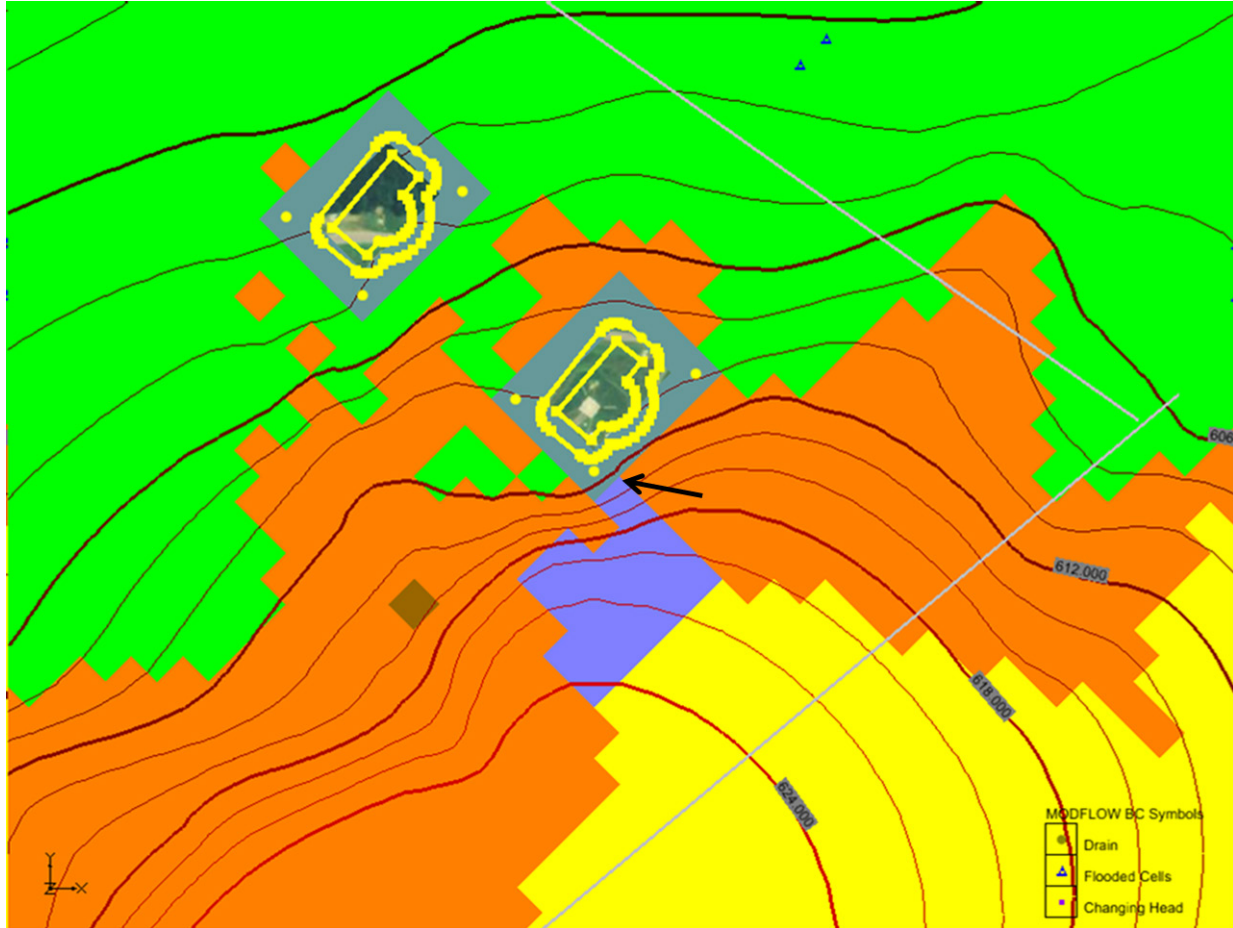


Figure 58. Detail from the post-construction groundwater model showing the locations of the predicted heads at the corners of the reactor units

Table 8. Averaged observed head (calibration target), maximum observed head, and simulated equivalent head from the calibrated H4R1D1 model for three wells near the desired location of predicted head. All heads in feet.

	MW-1205c	MW-1213c	MW-1202a
Average Observed Head	609.7	609.8	607.2
Maximum Observed Head	613.3	612.6	610.7
Calibrated Head	614.7	612.6	609.8

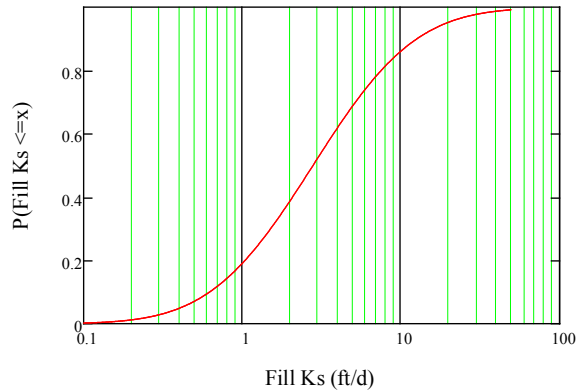


Figure 59. Prior parameter distribution for the hydraulic conductivity of the fill material

The error bars in Figure 60 are the upper limits of the 95% confidence intervals computed from the predicted value variances. The three different colors indicate the contribution to that variance: parameter uncertainty only as given by Eq. (12) (shown in blue), or parameter uncertainty plus model uncertainty as given by the squared quantity on the right hand side of Eq. (16) (shown in red and green). The contribution from model uncertainty is the variance of the individual model prediction about the model-averaged mean prediction. The model-averaged mean prediction [Eq. (15)] used in Eq. (16) can be calculated using either *A/Cc* or *K/C*; results from both are shown in Figure 60. For the H4 models, model uncertainty has a minor effect when using *A/Cc* and no effect when using *K/C*. For the H3 models, the effect of model uncertainty is significant. This reflects the fact that the model-averaged predicted values are much closer to the H4 individual model predictions than to the H3 individual model predictions.

Model-average uncertainty (indicated by the error bars on the rightmost group of Figure 60) is equivalent to the H4 individual model results when using *K/C*. For *A/Cc*, the model-average uncertainty is influenced by the larger uncertainties of the H3 models since 27% of the probability is assigned to these models, as discussed above. The upper limit of the 95% confidence interval is 3.5 or 4.0 ft. larger than the model-average predicted value (depending on whether *K/C* or *A/Cc* is used). The inclusion of uncertainty in the groundwater head value for comparison with the design criterion thus adds a considerable degree of conservatism to the evaluation.

Figure 61 shows the model-averaged predictions and uncertainty measure for the case in which the uncertainty of the fill material hydraulic conductivity was included (w/ Fill, equivalent to the rightmost group of Figure 60) and the case in which the hydraulic conductivity was assumed to be known and assigned its geometric mean value (w/o Fill). The predicted values (top of the colored bars) are unaffected by the inclusion of uncertainty in the fill conductivity since both results use the mean value. The upper limit of the 95% confidence interval is increased by the inclusion of fill conductivity uncertainty, as much as by one foot when using *K/C*. Whether or not this is significant would depend on the margin between the upper limit and the design criterion.

The results of the example demonstrate the potential importance of even localized changes to the model under post-construction conditions. The fill material occupies a small portion of the model domain, but it is a potentially critical feature given that the design criterion for maximum groundwater head is within the excavation. In this case, including a reasonable uncertainty

estimate for this material of limited extent had a noticeable impact on the predicted regulatory value to be compared to this design criterion.

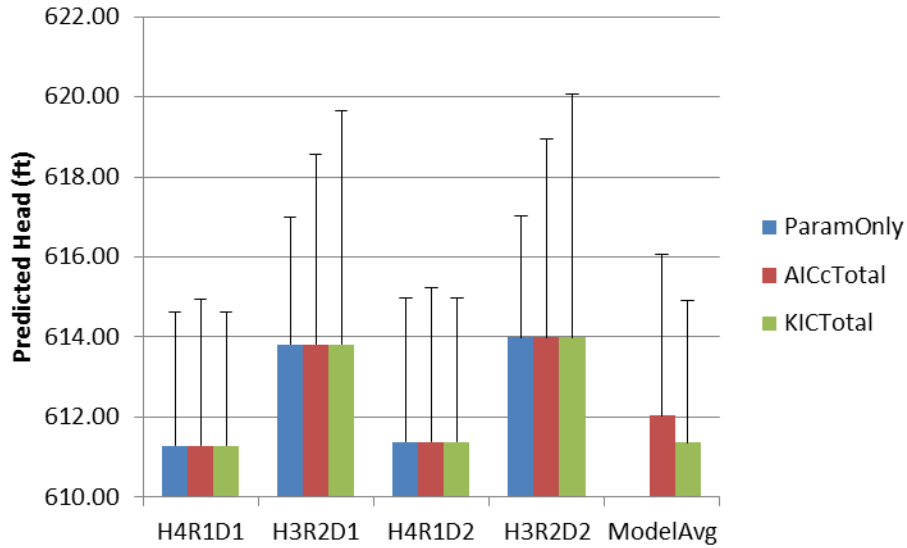


Figure 60. Predicted heads (top of colored bars) and 95% confidence interval upper limits for the individual models and the model average

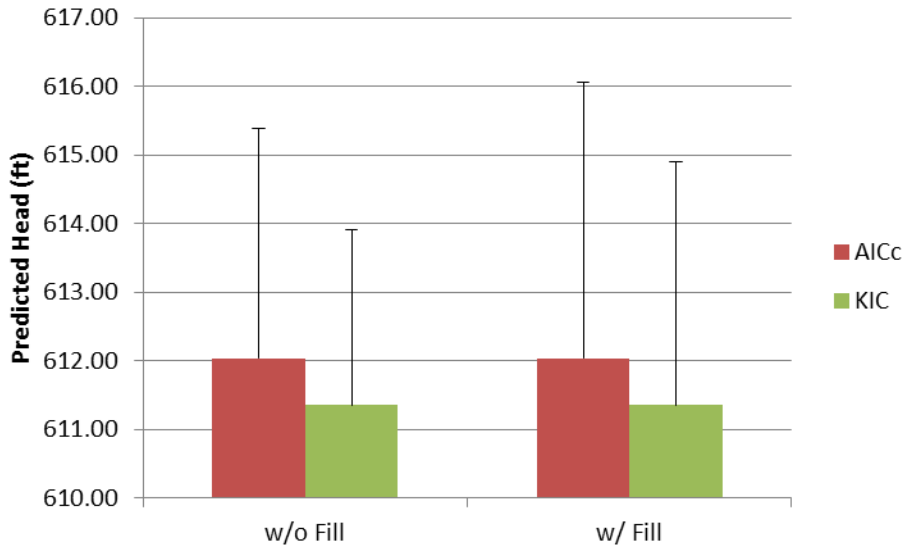


Figure 61. Effect on model-averaged predicted head of including the fill material hydraulic conductivity uncertainty

5 CONCLUSIONS

This report describes a methodology to assess predictive uncertainty in hydrologic model analyses carried out in support of safety and environmental evaluations of nuclear reactor applications. Current review criteria and technical procedures contained in NRC staff guidance (e.g., NRC, 2007) describe a predominantly deterministic approach that emphasizes conservatism in the analysis. It is recommended in this report that the focus be on making conservative decisions instead of focusing on the conservatism of models (e.g., bounding assumptions and extreme parameter values). A focus on conservative decisions requires that uncertainties in model outcomes be properly accounted for when comparing these outcomes to regulatory or design requirements, as illustrated in the report using a simple groundwater transport modeling example. This is consistent with a risk-informed approach, and it allows for the natural consideration of consequences (e.g., the safety consequences of exceeding a design flood elevation).

The uncertainty methodology described in this report considers the combined impact of uncertainties associated with the conceptual-mathematical basis of a model, the model parameters, and the scenarios to which the model is applied. The methodology was applied to groundwater issues commonly arising in the review of nuclear power plant applications under Section 2.4.12 of the Standard Review Plan (NRC 2007). This example used publicly available data from a combined license application. Some of the conclusions from the example are provided here.

Modeling expectations should be explicitly discussed in regulatory guidance and review plans, including the assessment of uncertainties and the consistent application of procedures, e.g., the discussion in ANS 2.17 (ANS 2010) and the guidelines for effective modeling in Hill and Tiedeman (2007). This may result in better integration of site characterization and modeling, and fewer requests for additional information.

Following standard procedures for uncertainty analyses can reveal limitations of the hydrologic analyses, e.g., unexamined parameter correlations and outstanding data needs. In addition, the use of standard procedures promotes consistent reviews.

To the extent possible, existing software was used to implement the uncertainty methodology. Parameter estimation and uncertainty calculations were primarily carried out using UCODE and PEST. UCODE provides a well-integrated set of essential tools. PEST has advanced capabilities, but is less well integrated and the version used here has a limitation when adding uncertain parameters to the predictive model. Uncertainty software is incompletely integrated with modeling platforms such as GMS and thus requires hand manipulation of files and completion of tasks outside of GMS. Calculation of model selection criteria for multi-model analysis was completed using custom spreadsheets because, for one of the criteria, the UCODE and PEST calculations depend on whether parameters are log transformed in the model calibrations. Calculation of model probabilities and model-averaged predictions were also completed in these spreadsheets.

Predictive models should include not only the uncertainties evaluated in the history-matching period (through model calibration), but also any additional uncertainties that might apply only in the predictive period. The example demonstrated the potential importance of even localized changes to the model under post-construction conditions. Including a reasonable uncertainty estimate for the hydraulic conductivity of the fill material, which occupied a very limited extent of

the model domain, had a noticeable impact on the predicted regulatory value to be compared to the design criterion.

The example also demonstrated that not all model uncertainties can be quantified. Data limitations led to the use of a steady-state groundwater flow model, a non-conservative choice when evaluating maximum groundwater head. It was important in this case to acknowledge the additional uncertainty this decision introduced to the analysis and to qualitatively evaluate its effect on the uncertainty in the predicted value.

Out of the sixteen alternative models considered in the multi-model analysis, four were assigned substantial model probabilities by the methodology. Model-averaged predicted values and predictive uncertainty were found to depend on the model selection criterion used to calculate the model probabilities. These results are consistent with other studies. Since no single criterion has been shown to be superior in all cases, multiple criteria should be used.

Explicit consideration of alternative models is likely more valuable than quantitative model averaging. However, model averaging has been shown in other studies to improve model predictive performance over the use of a single model. Using linear uncertainty methods, model averages can be easily completed and should be considered.

Relatively simple and practical approaches to uncertainty evaluation should be integrated into the hydrologic analyses of NRC staff. These approaches contribute to estimates of the degree of conservatism in the analysis, demonstrate an understanding of the systems being evaluated, and provide evidence of the staff's due diligence.

6 REFERENCES

ANS, *Evaluation of Subsurface Radionuclide Transport at Commercial Nuclear Power Plants*, ANSI/ANS-2.17-2010, American Nuclear Society, La Grange Park, Illinois, 2010.

ASTM, *Standard Guide for Developing Conceptual Site Models for Contaminated Sites*, ASTM E1689-95 (2008), ASTM International, West Conshohocken, Pennsylvania, 2008.

ASTM, *Standard Guide for Application of a Ground-Water Flow Model to a Site-Specific Problem*, ASTM D5447-04 (2010), ASTM International, West Conshohocken, Pennsylvania, 2010.

ASWP, "Alabama Water Quality Information System," Alabama State Water Program, Auburn, Alabama, 2006.

www.aces.edu/waterquality/gis_data/dogq_list_co.php3?County=Jackson&Code=101 and www.aces.edu/waterquality/gis_data/topo_data.htm.

Bredehoeft, J., Models and model analysis, *Ground Water*, 48(3):328, 2010.

Carrera J. and S.P. Neuman, Estimation of aquifer parameters under transient and steady state conditions: 1. Maximum likelihood method incorporating prior information, *Water Resour. Res.*, 22(2):199-210, 1986.

Cooley, R.L., Incorporation of prior information on parameters into nonlinear regression groundwater flow models: 2. Applications, *Water Resour. Res.*, 19(3):662-676, 1983.

Doherty, J., *PEST*, Model-Independent Parameter Estimation, User's Manual: 5th Edition, Watermark Numerical Computing, Australia, 2004. <http://www.pesthomepage.org/>

Doherty, J., *Addendum to the PEST Manual*, Watermark Numerical Computing, September, 2010. <http://www.pesthomepage.org/>

Draper, D., Assessment and propagation of model uncertainty, *J. Roy. Statist. Soc. Ser. B*, 57(1):45-97, 1995.

Findikakis, A.N. and M.K. Waterman, An industry perspective on groundwater flow model calibration, in Palmer, R.N. (ed.), *World Environmental and Water Resources Congress 2010: Challenges of Change*, American Society of Civil Engineers, pp. 737-743, 2010.

GM. *User's Manual for Global Mapper Version 6.09*, Global Mapper Software LLC, Parker, Colorado, 2005.

Harbaugh, A.W., E.R. Banta, M.C. Hill, and M.G. McDonald, *MODFLOW-2000, the U.S. Geological Survey modular ground-water model -- User guide to modularization concepts and the Ground-Water Flow Process*, U.S. Geological Survey Open-File Report 00-92, 121 pp., 2000.

Harbaugh, A.W., MODFLOW-2005, The U.S. Geological Survey Modular Ground-Water Model—the Ground-Water Flow Process. U.S. Geological Survey, Reston, Virginia. Techniques and Methods 6-A16, 2005.

- Helsel D.R. and R.M. Hirsch, *Statistical Methods in Water Resources*, Tech. Wat.-Resour. Invest., Book 4, Hydrologic Analysis and Interpretation, Chap. A3, U.S. Geological Survey, Reston, Virginia, 2002.
- Hill, M.C. and C.R. Tiedeman, *Effective Groundwater Model Calibration*, Wiley, New York, 455 pp., 2007.
- Hill, M.C., R.L. Cooley, and D.W. Pollock, A controlled experiment in ground-water flow model calibration using nonlinear regression, *Ground Water*, 36(3):520-535, 1998.
- Hoeting, J.A., D. Madigan, A.E. Raftery, and C.T. Volinsky, Bayesian model averaging: A tutorial, *Statist. Sci.*, 14(4):382-417, 1999.
- Irvin, G.D. and P.A. Dinterman, "Geologic Map of the Hollywood 7.5-Minute Quadrangle, Jackson County, Alabama," Quadrangle Series Map 52, Geological Survey of Alabama, Tuscaloosa, Alabama, 2009. www.ogb.state.al.us/gsa/QS_results.aspx?PubID=QS52
- McDonald, M.G., and A.W. Harbaugh, "A Modular Three-Dimensional Finite-Difference Flow Model," In: *Techniques of Water Resources Investigations of the U.S. Geological Survey*, Book 6, U.S. Geological Survey, Reston, Virginia, 1988.
- Menne, M., I. Durre, R. Vose, B. Gleason, and T. Houston, "An Overview of the Global Historical Climatology Network-Daily Database," *J. Atmos. Oceanic Technol.*, in press, 2012.
- Meyer, P.D., M. Ye, M.L. Rockhold, S.P. Neuman, and K.J. Cantrell, *Combined Estimation of Hydrogeologic Conceptual Model, Parameter, and Scenario Uncertainty with Application to Uranium Transport at the Hanford Site 300 Area*, NUREG/CR-6940 (PNNL-16396), U.S. Nuclear Regulatory Commission, Washington, DC., 2007.
- Microsoft, "Microsoft Office Excel 2007." Microsoft Corp., Redmond, Washington, 2006.
- Miller, J.A, *Groundwater Atlas of the United States, Segment 6, Alabama, Florida, Georgia, and South Carolina*, Hydrol. Invest. Atlas HA 730-G, U.S. Geological Survey, Reston, VA, 1990. (http://pubs.usgs.gov/ha/ha730/ch_g/G-text9.html)
- Moore, C. and J. Doherty, The role of the calibration process in reducing model predictive error, *Water Resources Research*, Vol. 41, W05020, doi:10.1029/2004WR003501, 2005.
- National Research Council, *Models in Environmental Regulatory Decision Making*, The National Academies Press, Washington, D.C., 2007.
- National Research Council, *Assessing the Reliability of Complex Models: Mathematical and Statistical Foundations of Verification, Validation, and Uncertainty Quantification*, The National Academies Press, Washington, D.C., 2012.
- Neuman, S.P., Maximum likelihood Bayesian averaging of alternative conceptual-mathematical models, *Stochastic Environmental Research and Risk Assessment*, 17, DOI10.1007/s00477-003-0151-7, 2003.
- Neuman, S.P. and P.J. Wierenga, *A Comprehensive Strategy of Hydrogeologic Modeling and Uncertainty Analysis for Nuclear Facilities and Sites*, NUREG/CR-6805, U.S. Nuclear Regulatory Commission, Washington, D.C., 2003.

NRC, *U.S. Nuclear Regulatory Commission Environmental Standard Review Plan*, NUREG-1555, U.S. Nuclear Regulatory Commission, March, 1999.

NRC, *U.S. Nuclear Regulatory Commission Standard Review Plan*, NUREG-0800, Rev. 3, U.S. Nuclear Regulatory Commission, March, 2007.

NRC, *Transcript of Advisory Committee on Reactor Safeguards, ESBWR Subcommittee: North Anna COLA*, August 21, 2009, Accession Number ML092450200, accessed at <http://adams.nrc.gov/wba/>.

NRC, *Transcript of Advisory Committee on Reactor Safeguards, 573rd Meeting*, June 10, 2010, Accession Number ML101660400, accessed at <http://adams.nrc.gov/wba/>.

Pilkey, O.H. and L. Pilkey-Jarvis, *Useless Arithmetic: Why Environmental Scientists Can't Predict the Future*, Columbia Univ. Press, New York, 2007.

Poeter E.P., M.C. Hill, E.R. Banta, S.W. Mehl, and S. Christensen, *UCODE_2005 and Six Other Computer Codes for Universal Sensitivity Analysis, Inverse Modeling, and Uncertainty Evaluation*, U.S. Geological Survey Techniques and Methods Report TM 6-A11, U.S. Geological Survey, Denver, Colorado, 2005.

Poeter, E.P. and D. Anderson, Multimodel ranking and inference in ground water modeling, *Ground Water*, 43(4):597-605, 2005.

Poeter, E.P., and M.C. Hill, *MMA, A computer code for Multi-Model Analysis*, U.S. Geological Survey Techniques and Methods 6-E3, 113 pp., 2007.

Pollock, D.W., *User's Guide for MODPATH/MODPATH-PLOT, Version 3: A particle tracking post-processing package for MODFLOW, the U.S. Geological Survey finite-difference ground-water flow model*, U.S. Geological Survey Open-File Report 94-464, 1994.

Singh, A., S. Mishra, and G. Ruskauff, Model averaging techniques for quantifying conceptual model uncertainty, *Ground Water*, 48(5), DOI: 10.1111/j.1745-6584.2009.00642.x, 2010.

Tsai, F. T.-C., and X. Li, Inverse groundwater modeling for hydraulic conductivity estimation using Bayesian model averaging and variance window, *Water Resources Research*, 44(9), W09434, doi:10.1029/2007WR006576, 2008.

TVA, Bellefonte Nuclear Plant Units 3 & 4, COL Application, Part 2, Final Safety Analysis Report, Rev. 1, Tennessee Valley Authority, Knoxville, Tennessee, 2009.
www.nrc.gov/reactors/new-reactors/col/bellefonte/documents.html

USACE, *Corpscon: Version 6.x Technical Documentation and Operating Instructions*, U.S. Army Corps of Engineers, Alexandria, Virginia, 2004. www.agc.army.mil/corpscon/

USGS, "1/3-Arc Second National Elevation Dataset, Jackson County, Alabama," U.S. Geological Survey, Sioux Falls, South Dakota, 2009. www.alabamaview.org/10m_DEM.html

Ye, M., S.P. Neuman, and P.D. Meyer, Maximum likelihood Bayesian averaging of spatial variability models in unsaturated fractured tuff, *Water Resour. Res.*, 40, W05113, doi:10.1029/2003WR002557, 2004.

Ye, M., P. D. Meyer, and S. P. Neuman, On model selection criteria in multimodel analysis, *Water Resour. Res.*, 44, W03428, doi:10.1029/2008WR006803, 2008.

Zheng, C. and P.P. Wang, *MT3DMS, A modular three-dimensional multi-species transport model for simulation of advection, dispersion and chemical reactions of contaminants in groundwater systems; documentation and user's guide*, U.S. Army Engineer Research and Development Center Contract Report SERDP-99-1, Vicksburg, MS, 202 pp., 1999.

Zheng, C., *MT3DMS v5.2: Supplemental User's Guide*, University of Alabama, Tuscaloosa, Alabama, 2006. hydro.geo.ua.edu/mt3d

Zheng, C., M.C. Hill, and P.A. Hsieh, *Modflow-2000, the U.S. Geological Survey Modular Ground-Water Model—User Guide to the LMT6 Package, the Linkage with MT3DMS for Multi-Species Mass Transport Modeling*, U.S. Geological Survey, Reston, Virginia, Open File Report 01-82, 2001.

APPENDIX A

Dependence of KIC on Log Transformation of Parameters

APPENDIX A

Dependence of KIC on Log Transformation of Parameters

When calculating the model selection criterion KIC from least squares optimization results, parameter transformations need to be considered. PEST and UCODE allow parameters to be log-transformed during the regression. Both codes report the parameter covariance matrix in the transformed space using log base 10. As indicated by Meyer et al. (2007), multi-model comparisons using KIC must use untransformed parameter covariances. PEST and UCODE, however, report KIC values computed with transformed parameters. One solution to this problem is to recompute the covariance matrix with all parameters untransformed and fixed at the optimal values (obtained with some or all of the parameters log-transformed). Alternatively, the untransformed KIC values can be calculated directly from the transformed parameter covariance matrix as described below.

Ye et al. (2008) give an expression for calculating KIC,

$$KIC = N_z \ln \hat{\sigma}_{ML}^2 - 2 \ln p(\hat{\theta}) - P \ln 2\pi - \ln |\Sigma^{ML}| \quad (A.1)$$

where N_z is the number of observations, P is the number of estimated hydrologic parameters, $\hat{\theta}$ is the vector of maximum likelihood parameter estimates, $\hat{\sigma}_{ML}^2 = \frac{\mathbf{e}^T \boldsymbol{\omega} \mathbf{e}}{N_z} \Big|_{\theta_k = \hat{\theta}_k}$ is the maximum likelihood estimate of the common observation error variance, $\mathbf{e} = \hat{\mathbf{z}} - \mathbf{z}^*$ is the vector of residuals (the difference between $\hat{\mathbf{z}}$, the simulated observation evaluated at $\hat{\theta}$, and the observed values, \mathbf{z}^*), and Σ^{ML} is the parameter covariance matrix evaluated at $\hat{\theta}$. Because Σ^{ML} is a function of the parameter transformations under which regression is carried out, it must be evaluated without transformations for KIC calculation. Since

$$\ln |\Sigma^{ML}| = P \ln \hat{\sigma}_{ML}^2 - \ln |\mathbf{J}_k^T \boldsymbol{\omega} \mathbf{J}_k| \quad (A.2)$$

this entails evaluating the Jacobian matrix, \mathbf{J} , without transformations.

For a model characterized by parameters $\theta_j, j=1, \dots, P$, \mathbf{J} has elements $J_{ij} = \frac{\partial z_i}{\partial \theta_j}$. For a parameter that is log-transformed (base 10) during regression¹, $\tilde{J}_{ij} = \frac{\partial z_i}{\partial \log \theta_j} = \theta_j \ln 10 \frac{\partial z_i}{\partial \theta_j}$. As a result,

$$\begin{aligned} & \ln \left| \tilde{\mathbf{J}}_k^T \boldsymbol{\omega} \tilde{\mathbf{J}}_k \right| \\ &= 2L \ln(\ln 10) + 2 \sum_{j \in \mathcal{L}} \ln \hat{\theta}_j + \ln \left| \mathbf{J}_k^T \boldsymbol{\omega} \mathbf{J}_k \right| \end{aligned} \quad (\text{A.3})$$

where \mathcal{L} is the set of L parameters that are log-transformed during regression. As a result,

$$\begin{aligned} & \ln \left| \boldsymbol{\Sigma}^{ML} \right| \\ &= \ln \left| \tilde{\boldsymbol{\Sigma}}^{ML} \right| + 2L \ln(\ln 10) + 2 \sum_{j \in \mathcal{L}} \ln \hat{\theta}_j \end{aligned} \quad (\text{A.4})$$

and

$$\begin{aligned} & KIC \\ &= \tilde{KIC} + 2L \ln(\ln 10) + 2 \sum_{j \in \mathcal{L}} \ln \hat{\theta}_j \end{aligned} \quad (\text{A.5})$$

where $\tilde{\boldsymbol{\Sigma}}^{ML}$ and \tilde{KIC} are the parameter covariance matrix and KIC value reported by PEST or UCODE with log-transformed parameters.

¹ if $\beta = \log \theta$, then $\beta \ln 10 = \ln \theta$, and $\partial \beta = \partial \log \theta = (\theta \ln 10)^{-1} \partial \theta$

APPENDIX B

Data Used in Model Development

Table B-1. List of borehole data used to define the surface of contacts between geological units

Borehole Name ^a	Total Depth (ft)	Northing ^b (ft)	Easting ^b (ft)	Surface Elevation (ft)	Elev. of Top of Weathered Rock ^c (ft)	Elev. of Top of Competent Rock ^d (ft)	Elevation of Contact Between Specified Units ^e (ft)							
							NV/USR	USR/A	A/B	B/C	C/D	D/E	E/F	F/LSR
B-1000	185.9	1533129.7	628373.5	611.9	595.4	590.9						503	483	434
B-1001A	17.2	1533081.9	628359.4	611.3	594.5	583.3								
B-1002	120.5	1532906.7	628471.5	613.3	597.3	592.8					583			
B-1003	120.4	1532838.5	628359.6	613.6	598.8	587.4					591			
B-1004	150.2	1532950.0	628276.6	611.1	598.0	597.9						490	469	
B-1005	251	1532943.5	628407.1	608.9	598.0	592.9						465	444	394
B-1006	176	1532755.0	628259.7	614.5	595.7	588.9						460		
B-1007	120	1533041.2	628430.9	608.4	600.3	591.9						D		
B-1008	121.3	1533048.9	628211.6	614.1	598.1	592.6						519	498	
B-1009	75.8	1532957.3	628130.1	613.9	595.2	595.1						D		
B-1010	74	1532836.3	628178.5	611.7	598.2	595.5						D		
B-1011	75.3	1532610.4	628132.4	615.6	599.1	599.0					591			
B-1012	50	1532678.0	628247.8	616.7	602.8	600.2					585			
B-1013	50	1532758.8	628315.6	614.8	603.2	593.8					584			
B-1014	121.2	1532984.8	628354.3	609.1	604.1	598.6						D		
B-1015	75.4	1533020.6	628276.3	611.5	599.0	598.5						D		
B-1016	20.7	1532867.3	628224.3	611.6	595.3	594.1						D		
B-1017	50.6	1532937.4	628225.4	611.9	592.9	588.4						D		
B-1018	16.5	1532827.3	628217.6	612.7	603.1	596.5						D		
B-1019	35	1532716.2	628178.6	613.7	597.3	596.9						D		
B-1020	35	1532590.2	628188.0	616.7	606.7	595.7					C			
B-1021	35.4	1532997.4	628462.5	608.6	597.3	583.3						D		

Borehole Name ^a	Total Depth (ft)	Northing ^b (ft)	Easting ^b (ft)	Surface Elevation (ft)	Elev. of Top of Weathered Rock ^c (ft)	Elev. of Top of Competent Rock ^d (ft)	Elevation of Contact Between Specified Units ^e (ft)							
							NV/USR	USR/A	A/B	B/C	C/D	D/E	E/F	F/LSR
B-1022	76.1	1532633.2	628366.9	617.4	598.9	595.9					549			
B-1023	60.1	1532853.9	628421.0	613.4	602.3	597.4					582			
B-1024	175.4	1532702.4	628492.0	617.1	602.6	593.7					540			
B-1025	75	1532823.2	628567.9	616.9	600.9	590.6					547			
B-1026	50	1533363.2	628319.4	608.6	589.9	562.6						D		
B-1027	50	1532755.9	627608.5	608.6	596.2	592.3						578		
B-1028	88.1	1532272.0	628314.6	624.9	612.6	589.9				566				
B-1029	35.9	1533050.8	628111.8	612.6	607.6	603.8						D		
B-1031	35	1532538.5	628081.8	616.9	601.9	590.5					594			
B-1032	175.6	1533054.2	628254.8	613.0	592.0	581.8						513	492	443
B-1033	121.5	1532169.8	628888.6	625.9	613.4	609.4			556					
B-1034	249.5	1532442.6	629037.0	622.0	608.0	601.0			579	454	385			
B-1035	171.1	1532549.5	629112.9	616.1	603.5	600.1			585	461				
B-1036	55.3	1532263.9	628856.1	625.2	609.2	594.0			582	457				
B-1037	149.7	1532329.0	628980.8	621.4	607.4	606.6			569					
B-1038	65.8	1532091.5	628812.5	629.4	616.7	611.0			A					
B-1039	120	1532472.2	628859.9	620.2	610.2	610.1				B				
B-1040	119.7	1532554.0	629061.0	616.9	605.7	603.5			596					
B-1041	120.3	1532544.9	628845.0	620.1	608.6	605.1				510				
B-1042	124.3	1532377.2	628935.9	622.0	599.0	593.0			585					
B-1043A	75.6	1532424.3	628756.8	622.2	607.7	606.7				B				
B-1044	76	1532399.8	629086.6	618.7	610.7	602.7			563					
B-1045	75.1	1532482.4	628986.7	622.4	603.9	596.3			596					
B-1046	49.4	1532242.9	628945.3	625.5	601.9	599.1			A					
B-1047	120	1532622.2	628995.6	619.2	607.7	604.2				B				

Borehole Name ^a	Total Depth (ft)	Northing ^b (ft)	Easting ^b (ft)	Surface Elevation (ft)	Elev. of Top of Weathered Rock ^c (ft)	Elev. of Top of Competent Rock ^d (ft)	Elevation of Contact Between Specified Units ^e (ft)								
							NV/USR	USR/A	A/B	B/C	C/D	D/E	E/F	F/LSR	
B-1048	76.3	1532210.9	628709.9	627.8	608.3	602.3			601						
B-1049	128	1532539.2	628917.1	617.3	607.9	592.3				496					
B-1050	75	1532300.7	628780.2	624.1	610.1	603.9			603						
B-1051A	51.9	1532159.7	628729.8	629.1	608.5	590.4			586						
B-1052	79	1532330.9	628912.5	621.8	595.1	567.8			580						
B-1053	35	1532489.4	628910.4	620.2	608.3	599.6				B					
B-1054	35	1532232.5	628800.2	628.2	611.3	593.2			A						
B-1055	71.6	1532492.0	629080.8	619.6	608.1	600.8			581						
B-1056	45.7	1532231.0	628882.6	626.9	606.9	581.2			A						
B-1057	35.2	1532372.8	628836.1	621.6	608.0	603.1			606						
B-1058	65.2	1532351.3	629027.4	620.2	612.4	584.9			564						
B-1059	250	1532712.7	628706.2	619.0	605.5	593.5				569	500				
B-1060	176.3	1532444.1	629267.9	621.7	605.3	602.7		600	534						
B-1061	75.2	1532124.2	629092.1	630.2	622.6	620.6		573							
B-1062	150.8	1532323.8	629378.9	627.7	618.8	556.7		555	489						
B-1063	50.2	1531925.4	628928.3	634.7	630.7	630.6		USR							
B-1064	50	1532447.5	628574.8	623.9	609.7	602.6				B					
B-1065	41.5	1532496.4	629393.6	628.1	610.6	587.8		USR							
B-1066	124.4	1532293.3	629209.1	626.4	616.9	587.4		583	518						
B-1067	174.6	1532868.7	628839.9	614.4	605.6	604.9				574	506				
B-1068	50	1532280.8	627961.6	617.2	605.0	586.0					C				
B-1069	50	1531732.6	628733.3	635.8	626.5	594.8		USR							
B-1070	51	1530825.5	628348.8	647.2	644.0	596.2	601								
B-1071	75	1531172.7	626508.3	614.5	596.5	588.3						D			
B-1072	50.1	1530152.0	627504.4	627.1	620.3	596.0		USR							

Borehole Name ^a	Total Depth (ft)	Northing ^b (ft)	Easting ^b (ft)	Surface Elevation (ft)	Elev. of Top of Weathered Rock ^c (ft)	Elev. of Top of Competent Rock ^d (ft)	Elevation of Contact Between Specified Units ^e (ft)							
							NV/USR	USR/A	A/B	B/C	C/D	D/E	E/F	F/LSR
B-1073	75.3	1530642.8	627276.0	629.2	604.5	597.1				B				
B-1074	50	1530685.8	627635.9	637.4	631.7	596.4		621						
B-1075	75	1530444.8	627150.2	626.2	612.7	611.2				B				
B-1076	50	1532710.0	628084.9	612.7	604.4	592.0						D		
B-1077	15.8	1532870.6	626759.1	602.1	590.4	575.6								LSR
B-1078	75	1533819.2	627721.5	603.6	591.5	588.6								LSR
B-1079	150	1533742.4	628277.0	604.8	593.0	592.9								547
B-1080	35	1532389.9	630169.0	615.8	605.9	580.8	NV							
B-1081	33.5	1532026.1	628657.8	625.7	614.2	597.2			A					
B-1082	75	1532535.4	628502.6	621.0	613.6	584.3				574				
B-1083	75	1532571.1	629135.1	615.0	601.6	600.0			585					
B-1084	50.3	1532586.4	628991.9	614.8	607.7	602.1				B				
B-1085	6.9	1532807.8	627935.7	608.5	601.6	600.0						D		
B-1086	75.3	1533155.7	628520.7	607.2	599.7	599.6						D		
B-1087	35.4	1532677.2	629071.3	613.0	609.0	600.5				B				
B-1088	71.2	1533043.3	628497.2	608.1	599.6	597.1						D		
B-1089	40	1531668.7	628473.1	630.5	614.3	595.0			A					
B-1090	128	1533200.9	628455.8	609.9	603.4	586.9						D		
B-1091	35	1531925.1	629403.7	641.9	627.8	620.9	NV							
B-1092	56	1532370.7	628902.4	621.6	604.8	600.6			592					
B-1094	35	1533085.6	628571.3	607.6	596.0	591.6						D		
B-1095	50.1	1532077.1	628968.9	630.0	617.4	599.0		588						
B-1096	50.1	1532615.5	629217.0	616.5	607.5	605.9			577					
B-1097	50	1531841.7	628482.3	625.3	614.1	612.9			A					
B-1098	50	1532350.7	627838.6	616.4	601.0	589.9						D		

Borehole Name ^a	Total Depth (ft)	Northing ^b (ft)	Easting ^b (ft)	Surface Elevation (ft)	Elev. of Top of Weathered Rock ^c (ft)	Elev. of Top of Competent Rock ^d (ft)	Elevation of Contact Between Specified Units ^e (ft)							
							NV/USR	USR/A	A/B	B/C	C/D	D/E	E/F	F/LSR
B-1099	50	1533127.1	627932.7	604.8	595.6	578.8						573		

^a Boring information (names, depth, coordinates) was taken from FSAR Table 2.5-227.

^b State Plane Coordinate System (Alabama East), NAD83.

^c Top of Weathered Rock is the elevation of the Standard Penetration Test (SPT) refusal.

^d Top of Competent Rock is the elevation at which Rock Quality Designation (RQD) > 70, weathering = Fresh, and below which no significant weathered intervals exist. In the absence of such data, this elevation was arbitrarily set to 0.1 ft. below the top of the weathered rock.

^e The elevation of the contact between stratigraphic units is based on the borehole logs (see FSAR Appendix 2BB and Fig. 2.5-306). A text entry of a unit name indicates that the unit was encountered, but a contact between units could not be discerned. NV = Nashville Unit; USR = Upper Stones River Unit; A-F = Middle Stones River (MSR) Units; LSR = Lower Stones River Unit.

Table B-2. List of monitoring wells and their characteristics (based on FSAR Table 2.4.12-203)

Monitoring Well Name	Northing^a (ft)	Easting^a (ft)	Reference Elevation^b (ft)	Ground Elevation^b (ft)	Well Depth^c (ft bre)	Screen Length (ft)	Top of Screen^b (ft)	Bottom of Screen^{b,d} (ft)	Boring Depth^c (ft bgs)
MW-1201a	1532950	628276.6	613.91	611.05	12.91	5	606.45	601.45	10.05
MW-1201b	1532950	628276.6	613.78	611.04	77.81	10	546.42	536.42	75.07
MW-1201c	1532950	628276.6	613.65	610.91	119	20	515.1	495.1	116.26
MW-1202a	1532571.1	629135.1	617.52	614.99	15.42	5	607.55	602.55	12.89
MW-1202c	1532571.1	629135.1	617.62	614.93	53	10	575.07	565.07	50.31
MW-1203a	1532718.7	628698.8	621.93	619.02	12.57	5	614.81	609.81	9.66
MW-1203b	1532718.7	628698.8	621.86	619.14	32.9	10	599.41	589.41	30.18
MW-1203c	1532718.7	628698.8	621.7	619.04	121	20	521.15	501.15	118.34
MW-1204a	1532472.2	628859.9	623.1	620.45	12.95	5	615.6	610.6	10.3
MW-1204b	1532472.2	628859.9	623.16	620.48	53.2	10	580.41	570.41	50.52
MW-1204c	1532472.2	628859.9	623.1	620.49	124.2	20	519.35	499.35	121.59
MW-1205a	1532290.8	629211.7	629.42	627.04	13	5	621.87	616.87	10.62
MW-1205b	1532290.8	629211.7	629.34	627.01	33.16	10	606.63	596.63	30.83
MW-1205c	1532290.8	629211.7	629.14	626.89	49.11	10	590.48	580.48	46.86
MW-1206b	1530825.5	628348.8	650.35	647.57	27	10	633.8	623.8	24.22
MW-1206c	1530825.5	628348.8	649.95	647.4	52.8	10	607.6	597.6	50.25
MW-1207a	1532280.8	627961.6	619.78	617.09	14.8	5	610.43	605.43	12.11
MW-1207b	1532280.8	627961.6	619.8	617.24	21	5	604.25	599.25	18.44
MW-1207c	1532280.8	627961.6	619.9	617.11	53.45	10	576.9	566.9	50.66
MW-1208a	1531172.7	626508.3	617.33	614.79	18.73	10	609.05	599.05	16.19
MW-1208b	1531172.7	626508.3	617.22	614.72	32.15	5	590.52	585.52	29.65
MW-1208c	1531172.7	626508.3	617.26	614.69	57.95	10	569.76	559.76	55.38
MW-1209b	1530685.8	627635.9	640.39	637.78	28	10	622.84	612.84	25.39
MW-1209c	1530685.8	627635.9	640.44	637.84	53.05	10	597.84	587.84	50.45

Monitoring Well Name	Northing ^a (ft)	Easting ^a (ft)	Reference Elevation ^b (ft)	Ground Elevation ^b (ft)	Well Depth ^c (ft bre)	Screen Length (ft)	Top of Screen ^b (ft)	Bottom of Screen ^{b,d} (ft)	Boring Depth ^c (ft bgs)
MW-1210a	1533742.4	628277	607.88	605.03	14.3	5	599.03	594.03	11.45
MW-1210b	1533742.4	628277	608.01	605.04	33.79	10	584.67	574.67	30.82
MW-1210c	1533742.4	628277	607.96	605.15	69.72	10	548.69	538.69	66.91
MW-1211a	1532389.9	630169	618.87	615.89	11.53	5	612.79	607.79	8.55
MW-1211c	1532389.9	630169	618.66	615.76	38.1	10	591.01	581.01	35.2
MW-1212a	1533819.2	627721.5	607	603.98	15.28	5	597.17	592.17	12.26
MW-1212b	1533819.2	627721.5	606.86	604.07	33.55	10	583.76	573.76	30.76
MW-1212c	1533819.2	627721.5	606.79	603.94	64	10	553.24	543.24	61.15
MW-1213b	1532159.7	628729.8	632.02	629.21	40	10	602.47	592.47	37.19
MW-1213c	1532159.7	628729.8	632.2	629.42	50	10	592.65	582.65	47.22
MW-1214a	1532755.9	627608.5	612.23	609.53	14	5	603.68	598.68	11.3
MW-1214b	1532755.9	627608.5	612.09	609.74	22.8	5	594.74	589.74	20.45
MW-1214c	1532755.9	627608.5	612.08	609.54	43.5	10	579.03	569.03	40.96
MW-1215a	1532957.7	628666.65	635.64	632.79	13.25	5	627.84	622.84	10.4
MW-1215b	1531700.65	628603.2	635.63	632.77	33	10	613.08	603.08	30.14
MW-1215c	1531700.65	628603.2	635.6	632.79	52.5	10	593.55	583.55	49.69
MW-1216a	1532870.6	626759.1	604.56	602.57	25.1	10	589.91	579.91	23.11
MW-1216c	1532870.6	626759.1	604.64	602.23	63	10	552.09	542.09	60.59
MW-1217a	1532752.4	628266.8	617.32	614.27	13.34	5	609.43	604.43	10.29
MW-1217b	1532752.4	628266.8	617.1	614.15	33.3	10	594.25	584.25	30.35
MW-1217c	1532752.4	628266.8	617.08	614.14	52.8	10	574.73	564.73	49.86
OW-1	1532758	628739.6	623.33	620.55	82.89	20	560.89	540.89	80.11
OW-2	1532723.1	628659.5	621.2	618.43	92.9	20	548.75	528.75	90.13
OW-3	1532669	628708	622.89	620.13	82.87	20	560.47	540.47	80.11
OW-4	1532751.6	628804.2	623.23	620.4	13.03	5	615.65	610.65	10.2
OW-5	1532819.5	628708.5	621.2	618.34	12.8	5	613.85	608.85	9.94

Monitoring Well Name	Northing ^a (ft)	Easting ^a (ft)	Reference Elevation ^b (ft)	Ground Elevation ^b (ft)	Well Depth ^c (ft bre)	Screen Length (ft)	Top of Screen ^b (ft)	Bottom of Screen ^{b,d} (ft)	Boring Depth ^c (ft bgs)
OW-6	1532631.7	628659.6	623.23	620.45	12.9	5	615.78	610.78	10.12
OW-7	1532793.7	628292.6	617.46	614.78	52.85	10	575.06	565.06	50.17
OW-8	1532706.9	628239.1	618	615.33	54.2	10	574.25	564.25	51.53
OW-9	1532802.3	628203.2	615.58	613.1	52.7	10	573.33	563.33	50.22
OW-10	1532835.4	628236.5	616.24	613.31	33.45	10	593.24	583.24	30.52
OW-11	1532839.7	628305.6	616.39	613.71	32.92	10	593.92	583.92	30.24
OW-12	1532780.6	628335.7	617.45	614.76	32.95	10	594.95	584.95	30.26

^a State Plane Coordinate System (Alabama East), NAD83. Coordinates are from the nearest borehole according to FSAR Figure 2.5-327.

^b Relative to the North American Vertical Datum of 1988 (NADV88).

^c "bre" = below reference elevation; "bgs" = below ground surface

^d A 0.45 ft-long cap is threaded onto the bottom of the screen. Thus the bottom of screen elevation equals the reference elevation minus the well depth plus 0.45 ft.

Table B-3. List of the observed hydraulic heads in monitoring wells

Well Name	Easting ^a (ft)	Northing ^a (ft)	Screen Center Elevation ^{b,c} (ft)	Observed Head Elevation ^b (ft)	Well Category ^d
1	627442.0	1540804.0	Assumed to be within Layer 1	609.0	1961
2	627255.0	1540308.0	Assumed to be within Layer 1	615.0	1961
3	627067.0	1539759.0	Assumed to be within Layer 1	617.0	1961
4	626397.0	1536021.0	Assumed to be within Layer 1	605.0	1961
5	625593.0	1537441.0	Assumed to be within Layer 1	619.0	1961
11	623382.0	1534667.0	Assumed to be within Layer 1	620.0	1961
12	620167.0	1533810.0	Assumed to be within Layer 1	609.0	1961
13	621198.0	1533046.0	Assumed to be within Layer 1	595.0	1961
14	623423.0	1531881.0	Assumed to be within Layer 1	591.0	1961
W9	632225.0	1535986.0	Assumed to be within Layer 1	593.9	2005
W19	632188.0	1535312.0	Assumed to be within Layer 1	596.0	2005

Well Name	Easting^a (ft)	Northing^a (ft)	Screen Center Elevation^{b,c} (ft)	Observed Head Elevation^b (ft)	Well Category^d
W22	632075.0	1534726.0	Assumed to be within Layer 1	607.4	2005
W20	631439.0	1533540.0	Assumed to be within Layer 1	597.9	2005
W12	629330.0	1531581.0	Assumed to be within Layer 1	595.8	2005
W30	628843.0	1534102.0	Assumed to be within Layer 1	595.3	2005
WT6	628281.0	1533066.0	Assumed to be within Layer 1	597.3	2005
WT5	628107.0	1532367.0	Assumed to be within Layer 1	605.1	2005
WT2	627333.0	1530919.0	Assumed to be within Layer 1	611.4	2005
WT3	627121.0	1532442.0	Assumed to be within Layer 1	598.3	2005
W16	627121.0	1528723.0	Assumed to be within Layer 1	625.8	2005
WT4	626946.0	1533815.0	Assumed to be within Layer 1	594.6	2005
P2	626572.0	1529659.0	Assumed to be within Layer 1	613.8	2005
P4	626073.0	1528823.0	Assumed to be within Layer 1	614.2	2005
P1	625973.0	1530770.0	Assumed to be within Layer 1	602.8	2005
WT1	625711.0	1531094.0	Assumed to be within Layer 1	603.7	2005
W17	625349.0	1529035.0	Assumed to be within Layer 1	610.8	2005
P3	625074.0	1530470.0	Assumed to be within Layer 1	597.5	2005
MW-1203b	628698.8	1532718.7	594.4	609.4	Average, Bedrock
MW-1204c	628859.9	1532472.2	509.4	609.6	Average, Bedrock
MW-1205b	629211.7	1532290.8	601.6	609.3	Average, Bedrock
MW-1205c	629211.7	1532290.8	585.5	609.7	Average, Bedrock
MW-1206b	628348.8	1530825.5	628.8	639.9	Average, Bedrock
MW-1206c	628348.8	1530825.5	602.6	634.5	Average, Bedrock
MW-1207c	627961.6	1532280.8	571.9	602.7	Average, Bedrock
MW-1208b	626508.3	1531172.7	588.0	607.7	Average, Bedrock
MW-1208c	626508.3	1531172.7	564.8	607.0	Average, Bedrock

Well Name	Easting^a (ft)	Northing^a (ft)	Screen Center Elevation^{b,c} (ft)	Observed Head Elevation^b (ft)	Well Category^d
MW-1209b	627635.9	1530685.8	617.8	619.2	Average, Bedrock
MW-1210b	628277.0	1533742.4	579.7	597.9	Average, Bedrock
MW-1211c	630169.0	1532389.9	586.0	609.9	Average, Bedrock
MW-1212b	627721.5	1533819.2	578.8	596.8	Average, Bedrock
MW-1212c	627721.5	1533819.2	548.2	595.5	Average, Bedrock
MW-1213b	628729.8	1532159.7	597.5	609.5	Average, Bedrock
MW-1213c	628729.8	1532159.7	587.7	609.8	Average, Bedrock
MW-1214b	627608.5	1532755.9	592.2	600.7	Average, Bedrock
MW-1214c	627608.5	1532755.9	574.0	600.7	Average, Bedrock
MW-1215b	628603.2	1531700.7	608.1	614.7	Average, Bedrock
MW-1215c	628603.2	1531700.7	588.6	614.4	Average, Bedrock
MW-1216c	626759.1	1532870.6	547.1	597.3	Average, Bedrock
MW-1217b	628266.8	1532752.4	589.3	600.8	Average, Bedrock
OW-11	628305.6	1532839.7	588.9	600.7	Average, Bedrock
OW-12	628335.7	1532780.6	590.0	600.9	Average, Bedrock
OW-8	628239.1	1532706.9	569.3	601.3	Average, Bedrock
MW-1202a ^e	629135.1	1532571.1	605.1	607.2	Average, Soil
MW-1208a	626508.3	1531172.7	604.1	607.8	Average, Soil
MW-1210a	628277.0	1533742.4	596.5	599.7	Average, Soil
MW-1212a	627721.5	1533819.2	594.7	597.5	Average, Soil
MW-1214a	627608.5	1532755.9	601.2	602.7	Average, Soil
MW-1216a	626759.1	1532870.6	584.9	597.4	Average, Soil
MW-1204a	628859.9	1532472.2	610.6	613.0	Average, Soil
MW-1217a	628266.8	1532752.4	604.4	604.8	Average, Soil
OW-4	628804.2	1532751.6	613.2	613.6	Average, Soil

Well Name	Easting ^a (ft)	Northing ^a (ft)	Screen Center Elevation ^{b,c} (ft)	Observed Head Elevation ^b (ft)	Well Category ^d
OW-5	628708.5	1532819.5	611.4	612.5	Average, Soil
OW-6	628659.6	1532631.7	613.3	616.0	Average, Soil

^a State Plane Coordinate System (Alabama East), NAD83. Coordinates are from the nearest borehole according to FSAR Figure 2.5-327.

^b Relative to the North American Vertical Datum of 1988 (NADV88).

^c Because of the data source for the 1961 and September 2005 data, no screen elevation information was available. Hence these wells were assigned to model Layer 1. The Average Bedrock and Average Soil data points are assigned to the appropriate model layer based on the screen center elevation, thus the categorization may differ from the effective location (i.e., a well may be in the "Bedrock" category, but the screen center could potentially fall within a model Layer 1 grid cell whose material designation is Soil or Weathered Rock).

^d The 1961 data consists of the values shown on FSAR [TVA, 2009] Figure 2.4.12-204. The September 2005 data consists of the values shown on FSAR Figure 2.4.12-210. Average Soil and Average Bedrock are based on data from the FSAR Table 2.4.12-204 as described in Section 1.2.5. These four categorizations are used to group wells for viewing calibration results, but all wells are used in the calibration regardless of category. Wells 6, 7, 8, 9, and 10 from the 1961 data set and well W32 from the September 2005 data set are outside of the model domain and are thus not used in the calibration process.

^e In the model, MW-1202a was moved 13.5 ft to the northeast so that this point would lie in an active grid cell in the post-construction simulations. The modified coordinates are (629146, 1532579).

APPENDIX C

Spreadsheets for Calculating Model Selection Criteria and Model-Averaged Quantities

Model	Num. Data	Num. Param.	WSSR	AIC	AICc	BIC	KIC	ln F	Model Probabilities					
									AIC	AICc	BIC	KIC		
H1R1D1	71	2	8010.42	341.53	341.89	344.06	349.90	9.51	0.00%	0.00%	0.00%	0.00%		
H2R1D1	71	3	6026.49	323.33	323.93	328.12	328.31	5.71	0.00%	0.00%	0.01%	0.01%		
H3R1D1	71	4	5590.22	319.99	320.92	327.04	323.02	3.33	0.01%	0.01%	0.03%	0.20%		
H4R1D1	71	5	4244.35	302.44	303.75	311.75	313.78	11.22	32.64%	39.59%	52.83%	20.25%		
H1R2D1	71	5	5137.42	316.00	317.31	325.31	354.44	38.32	0.04%	0.05%	0.06%	0.00%		
H2R2D1	71	6	4932.50	315.11	316.88	326.68	344.02	28.37	0.06%	0.06%	0.03%	0.00%		
H3R2D1	71	7	4021.04	302.60	304.92	316.44	337.15	33.58	30.09%	22.03%	5.07%	0.00%		
H4R2D1	71	8	4176.33	307.29	310.24	323.39	349.18	40.49	2.88%	1.54%	0.16%	0.00%		
H1R1D2	71	2	7767.93	339.35	339.71	341.88	347.91	9.71	0.00%	0.00%	0.00%	0.00%		
H2R1D2	71	3	6056.45	323.68	324.29	328.47	321.71	-1.25	0.00%	0.00%	0.01%	0.38%		
H3R1D2	71	4	5725.10	321.69	322.61	328.74	321.30	-0.08	0.00%	0.00%	0.01%	0.47%		
H4R1D2	71	5	4276.54	302.97	304.29	312.29	311.07	7.97	24.96%	30.28%	40.40%	78.68%		
H1R2D2	71	5	5227.29	317.23	318.54	326.54	354.05	36.70	0.02%	0.02%	0.03%	0.00%		
H2R2D2	71	6	4941.69	315.24	317.02	326.81	337.98	22.20	0.05%	0.05%	0.03%	0.00%		
H3R2D2	71	7	4184.85	305.43	307.76	319.27	337.38	30.98	7.29%	5.34%	1.23%	0.00%		
H4R2D2	71	8	4222.75	308.07	311.03	324.18	349.85	40.38	1.95%	1.04%	0.11%	0.00%		
denom = sum(exp(-0.5*((C-ICmin)) / (array formula)))									3.063546147	2.525996	1.89298	1.27092		

Figure C-2. Spreadsheet for calculating model probabilities

Post-construction groundwater head uncertainty - Standard Deviations of Predicted values from UCODE Three head predictions at the east, south, and west corners of each reactor block																			
0.085034014 Head Measurement Error Std Dev.																			
Post-construction models																			
H4R1D1				H3R2D1				H4R1D2				H3R2D2							
0.681908836 s_a		1.996564419 95% Critical value		0.674019 s_a		1.99773 95% Critical value		0.68449 s_a		1.996564 95% Critical value		0.68761 s_a		1.99773 95% Critical value					
Location	Predicted	Std Dev	Linear Upper Limits	Location	Predicted	Std Dev	Linear Upper Limits	Location	Predicted	Std Dev	Linear Upper Limits	Location	Predicted	Std Dev	Linear Upper Limits				
			Conf.Int.				Conf.Int.				Conf.Int.				Conf.Int.				
Unit3-01	601.67	0.92	603.51	603.96	Unit3-01	601.95	1.34	604.63	604.95	Unit3-01	601.80	0.89	603.57	604.04	Unit3-01	602.13	1.38	604.89	605.21
Unit3-02	604.11	1.07	606.25	606.64	Unit3-02	606.13	2.02	610.15	610.37	Unit3-02	604.03	1.00	606.04	606.46	Unit3-02	606.05	1.90	609.84	610.08
Unit3-03	603.15	0.83	604.81	605.30	Unit3-03	604.66	1.60	607.85	608.12	Unit3-03	602.99	0.77	604.53	605.05	Unit3-03	604.34	1.50	607.33	607.63
Unit4-01	610.10	0.70	611.49	612.05	Unit4-01	610.87	1.50	613.87	614.16	Unit4-01	610.12	0.78	611.68	612.19	Unit4-01	610.37	1.44	613.25	613.56
Unit4-02	611.29	1.17	613.63	613.99	Unit4-02	613.81	1.48	616.77	617.06	Unit4-02	611.38	1.30	613.98	614.32	Unit4-02	613.99	1.43	616.84	617.15
Unit4-03	609.83	0.58	610.99	611.62	Unit4-03	613.05	1.25	615.54	615.88	Unit4-03	609.72	0.74	611.19	611.73	Unit4-03	612.88	1.23	615.35	615.70
Std. Dev.																			
Model Probabilities				Unit4-02				Param+Model											
AICC	KIC	Pred.Val	Param.	AIC mean	KIC mean														
H4R1D1	39.59%	20.25%	611.29	1.17	1.39	1.17													
H3R2D1	22.03%	0.00%	613.81	1.48	2.31	2.86													
H4R1D2	30.28%	78.68%	611.38	1.30	1.46	1.30													
H3R2D2	5.34%	0.00%	613.99	1.43	2.42	2.99													
ModAvgMean	612.04	611.36																	
ModAvgSD	1.68	1.28																	
Conflnt	615.39	613.91																	
Error	3.355226	2.5556016																	

Figure C-3. Spreadsheet for calculating model-averaged predictions and predictive uncertainty

BIBLIOGRAPHIC DATA SHEET

(See instructions on the reverse)

NUREG/CR-7211

2. TITLE AND SUBTITLE

Application of a Hydrological Uncertainty Methodology to Nuclear Reactor Site Evaluations

3. DATE REPORT PUBLISHED

MONTH

YEAR

August

2016

4. FIN OR GRANT NUMBER

5. AUTHOR(S)

P. D. Meyer and C.D. Johnson

6. TYPE OF REPORT

final

7. PERIOD COVERED (Inclusive Dates)

8. PERFORMING ORGANIZATION NAME AND ADDRESS (If NRC, provide Division, Office or Region, U. S. Nuclear Regulatory Commission, and mailing address; if contractor, provide name and mailing address.)

Pacific Northwest National Laboratory
Richland, WA 99352

9. SPONSORING ORGANIZATION NAME AND ADDRESS (If NRC, type "Same as above" if contractor, provide NRC Division, Office or Region, U. S. Nuclear Regulatory Commission, and mailing address.)

DIVISION of Risk Analysis
Office of Nuclear Regulatory Research
U. S. Nuclear Regulatory Commission
Washington DC

10. SUPPLEMENTARY NOTES

11. ABSTRACT (200 words or less)

A variety of surface water and groundwater models are used to review applications for new nuclear power reactors. These models are used to evaluate current site hydrology and to provide estimates of future site conditions after facility construction. A simple groundwater transport modeling example illustrates how uncertainty concepts can be used to inform regulatory decisions under these conditions. An uncertainty analysis methodology that can be used to estimate the joint impact of parameter, conceptual model, and scenario uncertainties is described, along with available software tools that can be used in a practical implementation of this methodology. The uncertainty methodology is illustrated using an example of reviewing groundwater site characteristics as part of a safety evaluation for a new power reactor. The example uses publicly available information from the Bellefonte Nuclear Station Units 3 and 4 Combined License application. A detailed description of model development is included to illustrate typical modeling decisions that arise in actual reviews. Modeling and uncertainty analyses were carried out using the Groundwater Modeling System (GMS) software, PEST UCODE, and custom spreadsheets. The example illustrates that following standard procedures for uncertainty analyses can reveal limitations of the hydrologic analyses, e.g., unexamined parameter correlations and outstanding data needs. Explicit consideration of alternative models is likely more valuable than quantitative model averaging. However, model averages using linear uncertainty methods can be easily completed and should be considered. Simple approaches to uncertainty evaluation can have great value, contributing to estimates of the degree of conservatism in the analysis, demonstrating an understanding of the system, and providing evidence of due diligence.

12. KEY WORDS/DESCRIPTORS (List words or phrases that will assist researchers in locating the report.)

Hydrology uncertainty uncertainty methodology groundwater model, groundwater, Hydrological uncertainty methodology

13. AVAILABILITY STATEMENT

unlimited

14. SECURITY CLASSIFICATION

(This Page)

unclassified

(This Report)

unclassified

15. NUMBER OF PAGES

16. PRICE



Federal Recycling Program



**UNITED STATES
NUCLEAR REGULATORY COMMISSION**
WASHINGTON, DC 20555-0001

OFFICIAL BUSINESS



NUREG/CR-7211

**Application of a Hydrological Uncertainty Methodology
to Nuclear Reactor Site Evaluations**

August 2016